Coupling impedance in modern accelerators

S. A. Heifets and S. A. Kheifets

Stanford Linear Accelerator Center, Stanford University, Stanford, California 94309

A systematic review of theoretical results for the longitudinal and transverse impedances obtained by different methods is presented. Definitions, general theorems, modal analysis, diffraction model, and analytical results comprise the content of the paper. Several new results are included. In particular, necessary and sufficient conditions for the independence of the impedance on the beam longitudinal direction are given. The impedances of two basic simple structures—that of *a cavity* and that of *a step*—are studied in detail. The transition from the regime of a cavity to the regime of a step is explained, an approximate formula describing this transition is given, and the criterion for determining the applicability of each regime is established. The asymptotic behavior of the impedance for a finite number M of periodically arranged cavities as a function of M is studied. The difference in the behavior of the impedance for a single cavity and that for an infinite number of cavities is explained as the result of the interference of the diffracted waves. A criterion for determining the transition in the impedance behavior from small M to large M is presented.

CONTENTS

LIST OF SYMBOLS

Throughout the paper, boldface letters denote vectors.

Latin letters

$A(p)$	expansion coefficients
A_{LN}^{nl}	coefficients of Eq. (4.23)
a	beam pipe radius
$\mathbf{a}$	transverse vector defining an offset of a bunch
$B_n^{\pm}$	expansion coefficients
B_p	expansion coefficients
b	beam pipe radius
c	velocity of light
d	beam pipe radius
$d_n^{\pm}$	expansion coefficients
$\mathbf{E}(\mathbf{r},t)$	electric field
$\mathbf{E}_\omega(z,\mathbf{r},\theta)$	Fourier harmonic of the electric field
$\mathbf{E}_m$	azimuthal harmonic for mth mode
$E_m^{(\pm)}(k,r)$	azimuthal harmonics for mth mode
$\mathcal{E}$	particle energy
$\Delta\mathcal{E}$	energy loss
e	particle charge
$G_k(\mathbf{r},\mathbf{r}')$	time Fourier harmonic of the Green's function
$\hat{G}_{kp}(r,r')$	space Fourier harmonic of the Green's function
$G_1(r,d)$	$=K_1(\tau r)+I_1(\tau r)K_0(\tau d)/I_0(\tau d)$
$G_0(r,d)$	$=K_0(\tau r)-I_0(\tau r)K_0(\tau d)/I_0(\tau d)$
g	cavity gap
$\tilde{g}$	$=g/2b$
g_1	taper length
$\mathbf{H}(\mathbf{r},t)$	magnetic field
$\mathbf{H}_\omega(z,\mathbf{r},\theta)$	Fourier harmonic of the magnetic field

H_m	Hankel functions of the first kind of the mth order
I_m	modified Bessel function of the first kind of the mth order
J_m	Bessel functions of the first kind of the mth order
$\mathbf{j}_\omega$	Fourier harmonic of the current density
K_m	modified Bessel functions of the second kind of the mth order
k	$=\omega/c$, wave number
$\tilde{k}$	$=kb$
Δk	averaging interval of wave numbers
δk	difference between neighboring resonance frequencies
L	length of variation of the cavity shape
L	longitudinal period of a periodic structure
M	number of cavities in an array
m	azimuthal mode number; e.g., monopole $m=0$, dipole $m=1$, etc.
N	$=0,1,\ldots,M-1$, cavity number in an array
n_0	the integer closest to $\tilde{k}$
$\mathbf{n}$	the unit vector normal to the surface
P_L^l	right-hand sides of Eq. (4.23)
p_i	$=a_i/b$, $i=1,2$
Q	$=qk/\pi c\gamma^2\beta^2$
Q_λ	quality factor of a mode λ
q	$=eN$, total charge of a bunch
R	$=\lvert\mathbf{r}-\mathbf{r}'\rvert$ $=\sqrt{(z-z')^2+r^2+r'^2-2rr'\cos\theta}$
R_λ	shunt impedance of a mode λ
r_0	bunch offset
$\mathbf{r}$	transverse offset of the trailing particle
$r_b(z)$	equation for a boundary in the (r,z) plane
S	surface
$d\mathbf{S}$	$=\mathbf{n}\,dS$, surface element
s	distance inside a bunch
s_B	bunch spacing
t	time
U_λ	energy stored in a mode λ
dV	volume element
V_λ	eigenfunctions of a mode λ
$\mathbf{v}$	particle velocity
W	total field energy
$w_l(s)$	longitudinal point wake function
$w_\perp(s,\mathbf{r})$	transverse point wake function
w_l^R	longitudinal resistive point wake function
$w_\perp^R$	transverse resistive point wake function
x_n,t_n,y_n,z_n	normalized expansion coefficients
Y_m	Bessel functions of the second kind of the mth order
Z_l^R	longitudinal resistive impedance
$Z_\perp^R$	transverse resistive impedance
$Z_{\rm cav}(k)$	the impedance of a cavity
$Z_{\rm coll}(k)$	the impedance of a collimator
$Z_{\rm in}(k)$	the impedance of a step-in
$Z_{\rm out}(k)$	the impedance of a step-out
Z_T	longitudinal impedance of a taper
$Z_l(\omega,\mathbf{r})$	longitudinal impedance
$Z_\perp(\omega,\mathbf{r})$	transverse impedance
Z_0	$=4\pi/c\equiv 377\ \Omega$
Z_1	real part of the impedance
Z_2	imaginary part of the impedance
$Z_l^{\rm NB}$	narrow-band longitudinal impedance
$Z_\perp^{\rm NB}$	narrow-band transverse impedance

Greek letters

α_P^2	$=(2\pi ap/L)^2+4\pi ka^2p/L$
β	$=v/c$ relative particle velocity
γ	$=\mathcal{E}/mc^2$, Lorentz factor
γ_λ	resonance width of a mode λ
γ_{nm}	resonance width of a mode nm
$\delta(r)$	the Dirac's radial δ function
$\vartheta(x)$	step function, $\vartheta(x)=1$ for $x>0$, $\vartheta(x)=0$ for $x<0$.
ζ_n	effective surface impedance
ζ_N	local distance in the Nth cavity
η	parameter of a transition from a cavity regime to a step regime
κ_l	longitudinal loss factor
κ_λ^l	loss factor of a mode λ
$\kappa_{\rm in}^l$	loss factor of a step-in
$\kappa_{\rm out}^l$	loss factor of a step-out
$\kappa_\perp$	transverse loss factor
λ_n	$=n\pi/g$
λ_{dn}	$=\sqrt{k^2-\nu_n^2/d^2}$, $\mathrm{Im}\lambda_{dn}>0$
$\tilde{\lambda}_d$	$=\sqrt{\tilde{k}^2-\nu_n^2}$
μ_n	$=b\sqrt{k^2-\lambda_n^2}$
μ	$=gk/2$
ν_n	nth root of J_0, $\nu_1<\nu_2<\cdots<\nu_\infty$
χ_n	$=g\lambda_{bn}/2$
χ_p	$=a\Omega$
$\rho(s,\mathbf{r})$	normalized longitudinal charge density

ρ_ω	Fourier component of the charge density
σ	rms bunch length
$\sigma_\perp$	transverse rms size of a bunch
σ_R	resistivity
τ	$=k/\gamma\beta$
Ω	$=\sqrt{k^2-p^2+2ik\varepsilon}$, $\varepsilon\to 0$
ω_λ	frequency of a mode λ
$\omega_{c.o.}$	$\simeq c/a$ cutoff frequency
∇^2	the Laplace operator
$o(\varepsilon)$	terms of the order of ε

I. INTRODUCTION

The major problem of accelerator physics today is to increase the stored beam current. This is important for both existing and future high-energy accelerators, since the rate of events in experiments with high-energy particles drops with the energy $\mathcal{E}$ and increasing the beam current improves the yield.

The current stored in a modern high-energy accelerator is limited by collective instabilities (provided, of course, that the single-particle motion is stable, as is the case for all accelerators). Collective instabilities could arise either from direct electromagnetic (EM) interaction of particles in the same bunch or, indirectly, since a particle beam in an accelerator generates an electromagnetic field while passing through discontinuities and variations in the cross-sectional shape of the vacuum chamber.

Direct interaction between relativistic particles of the same bunch on a straight trajectory becomes negligible with the energy increase, since the Coulomb repulsion between the particles is compensated with an accuracy $1/\gamma^2 \ll 1$, $\gamma=\mathcal{E}/mc^2$ by their magnetic attraction. All the space charge effects [such as the Laslett tune shift (Laslett, 1963)] which are dominant at low particle energies, can be disregarded as $\gamma\to\infty$. The interaction of particles on a bend trajectory comprises a very interesting subject (Talman, 1986) but will not be considered in the present paper (see also Keil, 1985; Piwinski, 1985; Bassetti and Brandt, 1986; Channell, 1986; Lee, 1990).

Stability of the ultrarelativistic particle motion depends mostly (apart from the beam-beam interaction) on the interaction of the particle with electromagnetic *wakefields* generated in accelerator structures by the particles moving ahead of it. The wakefields in turn interact with the particles and may cause such collective effects as single- and multibunch collective instabilities, bunch lengthening, increase in the bunch energy spread, its emittance growth, etc. (Gygi-Hanney, 1983; Zisman *et al.*, 1986). The discussion of the collective effects can be found, for example, in the papers by Hoffman (1976), Chao (1982, 1983), and Pellegrini (1982). The properties of the wakefields and the methods for their calculation in the ultrarelativistic limit $\gamma\to\infty$ are the subject of the present paper.

The wakefield can be considered as a linear response of the system to an external excitation produced in our case by a beam current. In general, the response may be expressed in terms of a Green's function. However, in most cases it is sufficient to consider the average effect of the accelerator structure: an energy loss of a particle and a transverse abrupt change in the particle momenta ("kick"), which a particle experiences when passing through the structure. *Wake functions* describe such average effects of an accelerator structure. They depend both on the beam current distribution in the bunch and on the properties of the beam environment.

To find *the bunch wake function* excited in a given structure by *a bunch* of particles, it appears very helpful first to find *the point wake function* excited in it by *a point charge.* After the point wake function is found, the bunch wake function can be determined by its convolution with the charge distribution. Finding the point wake function requires study of the propagation, diffraction and interference of the radiated EM waves.

In general, the point wake function has three components. In what follows, we distinguish between two types of point wake functions:

(1) The *longitudinal* point wake function, i.e., its projection on the axis of the structure.

(2) The *transverse* point wake function, the two dimensional vector perpendicular to the axis of the structure.

The point wake function describes the interaction of a particle with its environment in the time domain (Bane *et al.*, 1984). The same interaction can also be described in the frequency domain by the Fourier transform of the point wake function—*the coupling impedance* (Bane and Wilson, 1980; Wilson, 1982). Correspondingly, in what follows we consider the *longitudinal* and *transverse* impedances.

The range of frequencies ω studied in the present paper extends up to some high-frequency which is well above the cutoff frequency of the beam pipe of radius a, but at the same time, such that the corresponding dimensionless wave number is still small in comparison to the particle Lorentz factor: $1\ll\omega a/c\ll\gamma$. This range is sufficient for studying the stability of the shortest bunches used in or designed for modern accelerators. Below the cutoff frequency, impedance is defined by a few eigenmodes and can easily be found by means of existing numerical codes. For $\omega > c\gamma/a$ the impedance falls off exponentially.

From its definition it is clear that the coupling impedance is a property of the beam environment, but not of the beam itself. This is the main advantage of the coupling impedance concept. The real (resistive) part of the longitudinal impedance describes the energy loss. The imaginary part of the impedance is responsible for an incoherent tune shift and bunch lengthening. If the frequency shifts of any two low-order synchrotron modes lead to the degeneracy, transverse mode coupling (also called fast head-tail instability) occurs. Other instabilities, such as the microwave longitudinal instability and transverse fast blowup instability, depend on the absolute value of the impedance. It is worthwhile to mention that single bunch instabilities are due to *the high-frequency*

impedance, whereas the multibunch instabilities depend on the low-frequency *narrow-band* impedance.

The narrow-band impedance may be described as a sum of narrow resonances. Each resonance is produced by a localized mode whose frequency is below or not much above the cutoff frequency of openings present in the structure. In the time domain, this corresponds to a slow-decaying oscillating wake function. In the high-frequency region, well above the cutoff frequency, the resonances overlap producing a smooth frequency dependence of the impedance. In the time domain, this defines the short-range behavior of the wake function.

The high-frequency impedance describes interaction of particles due to the presence of abrupt changes of the beam-pipe cross section as well as high-frequency tails of resonant structures such as RF cavities, bellows, vacuum ports, etc. It is significant if the bunch length is small in comparison to the beam-pipe radius. Until recently the bunch length in all accelerators has been larger than the beam-pipe radius, and consequently the detailed behavior of the high-frequency impedance was not of a major concern. It was usually approximated by single broad resonance parameters that were estimated from an experiment. This model of the high-frequency impedance is usually referred to as *a broadband impedance* (Hofmann and Zotter, 1989). However, the new generation of accelerators, such as high-energy colliders, synchrotron light sources, storage rings designed to yield large numbers of mesons (ϕ and B factories), etc., utilizes very short bunches. In this case, the energy loss is largely defined by the high-frequency impedance. That makes desirable a careful analytic analysis of the high-frequency behavior of the longitudinal impedance (Bisognano, 1990a). Our paper emphasizes this subject.

We restrict ourselves to theoretical methods and results for the impedance, and do not discuss measurement techniques or purely numerical methods of the impedance calculations.

The impedance of a given structure can be measured on a test bench either by using a small dielectric probe and then interpreting the results according to the Slatter (1950) theory, or by using a short current pulse sent through a wire (Sands and Rees, 1975; Gluckstern and Li, 1990). The impedance of the whole accelerator can be estimated from measurements of bunch lengthening, the coherent tune shifts, etc. We refer the reader to the lectures by Lambertson (1989) and by Palumbo and Vaccaro (1989) on this subject.

Numerical calculation of the point wake function is not a simple task due to the singularity of the charge distribution. Numerical methods are more appropriate for finding the bunch wake functions for nonsingular charge distributions (Weiland, 1980, 1982). They are also the only methods applicable to complex structures. Nevertheless, such calculations require significant time even with the most advanced computers.

A more conventional method consists of finding the impedance and using its inverse Fourier transformation to find the point wake function. Clearly, the utilization of this method demands knowing the impedance up to very high frequencies.

Direct numerical calculation of the impedance similarly faces difficulties from the enormous number of resonance contributions that should be taken into account (Wang and Zotter, 1989), which justifies development of the analytical and semianalytical methods described in the present paper. Such methods not only provide useful formulas for estimating the impedance but also give insight into the physics of the wakefield generation.

Whenever possible we check our results by the numerical code TBCI (Weiland, 1983a), which allows one to calculate the bunch wake functions in the time domain. Another useful code existing for this purpose is ABCI (Chin, 1988).

Throughout our discussion we assume that the particle energy is constant and does not change as the result of the radiation in the structure. We will also neglect small oscillations of a particle moving in an accelerator. In other words, we assume that the vector of the particle velocity $\mathbf{v}$ is constant (at least while traveling through the structure under consideration) and is directed parallel to the axis of the structure, which is the z axis in the coordinate system we have chosen. The particular case of a beam circulating in a toroidal cavity where $|\mathbf{v}|=$constant is considered in papers by Warnock and Morton (1988, 1990), Ng (1988, 1990), and Ng and Warnock (1989).

We also neglect the resistivity of the metal walls (exception in Sec. II.D). In the ultrarelativistic limit, the resistive corrections are negligibly small and are outside the scope of the present paper. The assumption of superconductivity allows us to impose simple boundary conditions on the EM field, which substantially simplify our derivations.

The main objective of the present paper is to review properties of the point wake function (in the time domain) or, equivalently, the behavior of the coupling impedance (in the frequency domain). The remainder of the paper is organized as follows: The basic concepts are defined in Sec. II. In Section III several general theorems concerning the impedances are stated. Here we give the Panofsky-Wenzel (1956) relation of the transverse and longitudinal point wake functions, and consequently the relation of the transverse and longitudinal impedances. We then present the radial dependence of impedance modes due to Weiland (1983b). Two useful results follow. One is an expression of the impedance in the high-frequency region in terms of low-frequency eigenmodes; the other is a proof of the independence of the impedance on the direction of the bunch motion along $\pm z$.

Section IV is devoted to evaluation of the narrow-band impedance for a step, a cavity, and a collimator using the field matching technique. A perturbation method is developed which simplifies calculations, and a hypothesis explaining the appearance of trapped modes is suggested.

In Sec. V, a simple diffraction approach for evaluating the high-frequency impedance is developed. For two

structures for which exact methods exist and the impedances are known, this simple approach is shown to give correct results.

In the last section (Sec. VI), we present some analytical calculations of the high-frequency impedance. This can only be done in limited, cylindrically symmetric simple cases, such as a cavity or a step in a waveguide cross section. Nevertheless, there are several reasons to consider these cases analytically.

- First, analytical considerations help us to better understand the details of the radiation process.
- Second, analytical results complement the purely numerical results of existing codes, and provide an answer in parameter regions where existing codes have difficulties.
- Third, analytical results for a cavity and for a step are interesting in themselves. Sometimes, other more complicated structures can be considered as combinations of cavities and steps. A good approximation for the coupling impedance of such a structure could be a sum of contributions of its parts. Solutions for several interesting structures can be obtained from the two cases studied here. For example, a cylindrical pipe of radius a ending with an infinite flange is a special case of a step in a pipe cross section from radius a to radius b in the limit as $b \to \infty$.

Due to the immensity of the field, we do not pretend to present here a comprehensive description of all the results obtained up to now. Neither were we able to mention all the papers relevant to our subject. Our aim was to give a rather representative list which will provide a reader with an introduction to the present status of the field. We regret, if by our oversight, some work was not referred to.

II. BASIC DEFINITIONS

A. The longitudinal impedance

The longitudinal point wake function w_l is defined as the energy loss $\Delta\mathcal{E}_1$ of a test particle with charge e, that follows, at a distance s, a pointlike bunch having total charge $q=eN$ (Bane and Wilson, 1980; Bane 1986):

$$\Delta\mathcal{E}_1 \equiv eqw_l(s) \ . \tag{2.1}$$

If the electric field $\mathbf{E}$ excited by the charge q is known, then the point wake function can be found by integrating the instantaneous work[1] produced by the field on a trailing ultrarelativistic particle with an offset $\mathbf{r}$:

$$w_l(s,\mathbf{r}) \equiv -\frac{1}{q}\int_{-\infty}^{\infty} dt\ \mathbf{v}\cdot\mathbf{E}(z,\mathbf{r},t)|_{z=vt-s}, \quad v\approx c \ . \tag{2.2}$$

Note that the field $\mathbf{E}(z,\mathbf{r},t)$ *does not* include the self-interaction of the particle. The radiated part of the field satisfies the homogeneous wave equation and the radiation condition $|\mathbf{E}|\to 0$ as $z\to\pm\infty$ (Jackson, 1975).

Equations (2.1) and (2.2) can also be derived by considering the energy flow of the EM field. The field of a particle moving along the axis z of a smooth pipe has only two nonzero components: the radial electric E_r and the azimuthal magnetic H_θ. The energy flow described by the Poynting vector $\mathbf{P}\sim\mathbf{E}\times\mathbf{H}$ is directed along the axis z and remains constant. There is no energy loss in this case. The field of a particle changes at a discontinuity of the vacuum pipe causing the energy loss. In the first approximation, the loss is given by the product of the z component of the electric field E_z at the discontinuity and the unperturbed azimuthal component H_θ. This gives a nonzero radial energy flux, producing Eqs. (2.1) and (2.2).

In general, the radiated field depends on the transverse offsets of both the trailing and the leading particles. The dependence on the transverse offset of the trailing particle $\mathbf{r}$ is explicitly indicated in Eq. (2.2).

We define the Fourier harmonic of a function $f(t)$ by

$$f(\omega) \equiv \int_{-\infty}^{\infty} dt\, f(t) e^{i\omega t} \ . \tag{2.3}$$

The longitudinal impedance $Z_l(\omega,\mathbf{r})$ is defined as a Fourier harmonic of the point wake function:

$$Z_l(\omega,\mathbf{r}) \equiv \frac{1}{v}\int_{-\infty}^{\infty} ds\, w_l(s,\mathbf{r}) e^{i\omega s/v} \ . \tag{2.4}$$

If the particle velocity has only the longitudinal component v_z, the longitudinal impedance is expressed in terms of the Fourier harmonic of the longitudinal electric field:

$$Z_l(\omega,\mathbf{r}) \equiv -\frac{1}{q}\int_{-\infty}^{\infty} dz\, E_{z\omega}(z,\mathbf{r}) e^{-i\omega z/v} \ . \tag{2.5}$$

For a single bunch, the energy loss κ_l per particle averaged over the particle distribution in the bunch is given by the convolution of the point wake function with the normalized longitudinal particle density $\rho(s,\mathbf{r})$ $\int ds\, d\mathbf{r}\, \rho(s,\mathbf{r})=1$:

$$\kappa_l \equiv \langle w_l(s)\rangle = \int d_1 d\mathbf{r}_1 ds_2 d\mathbf{r}_2 \rho(s_1,\mathbf{r}_1) \times \rho(s_2,\mathbf{r}_2) w_l(s_1-s_2,\mathbf{r}_1,\mathbf{r}_2) \ . \tag{2.6}$$

In the case when the transverse dimensions of the bunch are small, $\rho(s,\mathbf{r})$ can be approximated by $\rho(s)\delta(\mathbf{r})$ and the loss factor is

$$\kappa_l = \frac{1}{2\pi}\int d\omega\, Z_l(\omega)|\hat{\rho}(\omega)|^2 \ . \tag{2.7}$$

Here $Z_l(\omega)\equiv Z_l(\omega,0)$ and $\hat{\rho}(\omega)$ is the Fourier harmonic of $\rho(s)$.

For a particular case of a Gaussian longitudinal distri-

[1]The dimensions of the longitudinal wake function are V/C (volt per Coulomb) in the MKS system and 1/cm in the CGS system. For this reason we chose not to call this quantity the wake potential as is usually done. Correspondingly, dimensions of the longitudinal impedance in these systems are Ω (ohm) in the MKS system and sec/cm in the CGS system.

bution of the bunch density with the rms length σ

$$\rho(s)=\frac{1}{\sqrt{2\pi\sigma^2}}e^{-s^2/2\sigma^2}\ , \tag{2.8}$$

its Fourier harmonic is real

$$\hat{\rho}(\omega)=e^{-\omega^2\sigma^2/2c^2}\ , \tag{2.9}$$

and there is no need to take the absolute value in Eq. (2.7).

For resonance structures such as radio frequency (RF) resonators, cavities, etc., the impedance has narrow maxima at the resonance frequencies. Hence, the *narrow-band* impedance may be represented by the sum of resonances:

$$Z_l^{\rm NB}(\omega)=i\sum_\lambda \kappa_\lambda^l\left[\frac{1}{\omega-\omega_\lambda+i\gamma_\lambda}+\frac{1}{\omega+\omega_\lambda+i\gamma_\lambda}\right]\ , \tag{2.10}$$

where ω_λ, γ_λ and κ_λ^l are the frequencies, widths, and loss factors of the λth resonance, respectively. In the complex ω plane these parameters define the positions of the poles and their residues. Equation (2.10) is usually written in the form

$$Z_l^{\rm NB}(\omega)=\sum_\lambda \frac{R_\lambda}{1+iQ_\lambda(\omega_\lambda/\omega-\omega/\omega_\lambda)}\ , \tag{2.11}$$

where κ_λ^l and γ_λ are related to the shunt impedance R_λ and the quality factor Q_λ:

$$\kappa_\lambda^l=\frac{\omega_\lambda R_\lambda}{2Q_\lambda},\quad \gamma_\lambda^l=\frac{\omega_\lambda}{2Q_\lambda}\ . \tag{2.12}$$

For example, for the fundamental mode of a typical RF resonator $(R/Q)_0\approx 200\ \Omega$, and for $\omega_0\approx 500$ MHz, the loss factor $\kappa_0^1\approx 0.35\ {\rm cm}^{-1}$.[2] In the time domain, the point wake function which corresponds to the narrow-band impedance Eq. (2.10) is

$$w_l(s)=2\sum_\lambda \kappa_\lambda^l\cos(\omega_\lambda s/v)e^{-\omega_\lambda s/2Q_\lambda v},\quad s>0\ . \tag{2.13}$$

The action of a bunch on a trailing particle at some distance s is dominated by a few low-frequency higher-order modes (HOM). On the other hand, for $s=0$ (Wilson, 1978)

$$w_l(0)=\sum_\lambda \kappa_\lambda^l\ . \tag{2.14}$$

The seeming discrepancy of this formula with Eq. (2.13) is a consequence of the *fundamental theorem of beam loading* (Wilson, 1978). The factor $\frac{1}{2}$ appears from the fact that a particle is subject to the wake function produced only by the charge preceding it and, hence, "feels" on average $\frac{1}{2}$ of its own charge. Since there is no EM field in front of an ultrarelativistic particle, it follows from the causality principle that $w_l(s)=0$ for $s<0$.

The energy loss per particle into a single mode λ of an infinitely short bunch is

$$\Delta\mathcal{E}_\lambda/N=e^2\kappa_\lambda^l\ . \tag{2.15}$$

The loss factor κ_λ^l can be expressed (Wilson, 1978) in terms of the eigenfunction E_z^λ corresponding to the mode λ:

$$\kappa_\lambda^l=\frac{|V_\lambda|^2}{4U_\lambda}\ , \tag{2.16}$$

where

$$V_\lambda=\int dz E_z^\lambda(z)e^{-i\omega z/v} \tag{2.17}$$

and U_λ is the energy stored in the mode λ.

In practice, the loss factors and the resonance frequencies of the low modes are found numerically using a suitable computer code such as URMEL (Weiland, 1983c), SUPERFISH (Halbach and Holsinger, 1976), AMOS (DeFord *et al.*, 1989) or others for two-dimensional (2D) structures. For 3D calculations one can use code MAFIA (Klatt *et al.*, 1986), ARGUS (Mankofsky, 1988) or MAGIC (Coplen *et al.*, 1988).

In the case when the bunch wake functions are excited by a train of equidistant bunches with the bunch spacing s_B, the interference of the fields excited in the same structure by different bunches of the train has to be taken into account (Wilson, 1982). The loss factor of a given mode in the limit $v\to c$ should be multiplied by a factor $F(k_\lambda s_B/2Q_\lambda, k_\lambda s_B)$, where $k_\lambda=\omega_\lambda/c$ and Q_λ are the mode wave number and the quality factor, respectively. The function F of two arguments is

$$F(x,y)\equiv\frac{\sinh x}{\cosh x-\cos y}\ . \tag{2.18}$$

If $Q_\lambda\gg 1$ and the condition for the resonance excitation $k_\lambda s_B=2\pi n$, n an integer, is fulfilled, the loss factor can be substantially enhanced, i.e.,

$$F\sim 4Q_\lambda/2\pi n\ . \tag{2.19}$$

Modal analysis is an effective way to calculate the impedance for frequencies below or comparable to the cutoff frequency $\omega_{\rm c.o.}\sim c/a$, where a is the beam-pipe radius. For higher frequencies, the density of the resonances increases. In addition, since such an EM field may propagate in the beam pipe, the widths of the resonances get large. In this case the impedance as a function of the frequency becomes extremely complicated. Observable effects though, can always be described by an expression containing the convolution of the impedance with the spectral density of the bunch. Hence, only the average impedance plays a role. Such a *high-frequency impedance* is a smooth function of the frequency.

[2]Sometimes the loss factor is expressed in the units of volts per picocoulomb (V/pC), 1 V/pC$=1.11\ {\rm cm}^{-1}$.

B. The transverse impedance

The particle moving in a cylindrically symmetric structure that is uniform in the longitudinal direction with an offset, generates transverse EM field propagating with the particle. However, in the ultrarelativistic case, the transverse electric and magnetic forces cancel each other and, hence, the net transverse kick in this case is zero. Any distribution of the uniformity demotes this balance, and a particle experiences transverse force which depends on both the bunch and the particle offsets. For a small magnitude of the bunch offset r_0, the transverse EM field is proportional to r_0. The dependence on the bunch offset can be removed from all the expressions by dividing them by r_0. The conventional definition of the transverse wake function is done in this way. The price for this is different dimensions of the respective transverse and longitudinal wake functions, loss factors, and impedances.

Correspondingly, the transverse point wake function is defined as the integrated transverse kick caused by the transverse component of the radiated field divided by the bunch offset r_0:

$$w_\perp(s,\mathbf{r})\equiv-\frac{1}{qr_0}\int_{-\infty}^{\infty}dz\left[\mathbf{E}+\frac{\mathbf{v}}{c}\times\mathbf{H}\right]_\perp(z,\mathbf{r},t)|_{t=(z+s)/v}\ . \tag{2.20}$$

The transverse impedance $Z_\perp(\omega)$ is defined as the ωth Fourier harmonic of $-iw_\perp$:

$$Z_\perp(\omega,\mathbf{r})=-\frac{i}{v}\int_{-\infty}^{\infty}ds\,w_\perp(s,\mathbf{r})e^{i\omega s/v}\ , \tag{2.21}$$

or, cf. Eq. (2.5),

$$Z_\perp(\omega,\mathbf{r})=-\frac{i}{qr_0}\int_{-\infty}^{\infty}dz\left[\mathbf{E}_\omega+\frac{\mathbf{v}}{c}\times\mathbf{H}_\omega\right]_\perp e^{-i\omega z/v}\ . \tag{2.22}$$

The transverse loss factor is defined analogously to Eq. (2.7):

$$\kappa_\perp\equiv\langle w_\perp\rangle=\frac{i}{2\pi}\int d\omega|\hat{\rho}(\omega)|^2Z_\perp(\omega)\ . \tag{2.23}$$

Here $Z_\perp(\omega)\equiv Z_\perp(\omega,0)$.

The transverse narrow-band impedance can be represented by a sum over the pole terms:

$$Z_\perp^{\mathrm{NB}}(\omega)=i\sum_\lambda\kappa_\lambda^\perp\left[\frac{1}{\omega-\omega_\lambda+i\gamma_\lambda}-\frac{1}{\omega+\omega_\lambda+i\gamma_\lambda}\right]\ . \tag{2.24}$$

That gives the transverse point wake function

$$w_\perp(s)=2\sum_\lambda\kappa_\lambda^\perp\sin(\omega_\lambda s/v)e^{-\omega_\lambda s/2Q_\lambda v},\quad s>0\ . \tag{2.25}$$

Similarly to Eq. (2.16), the transverse loss factors $\kappa_\lambda^\perp$ can also be expressed (Bane, 1980; Bane *et al.*, 1984) in terms of the eigenfunctions V_λ:

$$\kappa_\lambda^\perp=\frac{c}{\omega_\lambda r_0}\frac{V_\lambda^*\nabla_\perp V_\lambda}{U_\lambda}\ , \tag{2.26}$$

where $\nabla_\perp$ means the derivative over r.

C. The loss factor for a step

To illustrate the concept of a longitudinal loss factor, we estimate it here for a simple example of an abrupt change in the cross section of a circular waveguide from radius a to radius b (a "step") (see Fig. 1).

We start by considering a particle moving in free space. It is convenient to direct the x axis along the particle trajectory. For an ultrarelativistic particle, a good approximation for the nonzero components of the field in the region $r<\gamma/k$ is

$$E_{\omega r}=\frac{2q}{cr}e^{ikz}\ , \tag{2.27}$$

$$H_{\omega\theta}=\frac{2q}{cr}e^{ikz}\ . \tag{2.28}$$

The field propagates synchronously with the charge. In the region $kr>\beta\gamma$ the field is exponentially small. The total field energy of the charge is given by

$$\begin{aligned}W&=2\pi\int_{-\infty}^{\infty}dt\int_0^{\infty}r\,dr\frac{c}{4\pi}(\mathbf{E}\times\mathbf{H})_z\\&=-2\pi c\int_{r_{\min}}^{\infty}r\,dr\int_0^{c\gamma/r}d\omega|E_{\omega r}|^2\ .\end{aligned} \tag{2.29}$$

Using the field from Eq. (2.27), the integral diverges at small r:

$$W\simeq\frac{q^2\gamma}{r_{\min}}\ . \tag{2.30}$$

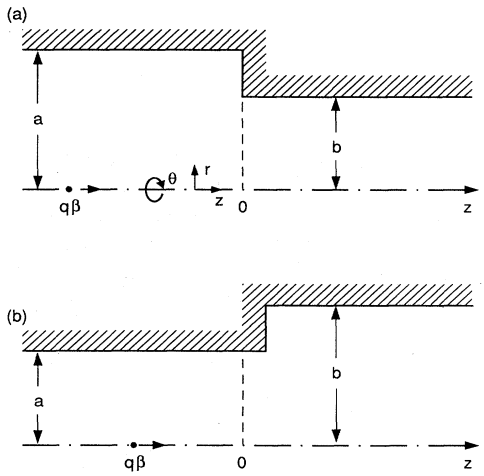

FIG. 1. Geometry of the waveguide cross section step and the coordinate system; (a) incoming charge, (b) outgoing charge.

(If $r_{\min}$ is the classical electron radius e^2/mc^2 the energy of the synchronous component of the field W is of the order of the energy of a particle $\mathcal{E}$: $W \simeq \mathcal{E}$, and it actually depends on the definition of the electron mass and the charge of a particle. For a rigid bunch of N particles the contribution of all particles

$$|E_{\omega r}|^2 = \left[\frac{2q}{cr}\right]^2 \sum_{i,j} e^{ik(z_i - z_j)} \tag{2.31}$$

can be found replacing the sum of the integral over the normalized distribution function $\rho(z)$:

$$|E_{\omega r}|^2 = \left[\frac{2Ne}{cr}\right]^2 \int dz_1 dz_2 \rho(z_1)\rho(z_2) e^{ik(z_1 - z_2)} . \tag{2.32}$$

For a Gaussian bunch with the rms length σ the energy per particle is

$$W = \frac{Ne^2}{\sqrt{\pi}\sigma} \ln \frac{\gamma\sigma}{r_{\min}} . \tag{2.33}$$

Consider now a particle moving in a circular waveguide of radius a. For $\gamma\sigma > a$ the energy of the synchronous component of the field moving with the particle is

$$W(a) = \frac{Ne^2}{\sqrt{\pi}\sigma} \ln \frac{a}{r_{\min}} . \tag{2.34}$$

Suppose now that the particle passes through an abrupt change of the pipe cross section. Then the change to the energy of the synchronous component of the field ΔW is the difference $W(a) - W(b)$:

$$\Delta W = \frac{Ne^2}{\sqrt{\pi}\sigma} \ln \frac{b}{a} . \tag{2.35}$$

We must distinguish two cases: a particle entering a narrowing pipe (a "step-in") and a particle exiting into a broadening pipe (a "step-out"). The energy loss in these two cases is defined by the term ΔW and the radiated energy $\Delta\mathcal{E}_{\text{rad}}$:

$$\kappa^l_{\text{in}} = \Delta\mathcal{E}_{\text{rad}} - \Delta W , \tag{2.36}$$

$$\kappa^l_{\text{out}} = \Delta\mathcal{E}_{\text{rad}} + \Delta W . \tag{2.37}$$

For the step-in case, the radiation propagates in the opposite direction with respect to the particle motion. Hence, the interaction of the field with the particle is small, $\kappa^l_{\text{in}} \approx 0$. The energy of the radiation is taken out from the synchronous component of the field: $\Delta\mathcal{E}_{\text{rad}} \approx \Delta W$. From Eq. (2.37) for the step-out case, we obtain

$$\kappa^l_{\text{out}} = 2\Delta W = \frac{2Ne^2}{\sqrt{\pi}\sigma} \ln \frac{b}{a} . \tag{2.38}$$

More accurate calculation shows that κ^l_{in} is not exactly zero, but has a small negative value. That corresponds to the gain of energy (Kheifets and Heifets, 1986a; Chan and Schweinfurth, 1987) that can be interpreted as the attraction by the image charge. Respectively, κ^l_{out} is less than given by Eq. (2.38). Nevertheless, the difference is always the constant

$$\kappa^l_{\text{out}} - \kappa^l_{\text{in}} = 2\Delta W = \frac{2Ne^2}{\sqrt{\pi}\sigma} \ln \frac{b}{a} . \tag{2.39}$$

Since below the cutoff frequency of a pipe no radiation occurs, $\Delta\mathcal{E}_{\text{rad}} = 0$, for a long bunch $\sigma > a$ it follows from Eqs. (2.36) and (2.37) that $\kappa^l_{\text{in}} = -\Delta W$ and $\kappa^l_{\text{out}} = \Delta W$; i.e., the absolute value of the energy loss or gain ΔW in such a case equals half the value of the energy loss κ^l_{out} for a step-out. The above consideration for the energy loss is also applicable to the longitudinal impedance; see Sec. IV.C.

D. The resistive wall impedance

One particular source of the high-frequency impedance is the resistivity of the beam-pipe walls. Although the effects of the resistivity in the ultrarelativistic case are small and neglected in the present paper, we give here formulas for the point wake functions and the impedances for comparison with those produced by discontinuities of the waveguide.

The longitudinal point wake function generated by the image current flowing in the wall of radius a with the resistivity σ_R decays asymptotically with the distance s behind the leading particle as $s^{-3/2}$ (Morton *et al.*, 1966; Chao, 1982);

$$w_l^R(s) = \frac{1}{2\pi a}\left[\frac{c}{\sigma_R}\right]^{1/2}\left[\frac{1}{s}\right]^{3/2} \quad \text{for } s > 0 . \tag{2.40}$$

The corresponding resistive impedance per unit length is inductive and increases with frequency:

$$Z_l^R = (1-i)\frac{Z_0}{4\pi a}\left[\frac{\omega}{2\pi\sigma_R}\right]^{1/2} . \tag{2.41}$$

Here $Z_0 = 4\pi/c \equiv 377\ \Omega$.

Similarly, the transverse point wake function decays asymptotically with the distance s behind the leading particle as $s^{-1/2}$:

$$w_\perp^R = \frac{1}{\pi a^3}\left[\frac{c}{\sigma_R s}\right]^{1/2} \quad \text{for } s > 0 . \tag{2.42}$$

The corresponding resistive impedance per unit length decreases with frequency:

$$Z_\perp^R = (1-i)\frac{1}{a^3}\left[\frac{1}{2\pi\sigma_R\omega}\right]^{1/2} . \tag{2.43}$$

III. SOME GENERAL THEOREMS

In this section we discuss several useful general statements regarding the coupling impedances.

A. The Panofsky-Wenzel theorem

The Panofsky-Wenzel theorem (Panofsky and Wenzel, 1956) gives the relation between the longitudinal and transverse point wake functions:

$$\frac{\partial w_\perp(s,\mathbf{r})}{\partial s}=\frac{1}{r_0}\nabla_\perp w_l(s,\mathbf{r}) . \tag{3.1}$$

This relationship follows directly from the definitions of Eqs. (2.2), (2.20), and Maxwell's equation $ik\mathbf{H}=\nabla\times\mathbf{E}$, provided that transverse components of the radiated field are zero at infinity:

$$\lim\mathbf{E}_\perp(z,\mathbf{r},t)=0 \quad \text{as } z\to\pm\infty . \tag{3.2}$$

By applying the Fourier transformation in the longitudinal coordinate s to both sides of Eq. (3.1), one obtains the expression for the transverse impedance in terms of the transverse gradient of the longitudinal impedance:

$$Z_\perp(s,\mathbf{r})=\frac{v}{\omega r_0}\nabla_\perp Z_l(s,\mathbf{r}) . \tag{3.3}$$

B. The radial dependence of the impedance

For *cylindrically symmetric* structures the radial dependence of the coupling impedances *in the ultrarelativistic case* is found explicitly by Weiland (1983b). To obtain his result, note that the radiated part of EM field satisfies the homogeneous wave equation. For its Fourier harmonic $\mathbf{E}_\omega$, the equation is

$$\nabla^2\mathbf{E}_\omega+k^2\mathbf{E}_\omega=0, \quad k=\omega/c . \tag{3.4}$$

The synchronous component of the field, i.e., the component whose phase velocity equals the velocity c of the particle, is then defined as follows:

$$\mathbf{E}_k(r,\theta)\equiv\int_{-\infty}^{\infty}dz\,\mathbf{E}_\omega(z,r,\theta)e^{-ikz} . \tag{3.5}$$

The boundary conditions for $\mathbf{E}_\omega(z,r,\theta)$ mix components of $\mathbf{E}_k(r,\theta)$ with different k. However for cylindrically symmetric structures, the boundary conditions do not mix the azimuthal harmonics $\mathbf{E}_m$, which are the coefficients in the expansion

$$\mathbf{E}_k(r,\theta)=\sum_m\mathbf{E}_m(k,r)e^{im\theta} . \tag{3.6}$$

Hence, the azimuthal harmonics can be treated independently from each other.

The equations for the projections of the azimuthal harmonics are easy to obtain using Eqs (3.4) and (3.5):

$$\left[\frac{1}{r}\frac{\partial}{\partial r}r\frac{\partial}{\partial r}-\frac{m^2}{r^2}\right]E_m^{(z)}(k,r)=0 , \tag{3.7}$$

$$\left[\frac{1}{r}\frac{\partial}{\partial r}r\frac{\partial}{\partial r}-\frac{(m\pm1)^2}{r^2}\right]E_m^{(\pm)}(k,r)=0 , \tag{3.8}$$

where $E_m^{(\pm)}\equiv E_m^{(r)}\pm iE_m^{(\theta)}$. The solutions of Eqs. (3.7) and (3.8) which are finite on the axis $r=0$ are

$$E_m^{(z)}(k,r)=\Upsilon_m^{(z)}(k)r^m, \quad m\geq0 , \tag{3.9}$$

$$E_m^{(\pm)}(k,r)=\Upsilon_m^{(\pm)}(k)r^{m\pm1}, \quad (m\pm1)\geq0 , \tag{3.10}$$

where functions $\Upsilon_m^{(z)}(k)$ and $\Upsilon_m^{(\pm)}(k)$ are defined by the boundary condition for $\mathbf{E}_k(r,\theta)$ Under the conditions considered here, the longitudinal and transverse impedances for each mode m can be expressed in terms of $E_m^{(z)}(k,r)$:

$$Z_{lm}=-\frac{E_m^{(z)}(k,r)}{q}=-\frac{\Upsilon_m^{(z)}(k)}{q}r^m, \quad m\geq0 , \tag{3.11}$$

$$Z_{rm}=-\frac{1}{qk}\frac{\partial E_m^{(z)}(k,r)}{\partial r}=-\frac{m\Upsilon_m^{(z)}(k)}{qk}r^{m-1}, \quad m\geq1 , \tag{3.12}$$

$$Z_{\theta m}=-\frac{im}{qk}\frac{E_m^{(z)}(k,r)}{r}=-\frac{im\Upsilon_m^{(z)}(k)}{qk}r^{m-1}, \quad m\geq1 . \tag{3.13}$$

These formulas, which are in agreement with the Panofsky-Wenzel theorem Eq. (3.3), give the scaling of the impedance with the offset r of the trailing particle. In the dimensionless form, $Z_{lm}\sim(r/a)^m$, and $Z_{\perp m}\sim(r/a)^{m-1}$ where a is a characteristic transverse dimension—for example the pipe radius. Usually the transverse size of the bunch $\sigma_\perp$ is much smaller than a [to prevent particle losses, usually $a\geq(10-20)\sigma_\perp$]. Hence, the monopole mode ($m=0$) dominates the longitudinal impedance, while the dipole mode ($m=1$) dominates the transverse impedance. Higher-order modes $m\geq2$ can dilute the transverse emittance of a bunch. However, the effect is usually negligible

From Eqs. (3.11)–(3.13), it follows that the longitudinal impedance of the azimuthally symmetric monopole mode ($m=0$) is independent of the coordinate r. The transverse impedance of this mode is zero. Hence, in this case the longitudinal impedance can be calculated by integrating the field over z at any value of the coordinate r. In particular, it is convenient to integrate the field along the pipe wall and its continuation inside the structure. Since the longitudinal field on the wall is zero, the integration is restricted to the line inside the structure only. With subsequent rescaling of the respective impedance with the offset r, this procedure can be applied to any other mode m as well.

For *the dipole* mode $m=1$ from Eq. (3.12), it follows that

$$Z_{r1}=\frac{Z_{l1}|_{r=a}}{ka} . \tag{3.14}$$

In what follows we consider the longitudinal impedance. The transverse impedance can be obtained from it by applying either Eq. (3.14) for $m=1$, or the Panofsky-Wenzel theorem for any m.

C. Dispersion relations and the finite frequency sum rule

Several important properties of the impedance can be derived from the analytic continuation of the impedance into the complex ω plane. First of all, the point wake function is real by definition. Therefore,

$$Z_l(-\omega^*)=+Z_l^*(\omega)\ , \tag{3.15}$$

where an asterisk indicates the complex conjugate value. As follows from this equation $\mathrm{Im}Z_l(0)=0$. [Note that according to the definition of the transverse impedance Eq. (2.22), $Z_\perp(-\omega^*)=-Z_\perp^*(\omega)$.]

Next, causality requires that in the ultrarelativistic limit $\gamma\to\infty$ there is no field in front of the charge:

$$w(s)=0 \quad \text{for } s<0\ . \tag{3.16}$$

Therefore, all the singularities of the impedance must lie in the lower half of the complex ω plane. Provided that $Z_l(\omega)$ tends to zero as $|\omega|\to\infty$, the Cauchy integral formulas give the following Kramers-Kronig dispersion relations between $Z_1(\omega)$ and $Z_2(\omega)$, the real and imaginary part of the longitudinal impedance, respectively:

$$Z_1(\omega)=\frac{2}{\pi}PV\int_0^\infty d\nu\frac{\nu Z_2(\nu)}{\nu^2-\omega^2}\ , \tag{3.17}$$

$$Z_2(\omega)=-\frac{2\omega}{\pi}PV\int_0^\infty d\nu\frac{Z_1(\nu)}{\nu^2-\omega^2}\ , \tag{3.18}$$

where PV denotes the principal value of the integral. If the impedance tends to a finite limit as $|\omega|\to\infty$, similar dispersion relations hold for the difference of the impedance at finite and infinite ω, respectively. The dispersion relations allow one to find the impedance by calculating either the real or the imaginary part only.

The dispersion relations can be used to determine the asymptotic behavior of the impedance from the parameters of its low-frequency resonances (Heifets, 1990d). Derivation of this formula is similar to that of the finite-energy sum rule (Horn *et al.*, 1968). Analogously, we call this the finite-frequency sum rule.

Suppose, for example, that the high-frequency tail of the impedance of some structure decreases with frequency as $\omega^{-1/2}$; see Eq. (6.32), and that it can be expanded for large ω into a power series in $\omega^{-1/2}$ (to the end of Sec. III.C, we restrict frequency ω to positive values, $\omega>0$). We know that such asymptotic behavior has, for example, the impedance of a cavity with side pipes (Lawson, 1968, 1990; Dôme, 1985; Heifets and Kheifets, 1987, 1990). In this case, Eq. (3.15) gives

$$Z_l(\omega)=\alpha\frac{(1+i)}{\sqrt{\omega}}+\frac{i\zeta}{\omega}+o(\omega^{-3/2})\ , \tag{3.19}$$

where α and ζ are two unknown real constants. We keep here the first few terms of the impedance expansion.

Consider the difference

$$\tilde{Z}(\omega)=Z_l(\omega)-\frac{\alpha(1+i)}{\sqrt{\omega}}-\frac{i\zeta}{\omega}\ . \tag{3.20}$$

The function $\tilde{Z}(\omega)$ decreases asymptotically, at least as $\omega^{-3/2}$. Its real part $\tilde{Z}_1$ satisfies the dispersion relation, Eq. (3.17). Its imaginary part $\tilde{Z}_2$ has an additional pole at $\omega=0$. Hence the dispersion relation for it must be

$$\tilde{Z}_2(\omega)=-\frac{\zeta}{\omega}-\frac{2\omega}{\pi}PV\int_0^\infty d\nu\frac{\tilde{Z}_1(\nu)}{\nu^2-\omega^2}\ . \tag{3.21}$$

To assure the correct asymptotic behavior $\tilde{Z}_2(\omega)\approx\omega^{-3/2}$ for $|\omega|\to\infty$, the following "superconvergence relation" must hold:

$$\int_0^\infty d\nu\,\tilde{Z}_1(\nu)=\frac{\pi\zeta}{2}\ . \tag{3.22}$$

Otherwise, $\tilde{Z}_2(\omega)$ would fall off as ω^{-1}, which is too slow.

Define now a sufficiently large frequency ω_c such that for any $\omega>\omega_c$

$$Z_1(\omega)=\frac{\alpha}{\sqrt{\omega}}\left[1+o\left[\frac{\omega_c}{\omega}\right]\right]\ . \tag{3.23}$$

Then, for any $\Omega>\omega_c$, Eq. (3.22) give

$$\int_0^\Omega d\nu\left[Z_1(\nu)-\frac{\alpha}{\sqrt{\omega}}\right]=\frac{\pi\zeta}{2}\left[1+o\left[\frac{\alpha\omega_c}{\sqrt{\Omega}}\right]\right]\ . \tag{3.24}$$

or

$$\alpha=\frac{1}{2\sqrt{\Omega}}\left[\int_0^\Omega d\nu\,Z_1(\nu)-\frac{\pi\zeta}{2}\right]\left[1+o\left[\frac{\omega_c}{\sqrt{\Omega}}\right]\right]\ . \tag{3.35}$$

Note that the right-hand side of this expression is independent of Ω, since α is a constant independent of ω.

In the region $\omega<\Omega$, $Z_1(\omega)$ can be represented as the sum of resonant terms. Using Eq. (2.10) we obtain

$$\alpha=\frac{\pi}{2\sqrt{\Omega}}\left[\sum_{\omega_\lambda<\Omega}\kappa_\lambda-\frac{\zeta}{2}\right]\ . \tag{3.26}$$

Equation (3.19) now defines the impedance for all ω in terms of the parameters of several low-frequency resonances:

$$Z_l(\omega)=i\vartheta(\Omega-\omega)\sum_{\omega_\lambda<\Omega}\kappa_\lambda^l\left[\frac{1}{\omega-\omega_\lambda+i\gamma_\lambda}+\frac{1}{\omega+\omega_\lambda+i\gamma_\lambda}\right]+\vartheta(\omega-\Omega)\frac{\pi(1+i)}{2\sqrt{\omega\Omega}}\left[\sum_{\omega_\lambda<\Omega}\kappa_\lambda-\frac{\zeta}{2}\right]\ . \tag{3.27}$$

Here $\vartheta(x)$ is the step function: $\vartheta(x)=1$ for $x>0$ and $\vartheta(x)=0$ for $x<0$. The parameters κ_λ^l, ω_λ, and γ_λ can easily be found for any given structure by one of the existing computer codes; e.g., URMEL. If Ω is large enough, $Z_l(\omega)$ obtained in this way is independent of the particu-

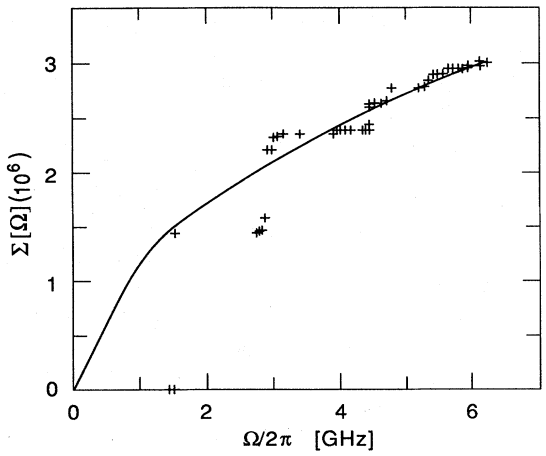

FIG. 2. The finite frequency sum rule [see Eq. (3.28)]. Crosses represent results of numerical calculations. The curve is a parametrization by Eq. (3.29).

lar choice of Ω. The sum

$$\Sigma(\Omega)\equiv\sum_{\omega_\lambda<\Omega}\kappa_\lambda \tag{3.28}$$

can be parametrized as

$$\Sigma(\Omega)=\frac{\zeta}{2}+\frac{2\alpha}{\pi}\sqrt{\Omega}+o\left[\frac{1}{\sqrt{\Omega}}\right], \tag{3.29}$$

from which both unknown parameters α and ζ can be found.

Figure 2 (Heifets, 1990a) illustrates this procedure. The sum Eq. (3.28) was calculated with the help of the code URMEL for the CEBAF cavity (the fundamental and cutoff frequencies are 1.5 and 3.2 GHz, respectively) and is plotted here as a function of Ω. Parametrization by Eq. (3.29) (solid line in Fig. 2) gives $\zeta=0$ and shows that α is independent of Ω for Ω larger than, say, twice the cutoff frequency.

D. The directional symmetry of the impedance

The independence of the impedance on bunch moving either in $+z$ or $-z$ direction is an important feature of an accelerator structure. Recently, Gluckstern and Zotter (1988) considered a cylindrically symmetric but longitudinally asymmetric cavity with side pipes of equal radii. They were able to prove that for a relativistic particle, the *longitudinal* impedance of a cavity with arbitrary shape is independent of the direction along the z-axis in which the bunch travels. Their result corroborates numerical observations of the independence of the bunch wake function obtained with the code TBCI. Bisognano (1990b) gives an elegant proof of the same statement. His approach is based on a reciprocity relation applied to the tensor Green's function.

We follow here his idea in a somewhat simpler way (Heifets, 1990c) to obtain a more general and physically transparent proof of this property for both *longitudinal* and *transverse* impedances. The result is valid for a cavity with no azimuthal symmetry, and for arbitrary particle velocity as long as it may be considered constant. At the same time it is shown that the impedance is directionally symmetric only if the entrance and exit side beam pipes have the same cross sections.

Consider the cavity of an arbitrary configuration and let a bunch travel through it along the axis z. We attach a subscript, "+" or "−", to all quantities pertaining to the respective cases when the bunch travels in the positive or negative direction parallel to the z axis. To examine both the longitudinal and transverse impedances, we assume that the bunch trajectory is offset from the axis by a transverse vector $\mathbf{a}$.

The current densities have only z components. The Fourier harmonics are

$$j_{\omega z+}=q\delta(\mathbf{r}-\mathbf{a})\exp(i\omega z/v),\quad \rho_{\omega+}=j_{\omega z+}/v\ , \tag{3.30}$$

$$j_{\omega z-}=-q\delta(\mathbf{r}-\mathbf{a})\exp(-i\omega z/v),\quad \rho_{\omega-}=-j_{\omega z-}/v\ . \tag{3.31}$$

Note that

$$\mathbf{j}_{\omega-}=-\mathbf{j}^*_{\omega+},\quad \rho_{\omega-}=\rho^*_{\omega+}\ . \tag{3.32}$$

The fields $\mathbf{E}_{\omega+}$ and $\mathbf{E}_{\omega-}$ excited by such sources satisfy the following wave equations:

$$\left[\nabla^2+\frac{\omega^2}{c^2}\right]\mathbf{E}_{\omega+}=4\pi\nabla\rho_{\omega+}-\frac{4\pi i\omega}{c^2}\mathbf{j}_{\omega+}\ , \tag{3.33}$$

$$\left[\nabla^2+\frac{\omega^2}{c^2}\right]\mathbf{E}_{\omega-}=4\pi\nabla\rho_{\omega-}-\frac{4\pi i\omega}{c^2}\mathbf{j}_{\omega-}\ , \tag{3.34}$$

as well as the boundary conditions for their tangential components:

$$\mathbf{E}_{\omega+}|_{\tan}=0,\quad \mathbf{E}_{\omega-}|_{\tan}=0\ , \tag{3.35}$$

and the radiation conditions for the radiated part of the EM field:

$$\lim\mathbf{E}^{\rm rad}_{+}(z,\mathbf{r},t)|_{t=(z+s)/v}=0,\quad \lim\mathbf{E}^{\rm rad}_{-}(z,\mathbf{r},t)|_{t=(z+s)/v}=0 \quad \text{as } z\to\pm\infty\ . \tag{3.36}$$

The longitudinal impedances Z_+ and Z_- are [see Eq. (2.5)]

$$Z_+(\omega,\mathbf{r})=-\frac{1}{q}\int_{-\infty}^{\infty}dz\,E_{z\omega+}(\mathbf{r},z)e^{-i\omega z/v}\ , \tag{3.37}$$

$$Z_-(\omega,\mathbf{r})=+\frac{1}{q}\int_{-\infty}^{\infty}dz\,E_{z\omega-}(\mathbf{r},z)e^{+i\omega z/v}\ . \tag{3.38}$$

Let us find out under what conditions the fields $\mathbf{E}_{\omega+}$ and $\mathbf{E}_{\omega-}$ are complex conjugates of one another. Substituting Eqs. (3.32) into (3.34) and taking its complex conjugate, we obtain

$$\left[\nabla^2+\frac{\omega^2}{c^2}\right]\mathbf{E}^*_{\omega-}=4\pi\nabla\rho_{\omega+}-\frac{4\pi i\omega}{c^2}\mathbf{j}_{\omega+}\ . \tag{3.39}$$

The boundary conditions shown in Eq. (3.35) are also valid for $\mathbf{E}^*_{\omega-}$. We now need only one additional assumption, that there are no incident waves accompanying particles "+" and "−"; then the equations and all the boundary conditions for $\mathbf{E}^*_{\omega-}$ and $\mathbf{E}_{\omega+}$ are the same, and we may conclude that

$$\mathbf{E}^*_{\omega-}=\mathbf{E}_{\omega+}\ . \tag{3.40}$$

From the Maxwell equation $i(\omega/c)\mathbf{H}_\pm=\nabla\times\mathbf{E}_\pm$, it follows that

$$\mathbf{H}^*_{\omega+}=-\mathbf{H}_{\omega-}\ . \tag{3.41}$$

We now multiply Eq. (3.33) by $\mathbf{E}_{\omega-}$ and Eq. (3.34) by $\mathbf{E}_{\omega+}$, subtract the results, and integrate the difference over the volume of the cavity and the side pipes bounded by imaginary cross sections at $z=\pm\xi$, $\xi\to\infty$. We then obtain the *Lorentz reciprocity theorem* (Collin, 1966):

$$\frac{4\pi}{c}\int dV(\mathbf{E}_{\omega-}\cdot\mathbf{j}_{\omega+}-\mathbf{E}_{\omega+}\cdot\mathbf{j}_{\omega-})$$
$$=\int d\mathbf{S}\cdot(\mathbf{E}_{\omega+}\times\mathbf{H}_{\omega-}-\mathbf{E}_{\omega-}\times\mathbf{H}_{\omega+})\ . \tag{3.42}$$

The integration on the right-hand side is performed over the surface enclosing the volume over which the integration on the left-hand side is performed, i.e., over the walls of the cavity, the walls of the side pipes, and the bounding cross sections. Since the tangential electric field on the walls is zero, it is sufficient to perform the integration only over these cross sections. The integration over the transverse coordinates in the left side of Eq. (3.42) is performed easily by using Eq. (3.30). The remaining integration over z gives the longitudinal impedance; see Eqs. (3.37) and (3.38). We obtain the following expression for the difference of the impedances for two directions of the bunch travel:

$$\frac{4\pi q^2}{c}[Z_-(\omega,\mathbf{r})-Z_+(\omega,\mathbf{r})]$$
$$=\int d\mathbf{S}\cdot[(E_{\omega+}\times\mathbf{H}_{\omega-}-\mathbf{E}_{\omega-}\times\mathbf{H}_{\omega+})_L$$
$$-(\mathbf{E}_{\omega+}\times\mathbf{H}_{\omega-}-E_{\omega-}\times\mathbf{H}_{\omega+})_R]\ , \tag{3.43}$$

where the subscripts R and L refer to the beam-pipe cross section at $z=\pm\xi$, respectively. Using Eqs. (3.40) and (3.41) this equation can be rewritten in the form:

$$\frac{4\pi q^2}{c}[Z_-(\omega,\mathbf{r})-Z_+(\omega,\mathbf{r})]$$
$$=\int d\mathbf{S}\cdot[(\mathbf{E}_{\omega+}\times\mathbf{H}^*_{\omega+}+\mathbf{E}^*_{\omega+}\times\mathbf{H}_{\omega+})_R$$
$$-(\mathbf{E}_{\omega+}\times\mathbf{H}^*_{\omega+}+\mathbf{E}^*_{\omega+}\times\mathbf{H}_{\omega+})_L]\ . \tag{3.44}$$

The right-hand side of this equation is real. Hence, the imaginary parts of the impedances are equal:

$$\mathrm{Im}Z_+(\omega,\mathbf{r})=\mathrm{Im}Z_-(\omega,\mathbf{r})\ . \tag{3.45}$$

The integrals in the right-hand side of Eq. (3.44) have a simple physical meaning. They give the EM field energy flow through the cross sections of the side pipes. If these cross sections are far enough from the cavity, then the only part of the EM field impinging on them is the synchronous component accompanying the bunch. This is a direct consequence of the radiation condition, Eq. (3.36), which is assumed to be fulfilled here. For the case when both side pipes have similar and equal cross sections, the synchronous components of the field at $z=\pm\infty$ are the same. It follows then from Eq. (3.44) that both longitudinal impedances are equal. Applying now the Panofsky-Wenzel theorem, Eq. (3.3), we see that the same is true for the transverse impedances.

However, for unequal or nonsimilar pipe cross sections, the synchronous components of the two fields are different, even at $z=\pm\infty$. We cannot say that Eqs. (3.40) and (3.41) are necessarily true. In this case the real parts of the impedances for two directions may differ by a constant.

In the ultrarelativistic case, $\gamma\to\infty$, for the side pipes with round cross sections, the difference of the energy of the synchronous components in the pipes with radii a and b is proportional to the constant $\ln(b/a)$ (Balakin and Novokhatski, 1983); see Sec. II.C. Hence, the difference of the real parts of the impedances is proportional to the same constant. The impedance for such a case is calculated in Sec. IV.C (Kheifets, 1986, 1987).

IV. THE MODAL ANALYSIS OF THE IMPEDANCE

We now turn to the study of the narrow-band impedance given by the sum of resonant contributions of *eigenmodes,* Eqs. (2.13) and (2.14). Effectively, only the modes which have frequencies below or comparable to the cutoff frequency $\omega_{\mathrm{c.o.}}\simeq c/a$ of the beam pipe with radius a contribute to the narrow-band impedance (Heifets, 1989). The widths of the resonance peaks above the cutoff frequencies rapidly become large and their height decreases. The resonance curves overlap, producing a smooth high-frequency impedance considered in Secs. V and VI.

The narrow-band impedance can be found analytically in the case when the structure may be divided into several parts for which the solution of the Maxwell equations is known. The field for the whole structure can then be found by *the field matching technique* (Keil and Zotter, 1972; Zotter and Bane, 1979), i.e., by requiring the field to be continuous across contiguous regions.

The field-matching technique is described in Sec. IV.A. Using it, one can derive the exact infinite system of linear equations for unknown coefficients of the field expansions into eigenmodes. For low-frequency modes, the system of the coupled equations can be solved either by perturbation methods or by series truncation. We demonstrate the method of truncation for a cavity and a collimator in Sec. IV.B, and for a step in the waveguide cross section in Sec. IV.C. The method of perturbation, applicable for

an arbitrary cylindrically symmetric cavity, is described next in the Sec. IV.D. Comparison of the two methods shows a good agreement. In Sec. IV.E., we briefly discuss the problem of trapped modes.

In cases of smoothly varying boundaries, the field matching technique is hard to apply. Structure of this type is widely used in accelerators in the form of bellows. Several methods have been developed for such cases (Chatard-Moulin and Papiernik, 1979; Krinsky, 1980; Cooper *et al.*, 1982; Kheifets, 1981; Krinsky and Gluckstern, 1981; Kheifets and Zotter, 1986; Kheifets and Gygi, 1985; and Kurennoy and Purtov, 1989). As an illustration of an approach for such cases, in Sec. IV.F we describe the calculation of the longitudinal narrow-band impedance for bellows (Krinsky and Gluckstern, 1986). Calculations of the transverse narrow-band impedance can be found in papers by Kheifets and Zotter (1986) and Kurennoy and Purtov (1989).

A. Field matching

The field matching technique (Keil and Zotter, 1972) will be demonstrated for axially symmetric structures, such as those sketched in Fig. 3 for a cavity (a) and a collimator (b). The symmetry axis is the z axis. We chose the interfaces to be at $z\pm g/2$. The point charge q is assumed to move on the axis with the speed v. The Fourier harmonic of the current density; cf. Eq. (3.30), has only the z component:

$$j_{\omega z}=q\delta(r)\exp(ikz/\beta)\ , \tag{4.1}$$

where $k=\omega/c$, $\beta=v/c$, and $\delta(r)$ is Dirac's radial δ function.

The Fourier components of the solution of the Maxwell equations which satisfy the boundary condition $E_z(z)=0$ on the pipe wall and the radiation condition at $z=\infty$ are known (Stratton, 1941). We shall denote such a solution for the region $z>g/2$ by the superscript "+" and for the region $z<-g/2$ by the superscript "−." It is convenient to introduce the following notations:

$$Q=qk/\pi c\gamma^2\beta^2\ ,$$

$$G_1(r,d)=K_1(\tau r)+I_1(\tau r)K_0(\tau d)/I_0(\tau d)\ , \tag{4.2}$$

$$G_0(r,d)=K_0(\tau r)-I_0(\tau r)K_0(\tau d)/I_0(\tau d)\ , \tag{4.3}$$

where d stands for a_1 or a_2, and $\tau=k/\gamma\beta$. K_0, K_1, I_0, and I_1 are modified Bessel functions of the second and first kind of the zeroth and first order, respectively. For $\gamma\gg1$, $\gamma QG_1(d,d)=Z_0q/4\pi^2d$, where $Z_0=377\ \Omega$. With these notations

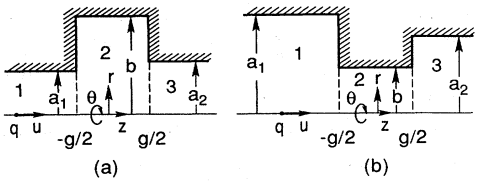

FIG. 3. Cylindrically symmetric structures of radius b and length g with side pipes of radii a_1 and a_2; (a) a cavity, (b) a collimator.

$$E^{\pm}_{\omega r}=\gamma QG_1(r,d)\exp(ikz/\beta)$$
$$-i\sum_n B^{\pm}_n(\nu_n/d)J_1(\nu_n r/d)\lambda_{dn}\exp(\pm iz\lambda_{dn})\ , \tag{4.4}$$

$$E^{\pm}_{\omega z}=-iQG_0(r,d)\exp(ikz/\beta)$$
$$+\sum_n B^{\pm}_n(\nu_n^2/d^2)J_0(\nu_n r/d)\exp(\pm iz\lambda_{dn})\ , \tag{4.5}$$

$$H^{\pm}_{\omega\theta}=\gamma\beta QG_1(r,d)\exp(ikz/\beta)$$
$$-ik\sum_n B^{\pm}_n(\nu_n/d)J_1(\nu_n r/d)\exp(\pm iz\lambda_{dn})\ . \tag{4.6}$$

Here J_0 and J_1 are Bessel functions of the first kind of the zeroth and the first order, correspondingly, and $\nu_1<\nu_2<\cdots<\infty$ are the roots of J_0. The sign of the imaginary parts of the propagation constants $\lambda_{dn}=\sqrt{k^2-\nu_n^2/d^2}$ should be chosen positive: $\mathrm{Im}\lambda_{dn}>0$. Such a choice is defined by the radiation condition; see Eq. (3.36).

The first terms in Eqs. (4.4)–(4.6) correspond to the synchronous component of the EM field. Each term in the sums of these expressions describes either (a) the nth diffracted wave propagating in the positive z direction, if $k>\nu_n/a_2$, or (b) an evanescent wave, if $k<\nu_n/a_2$. Similarly, for the reflected field each term describes either (a) the nth wave propagating in the negative z direction, if $k>\nu_n/a_1$, or (b) an evanscent wave, if $k<\nu_n/a_1$. For any given k, there are finite numbers of propagating waves and an infinite number of evanescent waves.

We also need to define similar expressions for the region $-g/2<z<g/2$ with radius b (region 2 in Fig. 3):

$$E^0_{\omega r}=\gamma QG_1(r,b)\exp(ikz/\beta)-i\sum_n(\nu_n/b)J_1(\nu_n r/b)\lambda_{bn}[C^+\exp(iz\lambda_{bn})-C^-\exp(-iz\lambda_{bn})]\ , \tag{4.7}$$

$$E^0_{\omega z}=-iQG_0(r,b)\exp(ikz/\beta)+\sum_n(\nu_n^2/b^2)J_0(\nu_n r/b)[C^+\exp(iz\lambda_{bn})+C^-\exp(-iz\lambda_{bn})]\ , \tag{4.8}$$

$$H^0_{\omega\theta}=\gamma\beta QG_1(r,b)\exp(ikz/\beta)-ik\sum_n(\nu_n/b)J_1(\nu_n r/b)[C^+\exp(iz\lambda_{bn})+C^-\exp(-iz\lambda_{bn})]\ . \tag{4.9}$$

For certainty, the same positive sign is chosen for the propagation constant in region 2: $\mathrm{Im}\lambda_{bn}>0$.

Expansions of the EM field are constructed in such a way as to fulfull the boundary condition on the wall of the pipe in any region with a constant pipe radius. For example, for $r=a_2$ and for all $z>g/2$, $E_z^+(z)=0$. On the other hand, unknown coefficients $B_n^{\pm}$ and $C^{\pm}$ have to be defined by the boundary and continuity conditions in the planes $z=\pm g/2$ between adjacent cylindrical regions:

(a) the radial component of the electric field on the inner side of the wall should be equal to zero for all r,

(b) all three components of the field should be continuous through the opening. For example, in the case of a cavity at $z=g/2$ for $a_2<r<b$,

$$E^0_{\omega r}(r)=0\ , \tag{4.10}$$

and for $r<a_2$,

$$E^+_{\omega z}(r)=E^0_{\omega z}(r)\ , \tag{4.11}$$

$$E^+_{\omega r}(r)=E^0_{\omega r}(r)\ . \tag{4.12}$$

Analogous expressions can be written for another cavity interface at $z=-g/2$, and for a collimator.

Introduce new dimensionless variables:

$$\tilde{k}=kb\ , \tag{4.13}$$

$$p_i=a_i/b\ ,\quad i=1,2 \tag{4.14}$$

$$\tilde{g}=g/2b\ . \tag{4.15}$$

In these variables the propagation constants are

$$\tilde{\lambda}_{ain}\equiv\lambda_{ain}b=\sqrt{\tilde{k}^2-\nu_n^2/p_i^2}\ ,\quad i=1,2 \tag{4.16}$$

$$\tilde{\lambda}_{bn}\equiv\lambda_{bn}b=\sqrt{\tilde{k}^2-\nu_n^2}\ . \tag{4.17}$$

It is also convenient to redefine the expansion coefficients

$$x_n=(i\pi c/2bQ)\exp[i\tilde{g}(\tilde{k}/\beta+\tilde{\lambda}_{a1n})]B_n^-\ , \tag{4.18}$$

$$t_n=(i\pi c/2bQ)\exp[-i\tilde{g}(\tilde{k}/\beta+\tilde{\lambda}_{bn})]C_n^-\ , \tag{4.19}$$

$$y_n=(i\pi c/2bQ)\exp[i\tilde{g}(\tilde{k}/\beta-\tilde{\lambda}_{bn})]C_n^+\ , \tag{4.20}$$

$$z_n=-(i\pi c/2bQ)\exp[-i\tilde{g}(\tilde{k}/\beta-\tilde{\lambda}_{a2n})]B_n^+\ . \tag{4.21}$$

The expressions for the field components (Kheifets, 1987) in the planes $z=-g/2$ and $z=g/2$ in these variables are, correspondingly:

$$E^-_{\omega r}=(2Q/\pi cb)\exp(-i\kappa\tilde{g}/\beta)\left[(\tilde{k}/2\gamma\beta^2)G_1(r,a_1)+(1/p_1)\sum_n x_n\nu_n J_1(\nu_n r/a_1)\lambda_{a1n}\right] \tag{4.4a}$$

$$E^0_{\omega r}=(2Q/\pi cb)\exp(-i\tilde{k}\tilde{g}/\beta)\left[(\tilde{k}/2\gamma\beta^2)G_1(r,b)+\sum_n \nu_n J_1(\nu_n r/b)\tilde{\lambda}_{bn}\{t_n\exp[2i\tilde{g}(\tilde{k}/\beta+\tilde{\lambda}_{bn})]-y_n\}\right] \tag{4.8a}$$

$$E^-_{\omega z}=-(2iQ/\pi cb)\exp(-i\tilde{k}\tilde{g}/\beta)\left[(\tilde{k}/2\gamma^2\beta^2)G_0(r,a_1)+(1/p_1^2)\sum_n x_n\nu_n^2 J_0(\nu_n r/a_1)\right] \tag{4.4b}$$

$$E^0_{\omega z}=-(2iQ/\pi cb)\exp(-i\tilde{k}\tilde{g}/\beta)\left[(\tilde{k}/2\gamma^2\beta^2)G_0(r,b)+\sum_n \nu_n^2 J_0(\nu_n r/b)\{t_n\exp[2i\tilde{g}(\tilde{k}/\beta+\tilde{\lambda}_{bn})]+y_n\}\right] \tag{4.8b}$$

TABLE I. Coefficients A^{nl}_{LN} and right-hand sides P^l_L of Eq. (4.23) for a cavity.

L \ N	1	2	3	4	P^l_L
1	$2p_1^2\tilde{\lambda}_{a1n}\phi_{ln}(p_1)$	$\tilde{\lambda}_{bn}J_1^2(\nu_n)\delta_{ln}$	$-\tilde{\lambda}_{bn}J_1^2(\nu_n)\delta_{nl}E_+$	0	$\dfrac{J_0(\nu_l p_1)}{I_0(\tau a_1)[\nu_l^2+(\tau b)^2]}$
2	$\nu_n^2 J_1^2(\nu_n)\delta_{ln}$	$-2p_1^2\nu_n^2\phi_{nl}(p_1)$	$-2p_1^2\nu_n^2\phi_{nl}(p_1)E_+$	0	$\dfrac{-(\tau b)p_1^2\nu_l J_1(\nu_l)I_0(\tau a_1)F(a_1)}{[\nu_l^2+(\tau a_1)^2]\gamma}$
3	0	$\tilde{\lambda}_{bn}J_1^2(\nu_n)\delta_{nl}E_-$	$-\tilde{\lambda}_{bn}J_1^2(\nu_n)\delta_{nl}$	$2p_2^2\tilde{\lambda}_{a2n}\phi_{ln}(p_2)$	$\dfrac{J_0(\nu_l p_2)}{I_0(\tau a_2)[\nu_l^2+(\tau b)^2]}$
4	0	$-2p_2^2\nu_n^2\phi_{nl}(p_2)E_-$	$-2p_2^2\nu_n^2\phi_{nl}(p_2)$	$-\nu_n^2 J_1^2(\nu_n)\delta_{ln}$	$\dfrac{-(\tau b)p_2^2\nu_l J_1(\nu_l)I_0(\tau a_2)F(a_2)}{[\nu_l^2+(\tau a_2)^2]\gamma}$

$E_+=\exp[2i\tilde{g}(\kappa/\beta+\tilde{\lambda}_{bn})]$, $E_-=\exp[-2i\tilde{g}(\kappa/\beta-\tilde{\lambda}_{bn})]$,

$F(a)=K_0(\tau b)/I_0(\tau b)-K_0(\tau a)/I_0(\tau a)$, $p_1=a_1/b$, $p_2=a_2/b$, $\tilde{g}=g/2b$

and

$$E^{+}_{\omega r}=(2Q/\pi cb)\exp(i\tilde{k}\tilde{g}/\beta)\left[(\tilde{k}/2\gamma\beta^2)G_1(r,a_2)+(1/p_2)\sum_n z_n\nu_n J_1(\nu_n r/a_2)\lambda_{a2n}\right] \tag{4.4c}$$

$$E^{0}_{\omega r}=(2Q/\pi cb)\exp(i\tilde{k}\tilde{g}/\beta)\left[(\tilde{k}/2\gamma\beta^2)G_1(r,b)+\sum_n \nu_n J_1(\nu_n r/b)\tilde{\lambda}_{bn}\{t_n-y_n\exp[-2i\tilde{g}(\tilde{k}/\beta-\tilde{\lambda}_{bn})]\}\right] \tag{4.8c}$$

$$E^{+}_{\omega z}=-(2iQ/\pi cb)\exp(i\tilde{k}\tilde{g}/\beta)\left[(\tilde{k}/2\gamma^2\beta^2)G_0(r,a_2)-(1/p_2^2)\sum_n z_n\nu_n^2 J_0(\nu_n r/a_2)\right] \tag{4.4d}$$

$$E^{0}_{\omega z}=-(2iQ/\pi cb)\exp(i\tilde{k}\tilde{g}/\beta)\left[(\tilde{k}/2\gamma^2\beta^2)G_0(r,b)+\sum_n \nu_n^2 J_0(\nu_n r/b)\{t_n+y_n\exp[-2i\tilde{g}(\tilde{k}/\beta+\tilde{\lambda}_{bn})]\}\right] \tag{4.8d}$$

These expressions are valid both for a cavity for which $p_i<1$, and for a collimator for which $p_i>1$.

The unknown coefficients x_n, y_n, t_n, and z_n are defined by the set of linear algebraic equations that are obtained by substituting expressions for the field components into Eqs. (4.10)–(4.12) for $z=g/2$, and into similar equations for the second interface, $z=-g/2$.

If we introduce a matrix of coefficients:

$$X_n^N\equiv\begin{bmatrix}X_n^1\\X_n^2\\X_n^3\\X_n^4\end{bmatrix}=\begin{bmatrix}x_n\\y_n\\t_n\\z_n\end{bmatrix},\quad N=1,2,3,4\ , \tag{4.22}$$

then the set of equations can be written in a compact form:

$$\sum_N\sum_n A_{LN}^{nl}X_n^N=P_L^l,\quad L,N=1,2,3,4\ ;\quad n,l=1,2,\ldots,\infty\ . \tag{4.23}$$

Equation (4.23) constitutes an infinite system of linear algebraic equations for unknown coefficients X_n^N. The coefficients A_{LN}^{nl} and the right-hand sides P_L^l of Eq. (4.23) are presented in Table I for a cavity and in Table II for a collimator (Kheifets, 1987). There

$$\phi_{mn}(p)=\begin{cases}\nu_n J_0(\nu_m p)J_1(\nu_n)/(\nu_n^2-p^2\nu_m^2), & \text{if } \nu_n\neq p\nu_m\ ,\\ \nu_n J_1^2(\nu_n)/(\nu_n+p\nu_m), & \text{if } \nu_n=p\nu_m\ .\end{cases} \tag{4.24}$$

In particular,

$$\phi_{mn}(1)=\delta_{nm}J_1^2(\nu_n)/2\ .$$

In a smooth pipe for which $p_1=p_2=1$, all $P_L^l=0$. Since $\mathrm{Det}|A_{LN}^{nl}|\neq 0$, only the trivial solution $X_n^N=0$ exists. This means that no radiation occurs in a smooth pipe.

TABLE II. Coefficients A_{LN}^{nl} and right-hand sides P_L^l of Eq. (4.23) for a collimator.

L \ N	1	2	3	4	P_L^l
1	$\tilde{\lambda}_{a1n}J_1^2(\nu_n)\delta_{nl}$	$2p_1^{-2}\tilde{\lambda}_{bn}\phi_{ln}(p_1^{-1})$	$-2p_1^{-2}\tilde{\lambda}_{bn}\phi_{ln}(p_1^{-1})E_+$	0	$\dfrac{-J_0(\nu_l/p_1)}{I_0(\tau a_1)[\nu_l^2+(\tau b)^2]}$
2	$2p_1^{-2}\nu_n^2\phi_{nl}(p_1^{-1})$	$-\nu_n^2J_1^2(\nu_n)\delta_{ln}$	$-\nu_n^2J_1^2(\nu_n)\delta_{ln}E_+$	0	$\dfrac{-(\tau b)\nu_l J_1(\nu_l)I_0(\tau a_1)F(a_1)}{p_1^2[\nu_l^2+(\tau a_1)^2]\gamma}$
3	0	$2p_2^{-2}\tilde{\lambda}_{bn}\phi_{ln}(p_2^{-1})E_-$	$-2p_2^{-2}\tilde{\lambda}_{bn}\phi_{ln}(p_2^{-1})$	$\tilde{\lambda}_{a2n}J_1^2(\nu_n)\delta_{nl}$	$\dfrac{-J_0(\nu_l/p_2)}{I_0(\tau a_2)[\nu_l^2+(\tau b)^2]}$
4	0	$-\nu_n^2J_1^2(\nu_n)\delta_{ln}E_-$	$-\nu_n^2J_1^2(\nu_n)\delta_{ln}$	$-2p_2^{-2}\nu_n^2\phi_{nl}(p_2^{-1})$	$\dfrac{-(\tau b)\nu_l J_1(\nu_l)I_0(\tau a_2)F(a_2)}{p_2^2[\nu_l^2+(\tau a_2)^2]\gamma}$

$[E_+=\exp[2i\tilde{g}(\kappa/\beta+\tilde{\lambda}_{bn})],\quad E_-=\exp[-2i\tilde{g}(\kappa/\beta-\tilde{\lambda}_{bn})],$

$F(a)=K_0(\tau b)/I_0(\tau b)-K_0(\tau a)/I_0(\tau a),\quad p_1=a_1,/b,\quad p_2=a_2/b,\quad \tilde{g}=g/2b$

An equivalent system of equations can also be obtained by matching the field on the surface $r=a$ (Henke, 1985a). For small openings, matching at $z=\pm g/2$ is preferable, because the field in the structure under consideration, in this case is close to the field of a pillbox cavity. This type of matching is also the only one possible when the tubes have different radii. In calculations with equal side-pipe radii, the two types of matching are in close agreement.

B. The impedance of a cavity and a collimator

Suppose that the coefficients X_n^N, defined as the solution of the system Eq. (4.23), are found. Using definitions Eqs. (4.18)–(4.21), we can now find the longitudinal component of the electric field $E_z(z)$ from Eqs. (4.5) and (4.8). Substituting it into formula Eq. (2.5) and performing the integration in it, we find

$$Z(k)=-\frac{Z_0}{\pi}\sum_n\left[\frac{x_n(\tilde{k}/\beta-\tilde{\lambda}_{aln})}{1+(\tau a_1/\nu_n)^2}+\frac{y_n(\tilde{k}/\beta+\tilde{\lambda}_b)}{1+(\tau b/\nu_n)^2}\exp\{[2i\tilde{g}(\tilde{\lambda}_b-\tilde{k}/\beta)]-1\}\right.$$
$$\left.-\frac{t_n(\tilde{k}/\beta-\tilde{\lambda}_b)}{1+(\tau b/\nu_n)^2}\exp\{[2i\tilde{g}(\tilde{\lambda}_b+\tilde{k}/\beta)]-1\}+\frac{z_n(\tilde{k}/\beta+\tilde{\lambda}_{a2n})}{1+(\tau a_2/\nu_n)^2}\right]. \tag{4.25}$$

Quantities $\tilde{k}$, $\tilde{g}$, and $\tilde{\lambda}$ are defined in Eqs. (4.13) through (4.17). Formula (4.25) is valid for both a cavity and a collimator, if the expansion coefficients x_n, y_n, t_n, and z_n in it are understood to be given by the solution of Eq. (4.23) for a cavity and for a collimator, respectively.

In the ultrarelativistic limit, $\gamma\to\infty$, the impedance can be found by integrating the field along any path displaced by r; see Sec. III.B (Weiland, 1983):

$$Z(k)=-(Z_0/\pi)\sum_n(x_nJ_0(\nu_nr/a_1)(\tilde{k}-\tilde{\lambda}_{a1n})+y_nJ_0(\nu_nr/b)(\tilde{k}+\tilde{\lambda}_b)\{\exp[2i\tilde{g}(\tilde{\lambda}_b-\tilde{k})]-1\}$$
$$-t_nJ_0(\nu_nr/b)(\tilde{k}-\tilde{\lambda}_b)\{\exp[2i\tilde{g}(\tilde{\lambda}_b+\tilde{k})]-1\}+z_nJ_0(\nu_nr/a_2)(\tilde{k}+\tilde{\lambda}_{a2n}))\,. \tag{4.26}$$

The remarkable feature of this formula is that the right-hand side of it *does not* depend on r in spite of its explicit presence there.

In particular, for a cavity with equal side-pipe radii a, $b=pa$, a convenient choice is $r=a$, since then the regions $z>g/2$ and $z<-g/2$ do not contribute to the value of the integral:

$$Z_{\rm cav}(k)=-(Z_0/\pi)\sum_n J_0(\nu_np)(y_n(\tilde{k}+\tilde{\lambda}_b)\{\exp[2i\tilde{g}(\tilde{\lambda}_b-\tilde{k})]-1\}-t_n(\tilde{k}-\tilde{\lambda}_b)\{\exp[2i\tilde{g}(\tilde{\lambda}_b+\tilde{k})]-1\})\,. \tag{4.27}$$

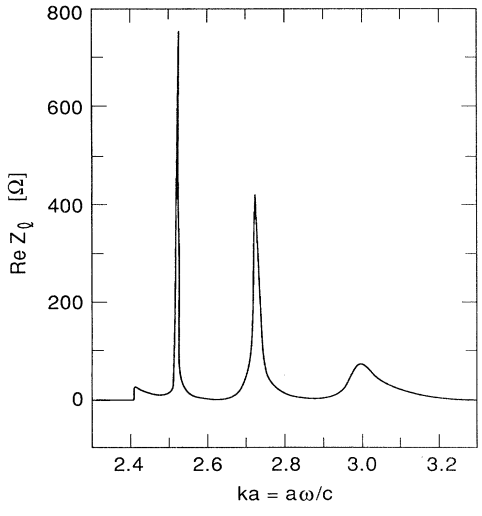

FIG. 4. The real part of the longitudinal impedance of a cavity as a function of dimensionless parameter $ka=a\omega/c$; $a=a_1=a_2$, $g/2b=0.302$, $a/b=0.152$.

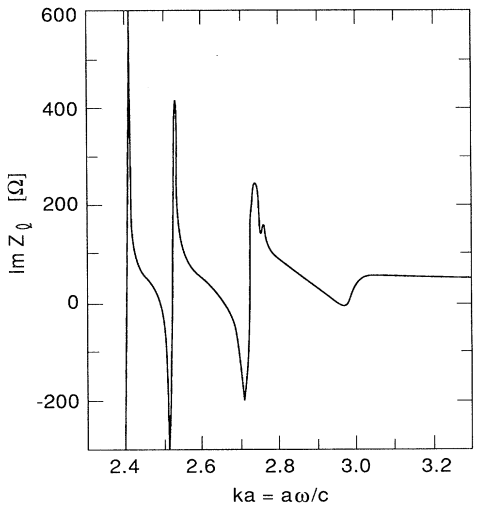

FIG. 5. The same as in Fig. 4, but for the imaginary part of the impedance.

For a collimator a convenient choice is $r=b$. In this case, the region $-g/2<z<g/2$ does not contribute to the value of the integral

$$Z_{\rm coll}(k)=-(Z_0/\pi)\sum_n [x_n J_0(\nu_n/p_1)(\tilde{k}-\tilde{\lambda}_b) + z_n J_0(\nu_n/p_2)(\tilde{k}+\tilde{\lambda}_b)] . \quad (4.28)$$

In general, a solution of Eq. (4.23) can be found only numerically. Two computer codes, RCVTY [for the geometry sketched in Fig. 3(a)] and RCLMTR [for the geometry sketched in Fig. 3(b)], exist for this purpose (Kheifets, 1987). An approximate solution is found by truncating the system to a finite size, inverting its matrix and solving for the coefficients. One can expect that such a solution is valid for modes with wavelengths larger than the diameter of the opening. For parameter values that are not too extreme, a matrix size of 20×20 is usually sufficient to obtain reasonable accuracy for the values of ka in the range $0\le ka\lesssim 3.0$. The results are independent of the matrix size up to the maximum size of 100×100 allowed by the codes.

The impedance of the same structure was also calculated by Henke (1985a) who matched the field on the surface $r=a$, $-g/2<z<g/2$. In Figs. 4 and 5 (Kheifets, 1987) we present the respective real and imaginary parts of the impedance calculated using the code RCVTY. One finds good agreement with the impedance calculated by Henke (1985a) for all frequencies except for a small region around the cutoff frequency of the pipe $ka=2.405$. More calculations of the narrow-band impedance of a cavity with the beam pipes can be found in papers by Warnock *et al.* (1982), Warnock and Bart (1984), Vos (1986, 1987), and van Rienen and Weiland (1986).

The dependence of the impedance on the particle energy is illustrated in Figs. 6 and 7 (Kheifets, 1987), where

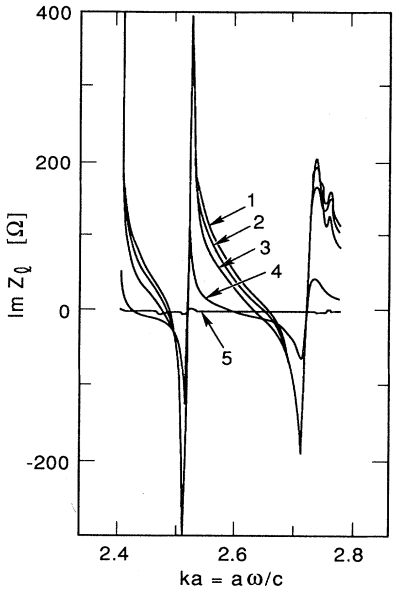

FIG. 7. The same as in Fig. 6 but for the imaginary part of the impedance.

the real and imaginary parts of the longitudinal impedance of a cavity are plotted for several different Lorentz factors γ. As we can see, the impedance at $\gamma=10$ is indistinguishable from its value at $\gamma=\infty$.

To illustrate the behavior of the impedance of a collimator, the respective real and imaginary parts of the impedance of a thin collimator for the SLAC geometry are plotted in Figs. 8 and 9 (Kheifets, 1987).

The transverse impedance of a cavity was calculated in papers by Kheifets *et al.* (1987a, 1987b) and by Henke (1985b).

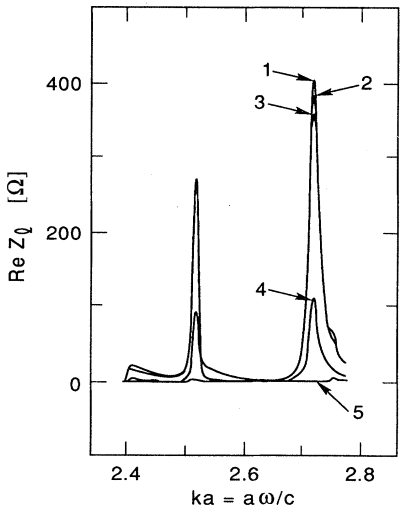

FIG. 6. An illustration of the dependence of the real part of the impedance on γ for the same cavity as in Fig. 4: (1) $\gamma=100$, (2) $\gamma=10$, (3) $\gamma=5$, (4) $\gamma=2$, (5) $\gamma=1.4$.

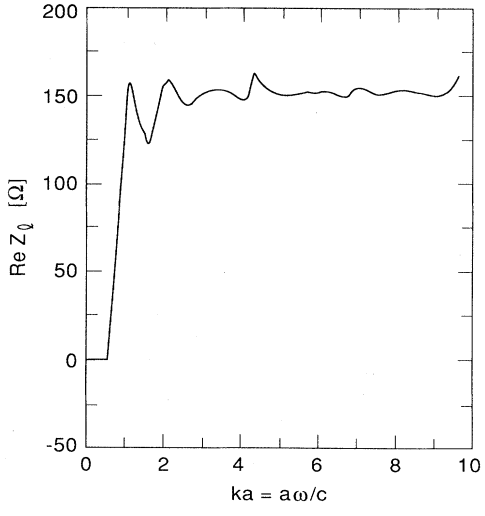

FIG. 8. The real part of the longitudinal impedance of a very thin collimator as a function of dimensionless parameter $ka=a\omega/c$; $a=a_1=a_2$, $g/2b=0.217$, $a/b=0.281$.

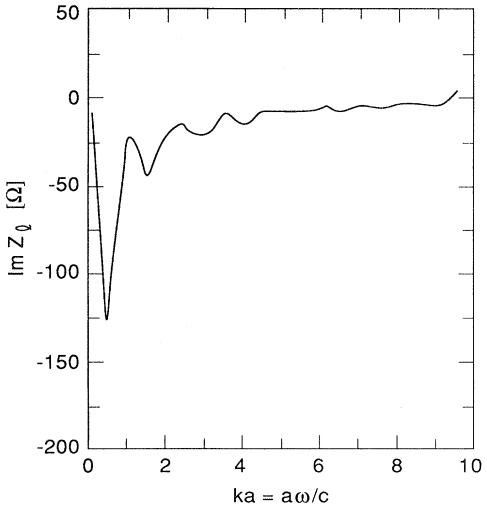

FIG. 9. The same as in Fig. 8, but for the imaginary part of the impedance.

C. The impedance of a step

Another important case is an infinitely-long straight pipe with an abrupt change of its cross section (a "step"). The coupling impedance of a step for a planar geometry was considered by Hereward (1975). We give here the calculation of the coupling impedance of a step in a cylindrical pipe (Kheifets and Heifets, 1986a, 1986b).

The geometry and the coordinate system are sketched in Fig. 1.

As discussed in Sec. III.D, one needs to distinguish two cases when considering a step:

In: A charge coming out of the bigger pipe of the cross section radius a and entering the narrow pipe of the cross section radius b. (We use a subscript "in" for this case.)

Out: A charge exiting from the narrow pipe and entering the bigger one. (We use a subscript "out" for this case.)

Both of these cases are included in the solution derived in the previous section. For example, case *In* of a charge passing through a *decreasing* cross section can be obtained by assuming $a_2=b$ (or equivalently, $p_2=1$), and $g=0$, in the equations describing a collimator. Similarly, case *Out* of a charge passing through an *increasing* cross section can be obtained by assuming $a_1=b$ (or equivalently, $p_1=1$) and $g=0$, in the same equations.

Using Eq. (4.25) we find that the narrow-band longitudinal coupling impedance for a charge entering the narrow pipe is

$$Z_{\rm in}(k)=-(Z_0/\pi)\sum_n [x_n(\tilde{k}-\tilde{\lambda}_a)+z_n(\tilde{k}+\tilde{\lambda}_b)] \ . \quad (4.29)$$

For a charge exiting the narrow pipe, respectively,

$$Z_{\rm out}(k)=-(Z_0/\pi)\sum_n [x_n(\tilde{k}-\tilde{\lambda}_b)+z_n(\tilde{k}+\tilde{\lambda}_a)] \ . \quad (4.30)$$

Coefficients x_n and z_n here are defined by solving an infinite system of linear algebraic equations which follow from Eq. (4.23) and Tables I and II:

$$\sum_m [T_{lm}\pm\delta_{lm}\tilde{\lambda}_{al}J_1^2(\nu_l)]g_m^{\pm}=P_l \ , \quad (4.31)$$

where

$$P_l=J_0(\nu_l p)/\nu_l^2 \ , \quad (4.32)$$

$$T_{lm}=4\nu_m^2 p^4 J_0(\nu_m p)J_0(\nu_l p) \times\sum_n \frac{\tilde{\lambda}_{bn}}{(\nu_n^2-\nu_m^2p^2)(\nu_n^2-\nu_l^2p^2)} \ , \quad (4.33)$$

$g_m^-\equiv -x_m$, $g_m^+\equiv z_m$, $p=b/a$, $\tilde{\lambda}_{al}=a\lambda_{al}$, $\tilde{\lambda}_{bl}=b\lambda_{bl}$; and $a=a_1$, $b=a_2$ for $Z_{\rm in}$, $b=a_1$, $a=a_2$ for $Z_{\rm out}$.

It is instructive to consider two limiting cases. If there is no step, i.e., $b=a$, then $P_l=0$ for all l, $x_l=0$, $z_l=0$ and no radiation occurs. In the opposite limit, when the pipe is closed, i.e., $b=0$, $p=0$, one obtains the exact solution

$$x_n=-\frac{1}{\nu_n^2 J_1^2(\nu_n)\sqrt{k^2a^2-\nu_n^2}} \ , \quad z_n=0 \ , \quad (4.34)$$

which gives the radiation produced in a Faraday cup.

An approximate solution of Eq. (4.31) has been found numerically by truncating its matrix to a finite size, inverting it and solving for the coefficients. For moderate values of parameters, a 20×20 matrix is sufficient to obtain reasonable accuracy. Since the magnitude of the coefficients $g_m^{\pm}$ fall off with increasing m rather rapidly,

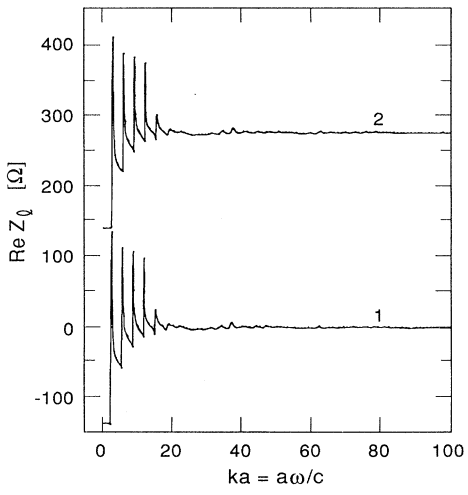

FIG. 10. The real part of the longitudinal coupling impedance of a cross section step as a function of parameter $ka=a\omega/c$; $b/a=0.1$; the matrix size is 60×60; (1) $\mathrm{Re}Z_{\rm in}$, (2) $\mathrm{Re}Z_{\rm out}$.

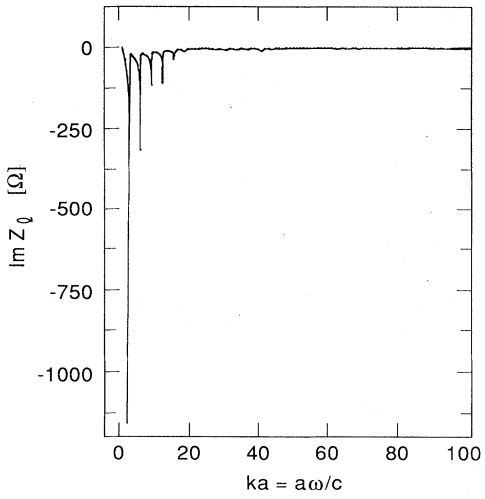

FIG. 11. The imaginary part of the longitudinal coupling impedance of a step as a function of parameter $ka=a\omega/c$; $b/a=0.1$; matrix size is 60×60. The imaginary parts of both $Z_{\rm in}$ and $Z_{\rm out}$ are found to be equal in agreement with Eq. (3.45).

the result does not change with a larger matrix size. An illustration of the narrow-band impedance behavior is presented in Figs. 10 and 11 (Kheifets and Heifets, 1986a), where the respective real and imaginary parts of longitudinal impedance are plotted for $p=0.1$ as functions of the normalized frequency ka. The resonant character of the impedance is clearly exhibited.

The impedances of narrowing and widening steps are similar except that the latter is shifted up by a constant. The shift is basically proportional to the difference of the EM field energy of a particle traveling in pipes with radii a and b. For a narrowing step, the radiated energy is taken out of the excess of the particle field energy in a wide pipe. As a result, the loss factor is small; see the area under curve 1 in Fig. 10. A careful examination shows that the loss factor is negative, corresponding to the gain of energy. The increase of the particle energy can be interpreted as a result of acceleration due to attraction by the image charge in the flange of the step. This effect is also noticed in a paper by Chan and Schweinfurth (1987). For a widening pipe, a restoration of the particle field takes place. The energy for this is taken away from the particle energy. Correspondingly, the loss factor is positive and large; see curve 2 in Fig. 10.

D. A perturbation method

An approximate solution of Eq. (4.23), obtained by truncation, is discussed in the previous sections. Another approximation for the narrow-band impedance of a cavity is achieved by using a perturbation method (Heifets, 1988, 1990a).

In a cavity with an opening to a waveguide (beam pipe, RF coupler, etc.), a mode above the cutoff frequency is coupled to modes propagating in the waveguide. That produces a finite width of the corresponding resonance in the narrow-band impedance (in addition to the width due to the finite wall resistivity). The existence of the narrow-band impedance is a consequence of the fact that this coupling is small. A perturbation theory in this small parameter can be developed.

In the zeroth approximation, the field pattern inside the cavity is the same as that of the closed cavity, and tangential components of the electric field are zero on the opening. In the first approximation the matching of the normal component of the electric field defined amplitudes of the longitudinal components of the waves propagating in the waveguide. The transverse components in the waveguide are then uniquely defined which, in turn, defines the tangential components of the field on the cavity opening. As a result, the relation between the normal and tangential components of the field on the opening inside the cavity can be written as

$$E_{rn}=\zeta_n H_{\theta n} , \tag{4.35}$$

where the coefficient $\zeta_n=\sqrt{1-(\nu_n/kb)^2}$ is the effective surface impedance of the opening. For example, the frequency shift of a nth mode caused by the opening can be calculated using the well-known result (Landau and Lifshitz, 1982) for the frequency shift due to surface impedance:

$$\omega_n-\omega_{0n}=-\frac{ic}{2}\frac{\int dS\,\zeta_n|\mathbf{H}_n|^2}{\int d\mathbf{S}\cdot\mathbf{r}(|\mathbf{H}_n|^2-|\mathbf{E}_n|^2)} . \tag{4.36}$$

The same idea that modes in the cavity with a small opening are almost the same as modes in the closed cavity may be utilized for an effective truncation of the exact system of equations obtained in the previous subsections. To obtain a set of equations suitable for the perturbation solution, we exclude coefficients x_n and z_n from Eq. (4.23) and make the following substitution:

$$y_n=i(d_n^+ + d_n^-)e^{i(\mu-\chi_n)} , \tag{4.37}$$

$$t_n=i(d_n^+ - d_n^-)e^{-i(\mu+\chi_n)} , \tag{4.38}$$

where $\chi_n=g\lambda_{bn}/2$, with λ_{bn} defined in Eq. (4.17), and $\mu=gk/2$. Such substitution corresponds to the decomposition of the field into standing waves. Coefficients $d_n^{\pm}$ are amplitudes of the longitudinal even (cosinelike) and odd (sinelike) modes, respectively. They satisfy two separate systems of equations:

$$d_n^+=\frac{i}{\sin\chi_n}\left[P_n\sin\mu+\frac{1}{2}\sum_m T_{mn}d_m^+\cos\chi_m\right] \tag{4.39}$$

and

$$d_n^-=\frac{i}{\cos\chi_n}\left[P_n\cos\mu-\frac{1}{2}\sum_m T_{mn}d_m^-\sin\chi_m\right] . \tag{4.40}$$

The coefficients T_{nm} and P_n are defined as

$$T_{nm}=\frac{4g\nu_m^2}{b\chi_n}\left[\frac{a}{b}\right]^4\frac{J_0(\nu_n a/b)J_0(\nu_m a/b)}{J_1^2(\nu_n)}\sigma_{nm}\ , \tag{4.41}$$

where

$$\sigma_{nm}=\sum_l\frac{\sqrt{(ka)^2-\nu_l^2}}{[\nu_l^2-(\nu_n a/b)^2][\nu_l^2-(\nu_m a/b)^2]} \tag{4.42}$$

and

$$P_n=(g/2b\chi_n)J_0(\nu_n a/b)/2\nu_n^2J_1^2(\nu_n)\ . \tag{4.43}$$

For the impedance in terms of d_n^+ and d_n^- we have

$$Z(\omega)=-\frac{Z_0}{\pi}\frac{g}{b}\sum_n\nu_n^2J_0(\nu_n a/b)\times\left[(d_n^++d_n^-)\frac{\sin(\mu-\chi_n)}{\mu-\chi_n}+(d_n^+-d_n^-)\frac{\sin(\mu+\chi_n)}{\mu+\chi_n}\right]. \tag{4.44}$$

The concept of narrow-band impedance presumes that the openings are small in comparison to the cavity surface. In this case, we may expect that the field pattern inside the cavity is perturbed by the presence of the side tubes only slightly, and is similar to that of the closed cavity (Dôme, 1985). Therefore, in the vicinity of the eigenfrequencies of the unperturbed cavity for which

$$\sin\chi_n\approx 0,\quad \chi_n\approx\chi_{nm}^0=m\pi,\quad \text{for } n \text{ even}\ , \tag{4.45}$$

and

$$\cos\chi_n\approx 0,\quad \chi_n\approx\chi_{nm}^0=(m+\tfrac{1}{2})\pi,\quad \text{for } n \text{ odd}\ , \tag{4.46}$$

only diagonal modes $d_n^\pm$ need to be retained in the sums in Eqs. (4.39) and (4.40). This gives

$$d_n^+=\frac{iP_n\sin\mu}{\sin\chi_n+(i/2)T_{nn}\cos\chi_n}\ , \tag{4.47}$$

and

$$d_n^-=\frac{iP_n\cos\mu}{\cos\chi_n-(i/2)T_{nn}\sin\chi_n}\ . \tag{4.48}$$

Other amplitudes $d_l^\pm$, where $l\neq n$, describe the mixing of the modes of a closed cavity and are zero in this approximation. This approximation can be refined, however, by substituting Eqs. (4.47) and (4.48) into the right-hand side of Eqs. (4.39) and (4.40). This will give $d_m^\pm\neq 0$. Repeating the substitution further refines the approximation.

Equations (4.47) and (4.48) have the typical resonance structure with width γ_{nm} and frequency ω_{nm} of the resonance given by

$$\gamma_{nm}=\frac{4c^2\chi_{nm}^0}{g^2\omega_{nm}}T_{nn},\quad \omega_{nm}=c\left[\frac{\nu_n^2}{b^2}+\frac{4\pi^2m^2}{g^2}\right]^{1/2}. \tag{4.49}$$

From this follows the estimate of the external Q factor: $Q=2\gamma_{nm}/\omega_{nm}$. The expression on the right-hand side of the first equation in Eq. (4.49) is simply the ratio of the energy flow $\dot{W}_{nm}$ of the mode labeled n,m, which is given by the integral of the Poynting vector over the cross section of the pipe to the energy W_{nl} stored in this mode:

$$\gamma_{nm}=-\frac{\dot{W}_{nm}}{W_{nm}}\ . \tag{4.50}$$

The loss factor κ_{nm}^l [see Eq. (2.10)] for a mode (n,m) can be found from Eqs. (4.44), (4.47), and (4.48). For a mode $\chi_n=m\pi$, it is

$$\kappa_{nm}^l=\frac{16}{g}\frac{J_0^2(va/b)}{\nu^2J_1^2(\nu)}\sin^2\frac{\omega_{nm}g}{2c}\ , \tag{4.51}$$

and for a mode $\chi_n=(m+\frac{1}{2})\pi$, it is

$$\kappa_{nm}^l=\frac{16}{g}\frac{J_0^2(va/b)}{\nu^2J_1^2(\nu)}\cos^2\frac{\omega_{nm}g}{2c}\ . \tag{4.52}$$

In calculating the longitudinal impedance, it is instructive to compare two approximate methods with each other and with purely numerical methods. The solid line in Fig. 12 (Heifets, 1990a) represents the real part of the longitudinal impedance $\mathrm{Re}Z(ka)$ obtained from Eq. (4.44) by the following procedure. For a given frequency, we find the number n_0 of the nearest resonance which satisfies Eqs. (4.45) or (4.46). Then the impedance is calculated, retaining in Eq. (4.44) a single term with the number n_0 while the coefficients $d_n^\pm$ are defined by Eqs. (4.47) and (4.48). The dashed line gives the contribution of the nonresonant modes in some band $\pm\Delta n$ around the resonance. The parameters used are $a/b=0.318$ and $g/2b=0.600$. Figure 13 shows for comparison the real part of the impedance calculated by truncating the set of Eqs. (4.39) and (4.40). In this example, the width of the band was $\Delta n=10$ (in total, twenty equations were retained). The agreement between the results shown in

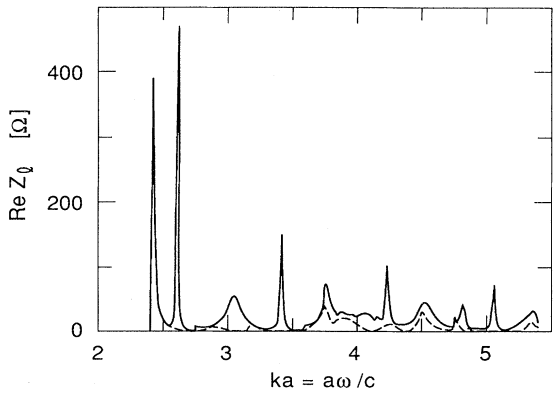

FIG. 12. The real part of the impedance according to the perturbation model. A single mode nearest to ka is taken into account, $a/b=0.318$, $g/2b=0.600$ (the solid line). The dashed line gives the contribution of the nonresonant modes (see text).

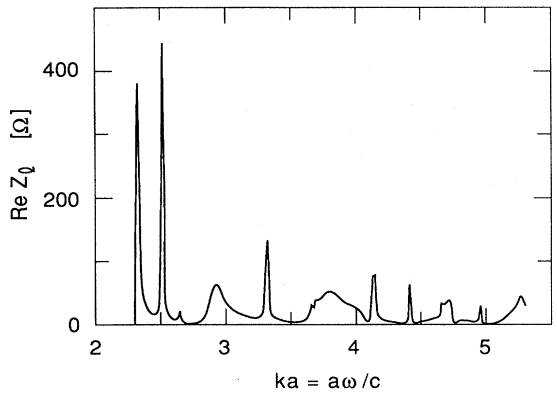

FIG. 13. The real part of the impedance obtained by truncating the system of equations; $a/b=0.318$, $g/2b=0.600$.

Figs. 12 and 13 could be even better if, instead of one, the two nearest resonance modes were retained in Eqs. (4.39) and (4.40). The broadening of the resonance obtained by the perturbation method for the CEBAF cavity is illustrated in Fig. 14. The real part of the impedance

$$\mathrm{Re}Z(\omega)=\sum_n\left[\frac{\kappa_n\gamma_n}{(\omega-k_nc)^2+\gamma_n^2}+\frac{\kappa_n\gamma_n}{(\omega+k_nc)^2+\gamma_n^2}\right] \tag{4.53}$$

is shown here (the solid line). The loss parameters κ_n and frequencies k_nc were calculated with the help of the program URMEL (Weiland, 1983c). The widths γ_n (related to the external Q factor) were calculated as defined in Eq. (4.49). The dashed line gives the impedance calculated with the widths caused by the finite conductivity of the walls (unloaded Q_0).

It is worth mentioning a calculation by Sands (1977)—closely related to the subject of the present paper—which gives the low-frequency radiation from a small hole in a vacuum chamber. Sands' derivation is based on the perturbation analytical solution obtained by Bethe (1944).

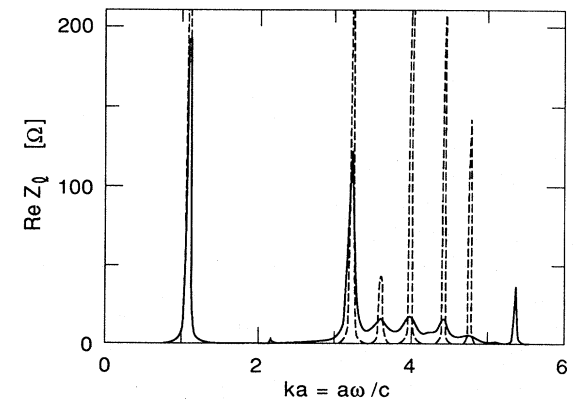

FIG. 14. The broadening of the higher resonances due to radiation; solid line, loaded Q; dashed line, unloaded Q_0.

E. Trapped modes

Trapped modes are narrow resonances observed *above* the cutoff frequency, both in experiments (Fornaca *et al.*, 1987) and in numerical calculations (Heifets, 1988). Their field pattern corresponds to modes localized within a cavity with a relatively large Q factor. A trapped mode of the pillbox cavity with side tubes can be seen in Fig. 13 as a small spike near $ka\approx4.5$. Its amplitude is actually much higher than it appears in Fig. 13 if plotted with higher resolution.

Calculations with different pipe lengths using URMEL confirmed the existence of a trapped mode for a cavity with parameters $a/b=0.318$, $g/2b=0.600$. For the mode with the frequency $f\approx233.3$ MHz, which corresponds to $ka\approx4.5$, the field outside of the cavity decreases rapidly to zero, thus conforming to the definition of trapped modes. The ratio R/Q for this mode is unusually small.

The origin of trapped modes is unclear at the present time. Several explanations have been suggested for this phenomenon. One of them maintains that the sharp edges of the cavities can cause multiple reflection of a wave and, as a result, give a long decay time to the mode. This explanation seems unsatisfactory, because above the cutoff frequency the reflection rate is relatively small, even for the sharp edges, and it goes rapidly to zero if the edges are rounded up. The reflection rate becomes exponentially small, when the function describing the edge boundary and all its derivatives are continuous.

Another hypothesis is that certain modes of a cavity produce waves in the tube that cancel each other. This assumption is probably also unsatisfactory if the modes are to be understood as those of a closed cavity unperturbed by the beam-pipe openings (Heifets, 1988).

However, a trapped mode may occur if two degenerate modes of the closed cavity are mixed by the perturbation brought about by the pipe openings. One of the mixed modes may become a trapped mode.

This idea was studied on a mode corresponding to $ka=4.5$. The mode was chosen because at the frequency $ka=4.5$ there is only one wave that can propagate in the tube. This wave is mostly generated by the coupling of the two degenerate modes in the cavity. The degree of the degeneracy of the modes can be varied by changing the parameters of the cavity. The analytical and numerical analysis supports the hypothesis of the connection between the mode degeneracy and the existence of the trapped modes. In particular, using the code URMEL it is shown that the mode remains trapped in a wide range of the cavity parameters, provided that the mode degeneracy is maintained.

F. The narrow-band impedance of bellows

Consider axially symmetric and longitudinally smooth periodic variations of a wall of a waveguide commonly known as *bellows*. Figure 15 illustrates the geometry and the coordinate system. In this case the application of the field matching technique used in previous subsections is very difficult. A more appropriate method for such cases will be described here. In general, all the Fourier harmonics of the polar angle θ, i.e., *modes* characterized by the number m, exist. However, our considerations will be restricted to an axial symmetric mode $m=0$ and, correspondingly, only the longitudinal impedance will be derived. Results for the dipole mode $m=1$ and, correspondingly, the transverse impedance, can be found in the paper by Kheifets and Zotter (1986).

Let us assume that the waveguide wall in the plane $\theta=$constant is described by the function

$$r=r_b(z)\ , \tag{4.54}$$

which is periodic in z with the period L. If the source particle moves along the axis of the waveguide, $r_0=0$, only the axial symmetric modes $m=0$ are excited. The series which gives the general solution of the Maxwell equations suitable for this case is found in the paper by Krinsky and Gluckstern (1981). The respective expansions of the longitudinal and radial components of the electric field with unknown coefficients B_p in the limit $\gamma\to\infty$ are

$$E_{\omega z}=\frac{iq}{\pi ca}e^{ikz}\sum_{p=-\infty}^{\infty}B_p e^{2i\pi pz/L}\frac{I_0(\alpha_p r/a)}{I_0(\alpha_p)}\ , \tag{4.55}$$

$$E_{\omega r}=\frac{q}{\pi ca}e^{ikz}\left[\frac{a}{r}+\sum_{p=-\infty}^{\infty}B_p e^{2i\pi pz/L}\left[ka+\frac{2\pi ap}{L}\right]\times\frac{I_1(\alpha_p r/a)}{\alpha_p I_0(\alpha_p)}\right]\ , \tag{4.56}$$

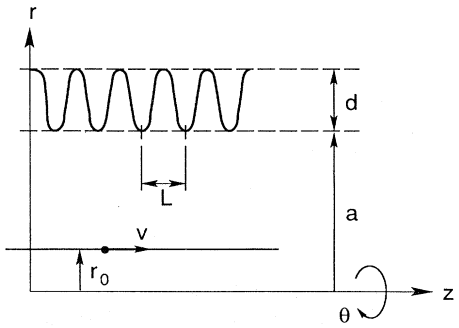

FIG. 15. Geometry of bellows and the coordinate system.

where I_0 and I_1 are modified Bessel functions of the first kind of the zeroth and first order, respectively. The quantity α_p is defined by

$$\alpha_p^2=\left[\frac{2\pi ap}{L}\right]^2+4\pi kap\frac{a}{L}\ . \tag{4.57}$$

The expansion coefficients B_p in this case are defined by the boundary condition (Krinsky and Gluckstern, 1981):

$$E_{\omega z}(r_b,z)=-E_{\omega r}(r_b,z)dr_b/dz\ , \tag{4.58}$$

which leads to the following infinite set of linear algebraic equations:

$$\sum_{p=-\infty}^{\infty}M_{np}B_p=N_n,\quad n=-\infty,\ldots,\infty\ , \tag{4.59}$$

where

$$M_{np}=\begin{cases}\left\langle\left[1-\frac{i}{2}kr_b(z)\frac{dr_b}{dz}\right]\exp\left[-\frac{2i\pi nz}{L}\right]\right\rangle, & p=0\ ,\\ \left[\left[\frac{2\pi a}{L}\right]^2 pn+\left[\frac{2\pi a}{L}\right]ka(p+n)\right]\left\langle\frac{I_0(\alpha_p r_b(z)/a)}{\alpha_p^2 I_0(\alpha_p)}\exp\left[-\frac{2i\pi(n-p)z}{L}\right]\right\rangle, & p\neq 0\ ,\end{cases} \tag{4.60}$$

and

$$N_n=\frac{2i\pi a}{L}\left\langle\frac{a}{r_b}\frac{dr_b(z)}{dz}\exp\left[-\frac{2i\pi nz}{L}\right]\right\rangle\ . \tag{4.61}$$

Here the brackets $\langle f\rangle$ are used to define the value of function $f(u)$ averaged over its period L. The longitudinal impedance per one period of bellows can be found using Eq. (2.5):

$$Z_l(k)=-iZ_0LB_0(k)/2\pi a\ . \tag{4.62}$$

The system of Eqs. (4.59) can be solved numerically. The computer code IMPASS [Impedances of Periodic Axially Symmetric Smooth Structures (Kheifets and Gygi, 1985)] enables one to calculate coefficients of the field expansions and to find both the longitudinal and the transverse impedances for $m=0$ and $m=1$ in the low-frequency region. The approach used here is not valid for the high-frequency region, where the impedance has a very complicated resonance structure.

Figure 16 (Kheifets and Gygi, 1985) presents the coefficient B_0 found with the help of IMPASS as a function

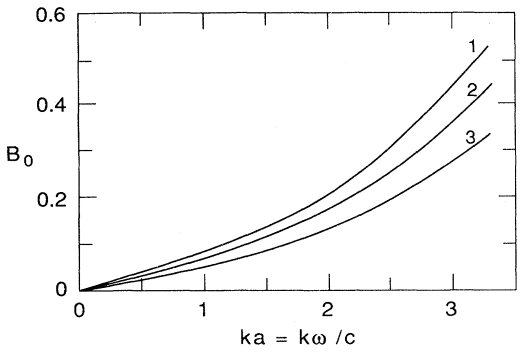

FIG. 16. Coefficient B_0 which defines the longitudinal impedance of bellows, see Eq. (4.62), for bellows with the boundary defined by equation $r_b(z)=a[1+\epsilon+(4\epsilon/\pi)\cos(2\pi z/L)]$ as a function of the parameter ka for three values of the parameter $\eta=2\pi a/L$: (1) $\eta=31.42$, (2) $\eta=20.94$, (3) $\eta=12.57$. The depth of corrugations is defined by $\epsilon\equiv d/2a=0.09$.

of the normalized frequency ka for three different values of bellows parameter $2\pi a/L$ and for the relative depth of the corrugations $d/2a=0.09$. More results can be found in the paper by Kheifets and Zotter (1986).

V. A DIFFRACTION MODEL FOR THE HIGH-FREQUENCY IMPEDANCE

In this section an approximate method is developed which is suitable for the study of the high-frequency behavior of the impedance. The integral equation which is equivalent to the Maxwell's equations is solved by iteration using approximate boundary conditions (Novokhatski, 1988; Heifets, 1989). This approach is very close to the diffraction models discussed by Bane and Sands (1987, 1990) and by Palmer (1986, 1989, 1990).

In the next subsection we define appropriate boundary conditions for the first iteration and study the implication of such a selection for a number of cases. In the next approximation the field on the boundary is assumed to be the field obtained on the previous step. For some structures—such as an array of irises—for which the interference of waves diffracted on different irises is of importance, the correct answer may be easily found by such a method (Sec. V.D). For other structures—such as a taper—for which there exists no known solution, the method gives an estimate of the impedance (Sec. V.E).

A. A method of iteration

Consider an arbitrary metal structure with openings. Let its volume be bounded by the surface S. The total field inside the volume excited by a relativistic particle is the sum of its synchronous field and the radiated field $\mathbf{E}_\omega$, $\mathbf{H}_\omega$. The radiated field satisfies the homogeneous wave equation and its value inside the volume is defined by the fields on its inner surface (Jackson, 1975):

$$\mathbf{E}_\omega=\int dS'[ik(\mathbf{n}'\times\mathbf{H}'_\omega)G_k+(\mathbf{n}'\cdot\mathbf{E}'_\omega)\cdot\nabla'G_k +(\mathbf{n}'\times\mathbf{E}'_\omega)\times\nabla'G_k]\ , \tag{5.1}$$

$$\mathbf{H}_\omega=\int dS'[-ik(\mathbf{n}'\times\mathbf{E}'_\omega)G_k+(\mathbf{n}'\cdot\mathbf{H}'_\omega)\cdot\nabla'G_k +(\mathbf{n}'\times\mathbf{H}'_\omega)\times\nabla'G_k]\ , \tag{5.2}$$

where $\mathbf{n}'$ is the unit vector normal to the surface pointed inside of the volume and

$$G_k(\mathbf{r},\mathbf{r}')=\frac{e^{ikR}}{4\pi R}\ , \qquad R=|\mathbf{r}-\mathbf{r}'|=\sqrt{(z-z')^2+r^2+r'^2-2rr'\cos\theta} \tag{5.3}$$

is the Green's function of the wave equation. It satisfies the equation

$$(\nabla^2+k^2)G_k=-\delta(\mathbf{r}-\mathbf{r}')\ .$$

In Eqs. (5.1) and (5.2), the derivatives in expression $\nabla'G_k$ are taken with respect to $\mathbf{r}'$.

For $k>0$ it can also be represented in the equivalent form:

$$G_k(\mathbf{r},\mathbf{r}')=\frac{i}{8\pi}\int_{-\infty}^{\infty}dp\,e^{ip(z-z')}\hat{G}_{kp}(r,r')\ , \tag{5.4}$$

where

$$\hat{G}_{kp}(r,r') \equiv\begin{cases}\displaystyle\sum_{m=0}^{\infty}A_mJ_m(\Omega r)H_m^{(1)}(\Omega r')\cos m\theta, & \text{for } r'>r\ ,\\ \displaystyle\sum_{m=0}^{\infty}A_mJ_m(\Omega r')H_m^{(1)}(\Omega r)\cos m\theta, & \text{for } r'<r\ .\end{cases} \tag{5.5}$$

Here $A_m=1$ for $m=0$, $A_m=2$ for all other m, and J_m and $H_m^{(1)}$ are the Bessel and the Hankel functions of the order m, respectively. Function $\Omega(k,p)$ has a cut along the negative axis in the plane of its argument p. We define it in the following way:

$$\Omega=\sqrt{k^2-p^2+2ik\varepsilon}\ ,\quad \varepsilon\to 0\ .$$

Correspondingly, functions $H_m^{(1)}$ of the purely imaginary argument ix are defined as $H_m^{(1)}(ix)=2(-i)^{m+1}K_m(x)/\pi$ (Gradshteyn and Ryzhik, 1980). For $k<0$, G_k is defined by $G_k=G^*_{-k}$.

Consider now the azimuthally symmetric structures with a particle traveling along its z axis with the velocity of light. Let the metal wall of the pipe be described by equation $r=r_b(z)$. In this case it is sufficient to consider only the monopole modes $m=0$. The method can also be extended to a general case $m\neq 0$.

The system of the integral equations (5.1), (5.2), can be solved approximately by the method of iteration. The

field on the boundary chosen on the first iteration defines the field on all the successive steps. The choice of the field for the first iteration is crucial for the convergence of the solution.

To define the field on the surface of a pipe of arbitrary shape, let us first consider the situation in a straight pipe $r_b=a=$constant. The EM field is a sum of the field of the particle in free space and the field of the image current in the wall (or the induced field). In the ultrarelativistic case, the electric field of a *particle* $\mathbf{E}_\omega^{(0)}$ has a large radial (i.e., the normal to the beam-pipe wall) component and a small longitudinal (tangential) component. The longitudinal component induces an image current in the wall. Since the image current has only a tangential component, it produces only a small tangential component of the *induced* field $\mathbf{E}_\omega^{(1)}$, which compensates for the tangential component of the particle field. The normal component of the induced electric field $E_{\omega n}^{(1)}$ and the tangential (azimuthal) component of the induced magnetic field $H_{\omega t}^{(1)}$ are zero on the pipe wall.

We now conjecture that in the high-frequency limit in the first approximation the boundary conditions for *the radiated* field in a pipe with a variable shape $r=r_b(z)$ are locally similar to those for a smooth pipe $a=$constant. The necessary condition for this assumption to be valid is that the length L of variation of the pipe shape, $dr_b/dz\approx a/L$, has to be large in comparison to the typical wavelength λ:

$$L\gg 1/k \ .$$

In other words, the assumption is that in the high-frequency limit in the first approximation the boundary conditions for the normal component of *the radiated* electric field is zero on any conductive boundary, as it is for a smooth pipe; i.e.,

$$E_{\omega n}^{(1)}=0, \quad \text{for } r=a(z-0) \ . \tag{5.6}$$

At the same time, the sum of the tangential component of the synchronous field of a particle $E_{t\omega}^{(0)}$ and the tangential component of the radiated field $E_{t\omega}^{(1)}$ on the metallic surface has to be zero:

$$E_{t\omega}^{(1)}=-E_{t\omega}^{(0)}, \quad \text{for } r=a(z-0) \ . \tag{5.7}$$

Hence, the components of the radiated field on the conductive boundaries are

$$E_{r\omega}^{(1)}=-E_{t\omega}^{(0)}\sin\alpha, \quad E_{z\omega}^{(1)}=-E_{t\omega}^{(0)}\cos\alpha \ , \tag{5.8}$$

where

$$E_{t\omega}^{(0)}=E_{r\omega}^{(0)}\sin\alpha+E_{z\omega}^{(0)}\cos\alpha \ . \tag{5.9}$$

Here $E_{r\omega}^{(0)}$ is given in Eq. (2.27) and $E_{z\omega}^{(0)}\approx 0$. The angle $\alpha=\alpha(z)$ is defined by $\tan\alpha=dr_b(z)/dz$.

The magnetic field in the azimuthally symmetric case has only azimuthal component $H_{\theta\omega}$. It can be shown (Heifets, 1989) that from Eq. (5.6) follows

$$H_{\omega\theta}^{(1)}=0, \quad \text{for } r=a(z-0) \ . \tag{5.10}$$

The radiated field on the cross sections $z=0$ and $z=g$ is the same as that in a straight pipe. For the azimuthally symmetric mode $m=0$ that means that the radiated field is zero.

Equations (5.8) and (5.10) specify the field on the boundary for the first iteration.

Equation (5.1) together with the radiation condition at infinity gives the component $E_z^{(1)}$ inside the pipe as the surface integral over the *metallic* walls of the pipe:

$$E_z^{(1)}=\int dS'\frac{\partial G_k}{\partial r'}E_t^{(0)}(r',z') \ . \tag{5.11}$$

For a smooth pipe $r_b(z)=a$, $dS=2\pi a\,dz$, and $E_t^{(0)}$ is defined in Eq. (5.9). In this case Eq. (5.11) gives

$$E_z^{(1)}=\frac{2iq\tau^2}{\omega}I_0(\tau r)K_0(\tau a)e^{ikz}, \quad \beta\approx 1 \ , \tag{5.12}$$

which agrees with the exact solution for a straight pipe given by the first term in Eq. (4.5). Note that in this approximation $I_0(\tau a)\approx 1$.

Equation (5.1) may be used to find the radiated field in a cavity iteratively. The field in the cavity found in the first approximation defines the radiated field on the boundaries, including beam-pipe openings. It may be taken as the value of the field on the boundary for the next iteration. The series obtained in this way are analogous to the Born's series of scattering theory. The expansion parameter of the series is the ratio of the amplitude of the tangential component of the radiated field $E_t^{(1)}$ to the amplitude of the tangential component of the particle field in Eq. (2.27). Note that the first approximation allows one to estimate this parameter and find the amplitude of the diffracted waves in the side pipes.

This method is next used to evaluate the impedance of a pillbox cavity with side pipes.

B. A diffraction model for a cavity

Consider a pillbox cavity of length g, radius b, and with side pipes of radius a. The surface integral Eq. (5.1) for this geometry is the sum of two integrals. The first integral, and the main contribution to the sum, is over the sides of the cavity at $z=0$ and $z=g$ for $a<r<b$. This is given by Eq. (5.11) with $E_t^{(0)}$ defined in Eq. (2.27). The second integral is over the cylindrical wall $r=b$ for $0<z<g$, which gives a negligibly small contribution of the order $(1/\gamma)^2$. Similar considerations are used in the papers by Gluckstern and Neri (1985, 1987a, 1987b) to obtain the narrow-band longitudinal impedance above the cutoff frequency of the beam pipe.

For the region $0<r<a$,

$$E_{\omega z}^{(1)}(r,z)=\frac{iq}{2c}\int_{-\infty}^{\infty}dp\,e^{ipz}[1-e^{i(k-p)g}]J_0(\Omega r) \times[H_0^{(1)}(\Omega b)-H_0^{(1)}(\Omega a)] \ . \tag{5.13}$$

This expression gives the first approximation for the diffracted field inside the cavity. Hence, to find the im-

pedance as defined in Eq. (2.5), we have to choose the path of integration along the beam-pipe wall $r=a$ in accordance with the discussion in Sec. III.B (Weiland, 1983b). Since on the pipe wall outside the cavity $E_{\omega z}(a,z)=0$, the range of integration in Eq. (2.5) is $0<z<g$. For $k>0$, we therefore have

$$Z_l(k)=\frac{Z_0}{2\pi}\int_{-\infty}^{\infty}\frac{dp}{k-p}J_0(\Omega a)[H_0^{(1)}(\Omega a)-H_0^{(1)}(\Omega b)] \times\sin^2\frac{g}{2}(k-p)\ . \tag{5.14}$$

An estimate of the integral in Eq. (5.14) is obtained in the paper by Heifets (1990d). For the region of parameters where $g\ll ka^2$ (a "cavity" regime) it reproduces the Lawson-Dôme formula (Lawson, 1968, 1990; Dôme, 1985):

$$Z_{\rm cav}(k)=(1+i)\frac{Z_0}{2\pi a}\left[\frac{g}{k\pi}\right]^{1/2}\ . \tag{5.15}$$

For the region of parameters where $ka^2\ll g\ll kb^2$, there is a transition regime

$$Z_{\rm trans}(k)=\frac{Z_0}{2\pi}\ln\frac{g}{ka^2}\ , \tag{5.16}$$

and for the region of parameters where $g\gg kb^2$, one obtains the impedance of a "step" found by Balakin and Novokhatski (1983) and independently by Kheifets (1987); see Eq. (6.79) in Sec. VI:

$$Z_S(k)=\frac{Z_0}{\pi}\ln\frac{b}{a}\ . \tag{5.17}$$

The difference between the impedances of a cavity Eq. (5.15) and a step Eq. (5.17) corresponds to different diffraction regimes. For $g\ll ka^2$ the transverse dimension of the area illuminated by the diffracted wave increases with z as $r\sim\sqrt{2z/k}$, which characterizes the Fresnel diffraction. For larger g for which $r\sim z/ka$, the Fraunhofer diffraction occurs.

The real part $\mathrm{Re}Z_l(k)$, Eq. (5.14), is produced by the values p in the range $-k<p<k$:

$$\mathrm{Re}Z_l(k)=\frac{Z_0}{2\pi}\int_{-k}^{k}\frac{dq}{k-p}J_0(\Omega a)[J_0(\Omega a)-J_0(\Omega b)] \times\sin^2\frac{g}{2}(k-p)\ . \tag{5.18}$$

The results of the numerical integration Eq. (5.18) are shown in Fig. 17 (Heifets, 1989), together with the estimate Eqs. (5.15) and (5.17). According to these calculations, the transition from the cavity to the step regime occurs for values of the cavity parameters such that

$$\eta=\frac{g}{k(b-a)^2}\approx 1\ . \tag{5.19}$$

Let us now evaluate the radial component of the radiated field $E_r^{(1)}$. It can be derived from Eq. (5.1), where the surface integral has to be taken over the surfaces $z=0$ and $z=g$, for $a<r<b$. In the high-frequency region $ka\gg 1$, neglecting terms of order of $1/ka$, we obtain

$$E_{\omega r}^{(1)}(r,z)=\frac{q}{2\pi c}\sum_{n=1}^{2}(z-z_n)e^{ikz_n} \times\int_0^{2\pi}d\theta\left[\frac{e^{ikR_n(a)}}{(a-r\cos\theta)R_n(a)} -\frac{e^{ikR_n(b)}}{(b-r\cos\theta)R_n(b)}\right], \tag{5.20}$$

where $R_n^2(x)=r^2+x^2-2rx\cos\theta+(z-z_n)^2$, $n=1,2$, and the summation is performed over two waves radiated from the surfaces $z_1=0$ and $z_2=g$. It is easy to see that the wave radiated from the surface $z=0$ does not contribute to $E_r^{(1)}$ at $z=0$. Only the wave scattered from the other surface changes the field in the next approximation. This is similar to the situation in scattering theory. The phase of this wave is proportional to the wave vector k and is large for $kg\gg 1$, giving, on average, a small correction. $E_{\omega r}^{(1)}(r,z)$ has a singularity $(r-a)^{-1/2}$ at $r=a$ as is well known (von Meixner, 1949). Note that at least in this approximation, a similar singularity appears also at $r=b$. These singularities leave the field energy finite. They are not essential in the evaluation of the integral in Eq. (5.1).

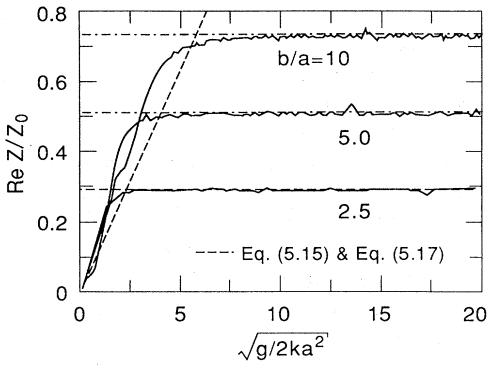

FIG. 17. The transition from a cavity regime to a step regime.

C. Loss factors in the diffraction model

The total impedance of the accelerator vacuum chamber is usually approximated by the sum of the impedances of its elements. This is equivalent to calculating the impedance of a given element while neglecting the diffracted EM field arising from all the other elements. In general this is incorrect. The interference of the EM field generated on different elements can be important. This will be illustrated below for an array of cavities. But even neglecting the interference, the estimate of the im-

pedance of a given element is not a simple task, especially for the high-frequency impedance.

Fortunately, in most cases an element can be represented either as a pillbox cavity with the beam pipes or as an abrupt change of the beam-pipe radius. The second structure (a step) can be considered as a very long cavity. The estimates of the impedances for these two types of structures (Bisognano *et al.*, 1988) according to the diffraction model discussed in the previous subsection give the correct dependence on all the physical parameters. This was verified by numerical calculations using the code TBCI over a wide range of parameters. The results are also valid for a very short bunch where direct numerical calculations require too much computing time and computer memory.

The high-frequency longitudinal impedance of a pillbox cavity with gap g, radius b, and side pipes of radii a, which is valid for $ka \gg 1$, is given by Eq. (5.15). The impedance falls off as $k^{-1/2}$ in an agreement with the results of the papers by Lawson (1968, 1990) and Dôme (1985). For a short Gaussian bunch, for which $\sigma \ll a$, this high-frequency tail of the impedance gives the main contribution to the energy loss for a cavity:

$$\kappa^{l}_{\rm cav}(\sigma)=\frac{\Gamma(\frac{1}{4})}{\pi a}\left[\frac{g}{\pi\sigma}\right]^{1/2}, \quad \frac{\Gamma(\frac{1}{4})}{\pi}=1.154 . \tag{5.21}$$

Equation (5.21) has been checked by the TBCI calculations for three different sets of parameters of CEBAF RF structures: (a) the fundamental power coupler, $a=3.5$ cm, $g=2.5$ cm, $b=5.5$ cm; (b) the higher-order mode coupler, $a=3.75$ cm, $g=3.75$ cm, $b=5.5$ cm; and (c) the gate valve $a=1.75$ cm, $g=2$ cm, $b=3.5$ cm. The rms length of the bunch σ was varied over the range 0.75–1.5 mm. The observed agreement is within 10%; see Fig. 18 (Bisognano *et al.*, 1988).

The transverse impedance can be estimated from the longitudinal impedance of the dipole mode using the Panofsky-Wenzel theorem (see Sec. III.A). The estimate

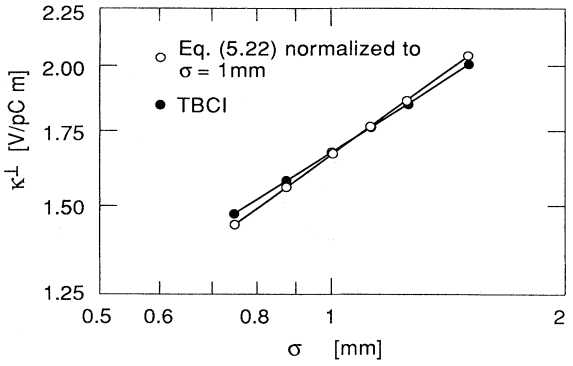

FIG. 19. The transverse loss factor ("kick") as a function of the rms bunch length; $a=3.5$ cm, $b=5.5$ cm, $g=2.5$ cm.

for the transverse loss factor is

$$\kappa^{\perp}_{\rm cav}(\sigma)=\frac{\sqrt{\pi g\sigma}}{a^3} . \tag{5.22}$$

This formula also agrees well with the results obtained by the code TBCI; see Fig. 19 (Bisognano *et al.*, 1988). For a very long cavity (a step), Eq. (5.21) is not applicable. The longitudinal impedance of a step is given by Eq. (5.17). Note that the frequency-independent impedance corresponds to a point wake function which is proportional to a δ function. The longitudinal loss factor for a step is

$$\kappa^{l}_{S}(\sigma)=\frac{2}{\sqrt{\pi}\,\sigma}\ln\frac{b}{a} . \tag{5.23}$$

The exact expression for the transverse loss factor of a step is unknown. In the paper by Bisognano *et al.* (1988), the following estimate is obtained:

$$\kappa^{\perp}_{S}(\sigma)=\frac{2}{\sqrt{\pi}\,a^2}\ln\frac{b}{a}\ln\frac{b}{\sigma} . \tag{5.24}$$

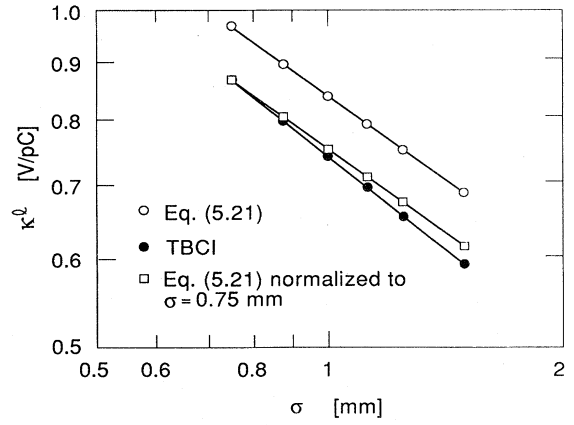

FIG. 18. The longitudinal loss factor as a function of the rms bunch length; $a=3.5$ cm, $b=5.5$ cm, $g=2.5$ cm.

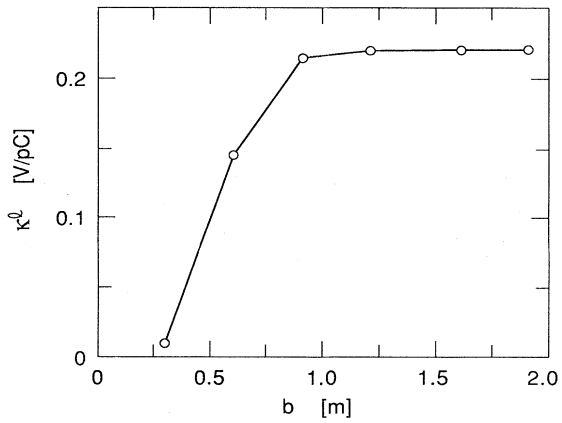

FIG. 20. The longitudinal loss factor as a function of b; $a=0.25$ m, $g=6.0$ m, $\sigma=0.06$ m.

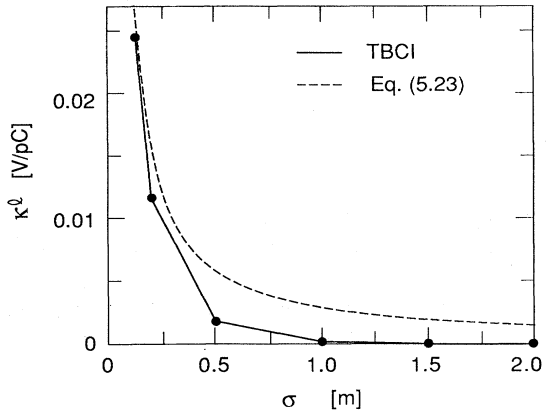

FIG. 21. The longitudinal loss factor as a function of σ; $a=1.5$ m, $b=2.0$ m, $g=20.0$ m.

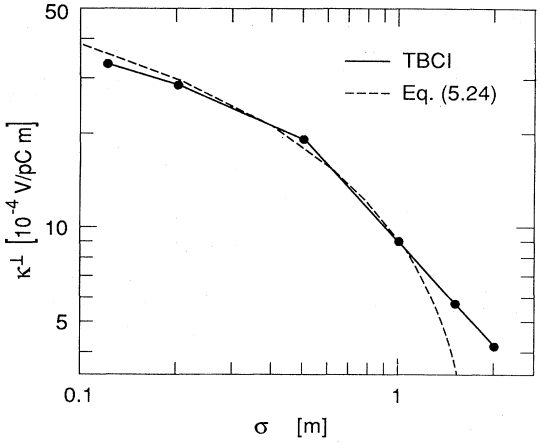

FIG. 22. The transverse loss factor as a function of σ; $a=1.5$ m, $b=2.0$ m, $g=20.0$ m.

These formulas contain both radii a and b, in contrast with Eqs. (5.15) and (5.21) for a short cavity. The regime of the cavity differs from the regime of the step by the fact that in the second case the signal from the outer wall of the cavity has enough time to reach a bunch traveling inside it, thus probing the outer radius of the cavity. If the parameter η, Eq. (5.19), for $k\sim 1/\sigma$,

$$\eta\equiv\frac{2g\sigma}{(b-a)^2} \tag{5.25}$$

is small, $\eta\ll 1$, the formulas for a cavity are valid. In the opposite case when $\eta\gg 1$, the regime of a step is fulfilled. This is illustrated in Fig. 20 (Bisognano *et al.*, 1988), where the dependence of the longitudinal κ_l loss factor on the radius b of the cavity is depicted. The longitudinal and transverse loss factors, as functions of the rms bunch length σ, are plotted in Figs. 21 and 22. In all cases the agreement of the estimates with numerical calculations is quite good. Equations (5.21)—(5.25) are convenient for a fast and reasonably accurate estimate of the impedance budget of an accelerator. However, Eq. (5.24) should be presently considered to be an empirical estimate.

D. A periodic array

The EM waves generated in one element of an accelerator propagate into the elements downstream of the system. There the waves interfere with the locally radiated field. Even if the impedance of each element assumed to be mutually independent is known, finding the impedance for the whole system is, in general, nontrivial.

In the high-frequency region, the previously described method of iteration is applicable. As an example of its application, we consider here a periodic structure. For an array of cavities where the number of cavities is large, the interference can drastically change the impedance. Another example where the interference is of importance (two adjacent cavities) is considered by Heifets (1989).

Let us consider a RF structure of a linear accelerator. It can be approximated by a periodic array of cavities built of irises in a waveguide. The irises, having equal round beam holes of radius a, are separated by a distance L. In the high-energy accelerator the signal reflected from the outer cavity wall does not reach the bunch moving with the velocity of light along the accelerator axis. For simplicity we therefore assume the outer radius to be infinitely large.

The radial component of the radiated field at location z of the accelerator, to good approximation, is the sum of the field Eq. (2.27) and a field of unknown amplitude $f(k,r)$ diffracted on the upstream irises:

$$E^{(0)}_{\omega r}(z,r)=-\frac{2q}{cr}e^{ikz/\beta}\vartheta(r-a)+\frac{2q}{c}f(k,r)e^{ikz}\vartheta(a-r)\ . \tag{5.26}$$

Here $\vartheta(x)$ is a step function. We use this expression as the zeroth approximation for E_t in Eq. (5.1). For the longitudinal field between the irises, $0<z<L$, Eq. (5.1) yields

$$E^{(1)}_{\omega z}(z,r)=\frac{iq}{2c}\int_{-\infty}^{\infty}dp\,e^{ipz}(1-e^{i(k-p)L})\times\int_0^{\infty}dr'[\vartheta(r'-a)-r'f(k,r')\vartheta(a-r')]\times\frac{\partial}{\partial r'}[J_0(\Omega r)H_0^{(1)}(\Omega r')\vartheta(r'-r)+J_0(\Omega r')H_0^{(1)}(\Omega r)\vartheta(r-r')]\ , \tag{5.27}$$

where $\Omega=\sqrt{k^2-p^2}$. The impedance per cell is

$$Z_l(k)=\frac{Z_0}{2\pi}\int_{-\infty}^{\infty}\frac{dp}{k-p}\sin^2\frac{L}{2}(k-p)J_0(\Omega a)H_0^{(1)}(\Omega a)[1+af(k,a)]$$
$$-\frac{2}{c}\int_{-\infty}^{\infty}\frac{dp}{k-p}\sin^2\frac{L}{2}(k-p)H_0^{(1)}(\Omega a)\int_0^a dr' J_0(\Omega r')\frac{\partial}{\partial r'}r' f(k,r') \ . \tag{5.28}$$

The first term here is the same as that for a single cavity, as given by Eq. (5.14), except for the additional factor $[1+af(k,a)]$. We will see that this factor is of order $1/k$. The second term in Eq. (5.28) is small. Hence, the high-frequency impedance of a periodic array becomes $Z_l(k)\propto k^{-3/2}$.

The equation defining function $f(k,r)$ can be obtained from the condition of periodicity for the radial component of the field $E_{\omega r}(z,r)$. The expression for $E_{\omega r}^{(1)}(z,r)$ can be found from the equation $\nabla\cdot\mathbf{E}=0$ and Eq. (5.27). At $z=L$ this yields

$$E_{\omega r}^{(1)}(L,r)=-\frac{q}{2c}\int_{-\infty}^{\infty}p\,dp\,e^{ipL}\int_0^{\infty}dr'[\vartheta(r'-a)-r'f(r')\vartheta(a-r')]$$
$$\times[J_1(\Omega r)H_1^{(1)}(\Omega r')\vartheta(r'-r)+J_1(\Omega r')H_1^{(1)}(\Omega r)\vartheta(r-r')] \ . \tag{5.29}$$

For $f(k,r)$ we thus obtain the following integral equation:

$$f(k,r)=\Phi(r)+\int_0^r r'dr'\Psi(r',r)f(k,r')$$
$$+\int_r^a r'dr'\Psi(r,r')f(k,r') \ , \tag{5.30}$$

where

$$\Psi(r,r')=\frac{1}{4}\int_{-\infty}^{\infty}p\,dp\,e^{-i(k-p)L}J_1(\Omega r)H_1^{(1)}(\Omega r') \tag{5.31}$$

and

$$\Phi(r)=-\int_a^b dr'\Psi(r,r') \ . \tag{5.32}$$

Note that $f(k,0)=0$.

Function $\Psi(r,r')$ describes the Fresnel diffraction on a circular hole. An estimate of the integral in Eq. (5.31) in the diffraction zone $r\simeq a$, $r'-r\gg\sqrt{2L/k}$ gives

$$\Psi(r,r')\simeq\Psi_0(r,r')$$
$$\equiv\left[\frac{k}{2\pi Lrr'}\right]^{1/2}$$
$$\times\exp\left[i\frac{k}{2L}(r-r')^2-i\frac{\pi}{4}\right] \ . \tag{5.33}$$

Equation (5.30) in this approximation simplifies to

$$f(k,r)=\Phi_0(r)+\int_0^a r'dr'\Psi_0(r,r')f(k,r') \ , \tag{5.34}$$

where

$$\Phi_0(r)\simeq\frac{-iL}{k}\frac{1}{a-r}\Psi_0(r,a) \ ,$$
$$\text{for } a-r\gg\sqrt{2L/k} \ . \tag{5.35}$$

Function $\Phi_0(r)$, describing the diffraction on a single iris, rapidly oscillates for $(a-r)>\sqrt{2L/k}$, and in this region is negligibly small. A solution of Eq. (5.34) can be found by an iterative procedure in which the solution f_n on the nth step is found by substituting f_{n-1} for $f(k,r)$ (with $f_1=\Phi_0$) in the integrand of Eq. (5.34). Subsequent iterations take into account the diffraction from the consecutive irises of the array. The iterative solution on the nth step is

$$f_n(k,r)\propto\exp\left[\frac{ik}{2L(n+1)}(r-a)^2\right] \ . \tag{5.36}$$

This function has a width which increases with n as $(a-r)\simeq\sqrt{(2L/k)(n+1)}$. Its amplitude decreases rapidly when the width becomes of the order of a; i.e., for $n>M\simeq ka^2/L$. Palmer (1987) noticed that M defines the minimal number of cavities sufficient for the impedance of a *finite* array to be approximated by the impedance of an *infinite* periodic structure. We discuss this in more detail in Section VI.

Function $\Psi_0(r,r')$ has a sharp peak as a function of $r-r'$. In the limit as $k\to\infty$ it can be approximated by the δ function:

$$\lim_{k\to\infty}\Psi_0(r,r')=\frac{1}{r}\delta(r-r') \ . \tag{5.37}$$

The solution of Eq. (5.34) in this limit is $f(\infty,a)=-1/a$. For finite but large $k\gg L/a^2$, we have $1+af(k,a)\sim(1/k)$; see below Eq. (5.41). The amplitude of the radiated field $f(k,r)$ at the iris increases from $f=0$ at $r=0$ to $f\approx-1/a$ at $r=a$, and then decreases as $-1/r$ for $r>a$. Recall that, for a single cavity, $E_{\omega r}^{(1)}$ has a discontinuity at $r=a$ changing from zero to $-1/a$. The continuity of the function $f(k,r)$, and, correspondingly, of the radiated field $E_{\omega r}^{(1)}$ at the point $r=a$ arises from the interference of the diffracted waves in the periodic structure. This is the reason that the asymptotic frequency dependence of the impedance for a single cavity differs from that of a periodic array of cavities.

To solve Eq. (5.34) numerically, it is convenient to introduce a new function, $F(a-r)$, defined by the expression

$$\frac{\partial}{\partial r} rf(k,r) = -\Lambda F(a-r) , \tag{5.38}$$

where

$$\Lambda = 1 + af(k,a) , \tag{5.39}$$

The function $F(a-r)$ satisfies the integral equation

$$F(a-r) = \sqrt{ra}\,\Psi_0(a,r) + \int_0^a dr' F(a-r')\sqrt{rr'}\Psi_0(r,r') , \tag{5.40}$$

with $\Psi_0(r,r')$ defined in Eq. (5.33). Equation (5.40) was solved numerically for different wave numbers k. The typical behavior of function $rf(k,r)$ is depicted in Fig. 23 (Heifets, 1989). The parameter $\Lambda(k)$ has been found from these calculations and its dependence on $ka^2/2L$ is shown in Fig. 24. It wobbles around (Heifets, 1989)

$$\Lambda \approx \frac{4\pi L}{ka^2} . \tag{5.41}$$

Function $F(a-r)$ oscillates rapidly (see Fig. 25); therefore, the last term in Eq. (5.30) is small. The remaining term has the same structure as that for a single cavity, but has an additional factor $\Lambda \propto 1/k$. Hence, the impedance of the periodic array decreases with the wave number as $k^{-3/2}$. For the real part of the impedance we obtain

$$\mathrm{Re}Z(k) = Z_0 \frac{2}{\sqrt{\pi}} \left[\frac{L}{ka^2}\right]^{3/2} , \tag{5.42}$$

while the same quantity decreases as $k^{-1/2}$ for a single cavity. The same dependence on k, i.e., $\mathrm{Re}Z(k) \propto k^{-3/2}$, was obtained in the optical resonator model (Vainshtein, 1963; Keil, 1972; Sessler, 1972; Brandt and Zotter, 1982). We give a more rigorous analytical derivation of these results in Sec. VI.D.

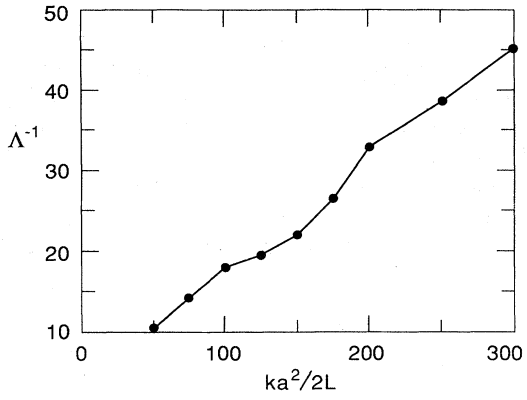

FIG. 24. Parameter Λ^{-1} as a function of $ka^2/2L$ (see text).

E. A taper

Consider a gradual transition—a *taper*—between two cross sections of the beam pipe from a smaller radius a to a larger radius b. We can expect that in such a case the energy loss of a bunch will be smaller than it would be while passing through a step. Until recently, no analytic methods for evaluating the effects of a taper were available. Here we use the method of iteration to derive an estimate of the effect of a linear taper; i.e., a taper in which the slope of the wall is constant. For short bunches, $\sigma \ll a < b$, the energy loss is dominated by the high-frequency modes $kb > ka \gg 1$. This allows one to estimate the loss and the impedance using Eq. (5.11).

Let us characterize the taper by an angle α at which the taper wall is inclined to the axis a: $\cot\alpha = g_1/(b-a)$, where g_1 is the length of the taper. For a step we have $g_1 = 0$, and $\alpha = \pi/2$. Based on the previous discussion,

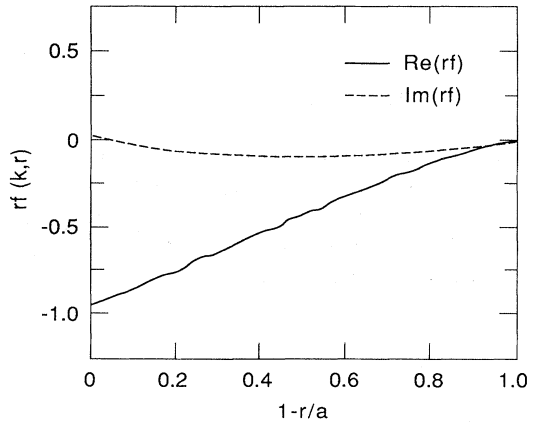

FIG. 23. Function $rf(k,r)$ (see text).

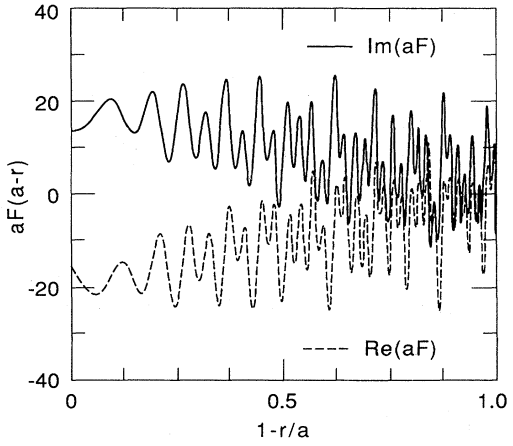

FIG. 25. Function $aF(a-r)$ (see text).

we can expect that the main contribution to the impedance comes from the waves with large k diffracted at small angles. The taper may be expected to reduce the impedance or the loss factor of the transition effectively, if its angle is comparable to or smaller than the Fresnel diffraction angle.

As shown below, for a bunch of rms length σ, the loss factor decreases with increasing taper length g_1 until it reaches a minimal value at $g_1 \simeq (b-a)^2/\sigma$, and it remains constant with further increases of g_1. A short taper, for which $g_1\sigma/2(b-a)^2 \ll 1$, is not effective in reducing the energy loss.

Consider a cylindrical cavity of total length g with slanted side walls comprising two symmetrical tapers of length g_1 on both sides. The symmetry of the cavity significantly simplifies calculations. We follow here the considerations of the paper by Heifets, 1989. Equation (5.11) for such a cavity gives

$$E^{(1)}_{\omega z}(r,z)=\frac{iq}{2c}\int_a^b dr'\int_{-\infty}^{\infty} dp\, e^{ipz}(\exp[i(k-p)(r'-a)\cot\alpha]-\exp\{i(k-p)[g-(r'-a)\cot\alpha]\})J_0(\Omega r)\frac{\partial H_0^{(1)}(\Omega r')}{\partial r'} . \tag{5.43}$$

Here $\Omega=\sqrt{k^2-p^2}$ and $\cot\alpha=g_1/(b-a)$. The two terms in Eq. (5.43) describe correspondingly the wave generated at the two tapers: the taper-out at $z=0$ and the taper-in at $z=g$. For $g_1=0$, it gives Eq. (5.14). The longitudinal impedance of a taper-out can be obtained by integrating the first term over z in the interval $0<z<L$ and considering the limit $L\to\infty$. A taper-in is considered in a similar way. This gives

$$Z_l(\omega)=\lim_{L\to\infty}(-1/c)\int_{-\infty}^{\infty}\frac{dp}{k-p}J_0(\Omega a)\{1-\exp[\mp i(k-p)L]\}\int_a^b dr'\exp[\pm i(k-p)(r'-a)\cot\alpha]\frac{\partial H_0^{(1)}(\Omega r')}{\partial r'} , \tag{5.44}$$

where the signs $\pm$ correspond to a taper-out and a taper-in. In the limit $L\to\infty$,

$$\lim_{L\to\infty}\frac{1}{k-p}(1-e^{\mp i(k-p)L})=\frac{1}{k-p}\pm i\pi\delta(k-p) ; \tag{5.45}$$

hence, the impedance is

$$Z_l(\omega)=\pm\frac{1}{c}\ln\frac{b}{a}-\frac{1}{2c}\int_{-\infty}^{\infty}\frac{dp}{k-p}J_0(\Omega a)\int_a^b dr'\exp[\pm i(k-p)(r'-a)\cot\alpha]\frac{\partial H_0^{(1)}(\Omega r')}{\partial r'} . \tag{5.46}$$

The first term corresponds to the difference in the field energies of a particle in the beam pipes of different radii. It is independent of the angle α. The real part of the second term describes the loss to the radiation, which is the same for a taper-out and a taper-in. The sum of the impedances of two tapers, calculated from Eq. (5.43), gives the impedance of the long tapered cavity. The difference of the losses for two tapers with the same angle α is independent of α:

$$\kappa^l_{\rm out}-\kappa^l_{\rm in}=\frac{2}{\sigma\sqrt{\pi}}\ln\frac{b}{a} . \tag{5.47}$$

This was noticed in numerical simulations (Chan, 1987). As was shown in a paper by Heifets (1988), a substantial contribution for a step is given by the region of variable p, for which $1/b \ll \Omega \ll 1/a$. Hence, if

$$\tan\alpha > \frac{b-a}{2ka^2} , \tag{5.48}$$

the exponent in Eq. (5.46) may be replaced by unity and the impedance of a taper is the same as the impedance of a step. In the opposite case of a small α, the exponent oscillates rapidly unless

$$(k-p)(r'-a)\cot\alpha \ll 1 . \tag{5.49}$$

Restricting the area of integration by this condition, we obtain for the real part of the impedance

$$\mathrm{Re}Z_l(\omega)=\mathrm{Re}Z_S(\omega)-\Delta Z_l(\omega) , \tag{5.50}$$

where Z_S is the impedance of a step, Eq. (5.17), and the correction term is

$$\Delta Z_l=\frac{1}{2c}\int_{-1}^{x_0}\frac{dx}{1-x}J_0(ka\sqrt{1-x^2}) \times[J_0(kr_m\sqrt{1-x^2})-J_0(kb\sqrt{1-x^2})] . \tag{5.51}$$

Here,

$$r_m=a+x_0,\quad x_0=\frac{\tan\alpha}{k(b-a)} . \tag{5.52}$$

To estimate the integral, we notice that ΔZ_l may be large only if the argument of the Bessel function in the integrand $\psi=kr_m\sqrt{1-x^2}$ is small within the range of integration. This is possible only if $ka\tan\alpha \ll 1$. If this condition is fulfilled, the correction term is

$$\Delta Z_l=\frac{1}{c}\ln\frac{1}{\zeta} , \tag{5.53}$$

where

$$\zeta=\begin{cases} a/b, & \text{if } kb\tan\alpha<1 , \\ 2ka\tan\alpha, & \text{if } 2kb\tan\alpha>1 . \end{cases} \tag{5.54}$$

The loss factor for a taper may be obtained by the convolution of Eq. (5.50) with the bunch distribution of rms length σ. In the case $b \gg a$, the correction term to the loss factor is

$$\Delta\kappa_l = \begin{cases} -\dfrac{1}{2\pi a}\cot\alpha, & \text{if } \tan\alpha \gg \sigma/a \ , \\ -\dfrac{1}{2\sigma\sqrt{\pi}}\ln\dfrac{b}{a}, & \text{if } \tan\alpha \ll \sigma/b \ . \end{cases} \tag{5.55}$$

Thus, the energy loss for a taper-out may be smaller than that for a step-out ($\alpha=\pi/2$) maximum by a factor of 2, even if the angle α is very small (Heifets, 1989; Yunn, 1989). For a long cavity tapered symmetrically from both ends, the correction Eq. (5.55) doubles, reducing for a sufficiently small angle, $\tan\alpha \ll \sigma/b$, the loss for a cavity to zero.

The dependence of the longitudinal loss factor of a one-sided taper on its angle can be approximated by the formula

$$\kappa_T^l = \frac{2}{\sigma\sqrt{\pi}}\left[1-\frac{\tilde{\eta}_1}{2}\right]\ln\frac{b}{a} \ , \tag{5.56}$$

where $\tilde{\eta}_1 = \min(1.0, \eta_1)$, and

$$\eta_1 = \frac{g_1\sigma}{(b-a)^2} \ . \tag{5.57}$$

For $\eta_1 > 1$, the loss factor of a taper reaches half the value of the loss factor for a step and remains constant with further increase of η_1.

A comparison of Eq. (5.56) with the calculations by the code TBCI is presented in Fig. 26 (Heifets, 1990b) for a cavity of length $g/a=115$, where $a=1$ cm, tapered from one side. The bunch length is assumed to be $\sigma/a=0.3$. Curves are plotted for the two respective ratios $b/a=4.0$ and $b/a=2.0$. The results of the TBCI calculations (solid lines) are in reasonably good agreement with those obtained from Eq. (5.56) (dashed lines).

For a symmetric taper, $\tilde{\eta}_1/2$ should be replaced by $\tilde{\eta}_1$:

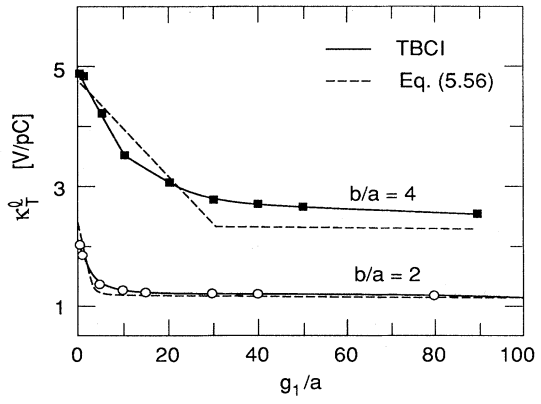

FIG. 26. The longitudinal loss factor of a taper as function of the radiative taper length g_1/a; $a=1$ cm, $\sigma/a=0.3$.

$$\kappa_T^l = \frac{2}{\sigma\sqrt{\pi}}(1-\tilde{\eta}_1)\ln\frac{b}{a} \ . \tag{5.58}$$

A long symmetric taper reduces losses to zero.

The independence of the losses on the direction of beam propagation is also confirmed in these calculations.

A quite different approach to the problem of a taper was recently developed by Yokoya (1990).

VI. ANALYTICAL RESULTS FOR THE HIGH-FREQUENCY IMPEDANCE

When the structure under consideration can be separated into simple parts for which the solutions of the Maxwell equations are known or can be found, a natural method for obtaining the solution for the whole structure is the field matching technique. The application of this method for calculating the narrow-band impedance is discussed in Sec. IV.A.

In the present section, using this method, we derive an exact system of equations that are suitable for the high-frequency region. An approximate solution of the system is obtained for several cylindrically symmetric structures. The high-frequency impedance is found for a step, for a cavity and for a periodic array of a finite number of cavities. It is shown that the observed transition from one regime (which is characteristic of a single cavity) to another regime (which is appropriate for an infinite periodic structure) can be explained by the interference of the EM waves diffracted from different cavities. The criterion governing such a transition is given. The results agree with the results obtained in the previous section using another approximation: the diffraction model. This supports the reliability of the approximations, and allows us to use them in more complicated cases where analytical methods do not exist. For example, a similar approach is used in the paper by Gluckstern and Neri (1989) to obtain the longitudinal impedance of a small obstacle.

The unique situation exists for a semi-infinite circular waveguide. In this case, an exact solution of the Maxwell equations can be found in a closed form. The Wiener-Hopf technique used for that purpose, and the derivation of the longitudinal impedance for that structure, are described in Sec. VI.F.

A. The basic system of algebraic equations

The starting point of the calculations of the high-frequency longitudinal impedance is a system of linear algebraic equations for unknown coefficients of the field expansion. We will derive the system of equations for the general case of a periodic array of M equal cylindrical cavities (Heifets and Kheifets, 1988, 1989) of radius b placed on an infinitely long beam pipe of constant radius a. A particle with charge q and velocity $v \sim c$ (i.e., $\beta \sim 1$) is assumed to move along the axis of the system $r_0=0$. We choose the plane $z=0$ to coincide with the beginning of the first cavity. Figure 27 gives the layout of the

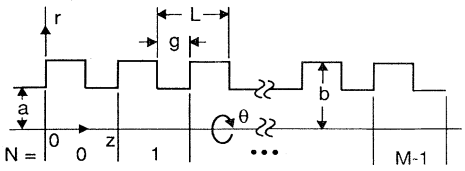

FIG. 27. A periodic array of cavities. The layout of geometry and the coordinate system.

geometry considered and the coordinate system used.

A particular case of a single cavity can be obtained by assuming $M=1$. Likewise, a particular case of a periodic array of cavities can be obtained in the limit as $M\to\infty$.

For the cylindrically symmetric (monopole) modes, the Fourier harmonics of the electric field generated by a particle can be written as a sum of *the field of a particle* in a pipe and *the radiation field* due to the presence of the cavities. The radiation field satisfies the homogeneous wave equation, and has to be finite at $r=0$. It can be represented as a superposition of cylindrical eigenfunctions with unknown coefficients $A(p)$. For the region inside the pipe, $r\le a$, the radial and longitudinal Fourier components of the electric field are, respectively,

$$E_{r\omega}=Q\gamma e^{ikz}G_1(r,a) -i\frac{qa}{\pi c}\int_{-\infty}^{\infty}dp\ A(p)\frac{p}{\Omega}J_1(\chi_p r/a)e^{ipz} \tag{6.1}$$

and

$$E_{z\omega}=-iQe^{ikz}G_0(r,a) +\frac{q}{\pi c}\int_{-\infty}^{\infty}dp\ A(p)J_0(\chi_p r/a)e^{ipz}\ , \tag{6.2}$$

where $k=\omega/c$, $Q=qk/\pi c\gamma^2$, and $G_{0,1}(r,a)$ are defined in Eqs. (4.3) and (4.2), and

$$\chi_p=a\Omega,\quad \Omega=\sqrt{k^2-p^2+2ik\varepsilon},\quad \varepsilon\to 0\ . \tag{6.3}$$

An infinitely small imaginary part ε is added to the wave number k to comply with the radiation condition.

The radiation field components inside the Nth cavity, $a<r<b$, $NL\le z<NL+g$, are

$$E_r^N=\sum_{n=0}^{\infty}\lambda_n D_n^N g_n^{(1)}(r)\sin(\lambda_n\zeta_N)\ , \tag{6.4}$$

and

$$E_z^N=\sum_{n=0}^{\infty}(\mu_n/b)D_n^N g_n^{(0)}(r)\cos(\lambda_n\zeta_N)\ , \tag{6.5}$$

where

$$g_n^{(0,1)}(r)=J_{0,1}(\mu_n r/b)Y_0(\mu_n)-Y_{0,1}(\mu_n r/b)J_0(\mu_n)\ , \tag{6.6}$$

$$\mu_n=b\sqrt{k^2-\lambda_n^2},\quad \lambda_n=n\pi/g,\quad \zeta_N=z-NL\ , \tag{6.7}$$

and D_n^N are unknown coefficients for the Nth cavity, $N=0,1,\ldots,M-1$. Here, $Y_{0,1}$ are Bessel functions of the second kind of the zeroth and first order, respectively. The field components in Eqs. (6.1), (6.2), (6.4), and (6.5) are constructed in such a way that their tangential projections are equal to zero on all the metallic surfaces: at $r=a$ in the pipe and $r=b$ in the cavities for appropriate values of z, and at $z=NL$ and $z=NL+g$ for arbitrary values of r in the interval $b>r>a$.

To find the unknown expansion coefficients D_n^N, one can use the field matching method described in Sec. IV.A. Matching the radial components of the field from Eqs. (6.1) and (6.4) in the Nth cavity on the surface $r=a$, $0\le\zeta_N<g$, defines the coefficients D_n^N in terms of the radial component of the radiation field. After that, matching the z components of the field Eqs. (6.2) and (6.5) at $r=a$ produces the following integral equation for the function $A(p)$:

$$A(p)=\sum_{N=0}^{M-1}\sum_{n=0}^{\infty}\frac{C_n(k)}{\pi g}\frac{V_n(p)}{J_0(\Omega)}\exp[i(k-p)NL]\left[\frac{i}{ka}V_n^*(k)+a\int_{-\infty}^{\infty}dp'V_n^*(p')\frac{J_1(\chi_{p'})}{\chi_{p'}}\exp[i(p'-k)NL]A(p')\right], \tag{6.8}$$

where the following notations are introduced:

$$C_n(k)=\frac{\mu_n}{b}\frac{g_n^{(0)}(a)}{g_n^{(1)}(a)} \approx\sqrt{k^2-\lambda_n^2}\tan[(b-a)\sqrt{k^2-\lambda_n^2}]\ , \tag{6.9}$$

$$V_n(p)=\int_0^g dz\,e^{-ipz}\cos(\lambda_n z)\ . \tag{6.10}$$

Notice that

$$|V_n(p)|^2=\frac{4p^2\sin^2\frac{g}{2}(p-\lambda_n)}{(p^2-\lambda_n^2)^2} \tag{6.11}$$

and that the functions $V_n(p)e^{-ipNL}$ are orthogonal

$$\int_{-\infty}^{\infty}dpV_n^*(p)V_m(p)\exp[-ipL(N-N')] =\pi g\delta_{n,m}\delta_{N,N'}\ . \tag{6.12}$$

The longitudinal impedance is given by the coefficient $A(k)$:

$$Z(k)=-Z_0 A(k), \quad Z_0=377\ \Omega\ . \tag{6.13}$$

In what follows we assume that $b>a$, since when $b=a$ all $C_n(k)=0$ identically. Consequently, all $A(p)=0$ which means that no radiation occurs in a smooth pipe.

We seek a solution of Eq. (6.8) in the form

$$A(p)=\sum_{N=0}^{M-1}\sum_{n=0}^{\infty} B_n^N \frac{V_n(p)}{J_0(\chi_p)}\exp[i(k-p)NL]\ , \tag{6.14}$$

which gives the following system of linear algebraic equations for B_n^N:

$$B_n^N=\frac{a}{\pi g}C_n(k)\left[\frac{i}{ka^2}V_n^*(k)+\sum_{N'=0}^{M-1}\sum_m \Gamma_{nm}^{N-N'}B_m^{N'}\right]\ . \tag{6.15}$$

Here $N=0,1,\ldots,M-1$, and the following notation for matrix elements $\Gamma_{nm}^{N-N'}$ is introduced:

$$\Gamma_{nm}^{N-N'}=\int_{-\infty}^{\infty}\frac{dp}{\chi_p}\frac{J_1(\chi_p)}{J_0(\chi_p)}V_n^*(p)V_m(p) \times\exp[i(p-k)L(N-N')]\ . \tag{6.16}$$

To evaluate this integral, we use analytical continuation of functions in its integrand into the complex plane of the variable p. According to the radiation condition, see Eq. (6.3), the path of integration in Eq. (6.16) must be shifted above the negative real axis and below the positive of that plane. Closing the path by a circle of large radius either in the upper or in the lower half-plane, it is easy to show that the integral is equal to the sum of residues of poles located in the zeros of the Bessel function $J_0(\nu_l)=0$:

$$\Gamma_{nm}^{N-N'}=\sum_l \frac{2\pi i}{u_l a^2}\begin{cases} V_n^*(u_l)V_m(u_l)\exp[iL(u_l-k)(N-N')] & \text{for } N>N'\ , \\ V_m^*(u_l)V_n(u_l)\exp[-iL(u_l+k)(N-N')] & \text{for } N<N'\ , \end{cases} \tag{6.17}$$

where

$$u_l=\begin{cases}\sqrt{k^2-(\nu_l/a)^2} & \text{for } \nu_l<ka\ , \\ i\sqrt{(\nu_l/a)^2-k^2} & \text{for } \nu_l>ka\ . \end{cases} \tag{6.18}$$

All terms with $\nu_l>ka$ in the sum of Eq. (6.17) are exponentially small. Hence, the summation over l may be truncated at $\nu_l=ka$. The imaginary part of the diagonal term is

$$\mathrm{Im}\Gamma_{nn}^0=\sum_{l=0}^{l_{\max}}\frac{2\pi}{u_l a^2}|V_n(u_l)|^2\ , \tag{6.19}$$

where the integer $l_{\max}$ on the upper limit of the summation is defined by the inequality $\nu_{l_{\max}}\le ka$.

The longitudinal impedance in terms of the coefficients B_n^N is

$$Z(k)=-Z_0\sum_{N=0}^{M-1}\sum_{n=0}^{\infty}V_n(k)B_n^N(k)\ . \tag{6.20}$$

So far, the system Eq. (6.15) constitutes the exact set of equations defining the radiation of an ultrarelativistic particle.

B. The impedance of a cavity in the zeroth-order approximation

In the high-frequency limit, we can expect that the system Eq. (6.15) can be solved by the method of iteration. In the zeroth-order approximation, we neglect the second term in brackets in Eq. (6.15):

$$B_n^N=\frac{iC_n(k)}{\pi gka}V_n^*(k)\ . \tag{6.21}$$

Then the impedance per cell is

$$\frac{Z}{M}=-i\frac{Z_0}{\pi gka}\sum_{n=0}^{\infty}|V_n(k)|^2C_n(k)\ . \tag{6.22}$$

Notice that in the zeroth-order approximation the impedance per cell given by this formula does not depend on the number of cells in the array and, as we will see shortly, is the impedance of a single cavity.

For large wave numbers k, the impedance, Eq. (6.22), is a fast changing function of k and goes to infinity at the resonance values

$$k_{nl}=\left[\left[\frac{\pi n}{g}\right]^2+\left[\frac{\pi(l+\frac{1}{2})}{b-a}\right]^2\right]^{1/2}\ , \tag{6.23}$$

defined by the equation $C_n^{-1}(k_{nl})=0$. The impedance can be presented as a sum of the resonances with infinitely small width. Representing $C_n^{-1}(k)$ in the vicinity of a resonance as

$$C_n^{-1}(k)=R_{nl}^{-1}(k-k_{nl}+i\varepsilon)\ , \tag{6.24}$$

with

$$R_{nl}=-\frac{[\pi(l+\frac{1}{2})]^2}{k_{nl}(b-a)^3}\ , \tag{6.25}$$

the real part of the impedance is given by the sum of δ-functional terms

$$\mathrm{Re}\frac{Z}{M}=\frac{Z_0\pi^2}{gka(b-a)^3} \times\sum_{n,l}|V_n(k)|^2\frac{(l+\frac{1}{2})^2}{k_{nl}}\delta(k-k_{nl})\ . \tag{6.26}$$

Practically, we are interested in ReZ averaged over some

interval of wave numbers Δk, which should be large in comparison with the difference between neighboring resonance frequencies δk, given by

$$\delta k = k_{n(l+1)} - k_{nl} \approx \frac{\pi l}{k(b-a)^2} . \tag{6.27}$$

We can choose an appropriate Δk in the following way. The factor $|V_n(k)|^2$ given by Eq. (6.11) has a maximum value of order of $(g/2)^2$ for $n = n_0$, where

$$n_0 = \left[\frac{kg}{\pi} \right] , \tag{6.28}$$

and decreases as $(n-n_0)^{-2}$ for $n \neq n_0$. The square brackets denote the integer part of an argument. The main contribution to the impedance is therefore given by mode n_0 which, of course, is different for different k. Hence, it is convenient to choose the interval of averaging as

$$\Delta k \approx \pi/2g , \tag{6.29}$$

which is large in comparison to δk if k is large.

For an estimate of the real part of the impedance in Eq. (6.26), it suffices to consider only the term $n = n_0$. The average impedance is then

$$\left\langle \mathrm{Re}\frac{Z}{M} \right\rangle = \frac{\pi^2 g}{4ka(b-a)^3} \frac{Z_0}{\Delta k} \sum_{l=0}^{l_{\max}} \frac{(l+\frac{1}{2})^2}{k_{n_0 l}} , \tag{6.30}$$

where

$$l_{\max} = (b-a)\sqrt{k/\pi g} . \tag{6.31}$$

This estimate of the real part of the impedance, with Δk defined by Eq. (6.29), differs from the real part of Lawson's estimate (Lawson, 1968)

$$\frac{Z}{M} = (1+i)\frac{Z_0}{2\pi}\sqrt{g/\pi a}\,\frac{1}{\sqrt{ka}} \tag{6.32}$$

only by a factor $\pi/3$. Numerical calculations confirm that this result is independent of the choice of the size of the interval Δk.

We conclude that the main contribution to the impedance comes, with good accuracy, from eigenmodes with eigennumbers

$$n = n_0 \quad \text{and} \quad 0 \le l \le l_{\max} . \tag{6.33}$$

This result has a simple physical meaning. The eigenmode with the eigennumbers $(n,l) \gg 1$ is characterized by the wave vector $\mathbf{k}$ with components $k_\perp = \pi l/(b-a)$ and $k_\parallel = n\pi/g$, corresponding to the wave number k_{nl} in Eq. (6.23) and the frequency $\omega \approx k_{nl} c$. The interaction of a particle with a mode substantially contributes to the impedance if, in the time of flight through the cavity g/v, the phase slippage is small:

$$(\omega - k_\parallel v)(g/v) < \pi/2 . \tag{6.34}$$

Substituting $v \approx c$ and $n = n_0$ from Eq. (6.28), we obtain the condition Eq. (6.33) with $l_{\max}$ from Eq. (6.31).

The zeroth-order approximation does not take into account either the interference of the radiation from different cavities or the energy escape into the cavity openings. In the next two subsections we derive a method which allows us to take into account both these effects.

C. The high-frequency impedance of a cavity in the diagonal approximation

We start with the somewhat simpler case of a single cavity, $M = 1$. In this case, the interference of the radiation from different cavities plays no role, but the energy flow into the side pipes must be taken into account. For $M = 1$, Eq. (6.15) takes the form

$$B_n = \frac{a}{\pi g} C_n(k) \left[\frac{iV_n^*(k)}{ka^2} + \sum_m \Gamma^0_{nm} B_m \right] . \tag{6.35}$$

In the zeroth-order approximation, the sum on the right-hand side of this equation is neglected altogether. In the next approximation, we include the main diagonal term $m = n$ contributing to the sum. All the other terms give only small corrections and can be taken into account by the method of iteration. In this *diagonal approximation* (Heifets and Kheifets, 1988, 1989), we obtain the following expression for the impedance:

$$Z(k) = -i\frac{Z_0}{ka^2} \sum_n \frac{|V_n(k)|^2}{y(k)} , \tag{6.36}$$

where we define

$$\begin{aligned} y(k) &\equiv \frac{\pi g}{a} C_n^{-1} - \Gamma^0_{nn} \\ &\approx \frac{\pi g}{a} \frac{\cot[(b-a)\sqrt{k^2-\lambda_n^2}\,]}{\sqrt{k^2-\lambda_n^2}} - \Gamma^0_{nn} . \end{aligned} \tag{6.37}$$

The sum in Eq. (6.36) is again mainly determined by terms $n \approx n_0$.

Similarly to the treatment of Eq. (6.22), the impedance given by Eq. (6.36) can be represented as a sum over the resonance terms with finite widths. The resonance frequencies are now given by the condition $\mathrm{Re}\, y(k) = 0$, while the resonance widths are defined by $\mathrm{Im}\Gamma^0_{nn}$. Evaluation of Γ^0_{nn} has been done by Heifets and Kheifets (1989). For large $k \approx n\pi/g$, a good estimate for Γ^0_{nn} is

$$\Gamma^0_{nn} = (i-1)\frac{g}{a}\left[\frac{\pi g}{2k}\right]^{1/2} . \tag{6.38}$$

The resonance frequency shift given by $\mathrm{Re}\Gamma^0_{nn}$ is small, and the expansion around a resonance frequency k_{nl} takes the form

$$y(k) = R_{nl}^{-1}(k - k_{nl} + i\gamma_{nl}) , \tag{6.39}$$

where

$$R_{nl}=-\frac{al^2}{g^2(b-a)l_{\max}^2} \tag{6.40}$$

and

$$\gamma_{nl}=\frac{1}{g\sqrt{2}}\left[\frac{l^2}{l_{\max}^3}\right] . \tag{6.41}$$

Hence, in the diagonal approximation, ReZ is not singular as it was in the zeroth approximation, Eq. (6.26), although it may have rather sharp peaks if γ_{nl} is small. This is the main qualitative feature of the diagonal approximation for a single cavity.

The ratio of the resonance width γ_{nl} to the distance δk between adjacent resonances is small for the resonances with $l<l_{\max}$:

$$\frac{\gamma_{nl}}{\delta k}\approx\frac{l}{l_{\max}}<1 . \tag{6.42}$$

Therefore, averaging over Δk for resonances with different l may be performed independently. Since the integral over a resonance curve does not depend on its width, the real part of the impedance is the same as given by Eq. (6.32). The diagonal approximation allows one to estimate correction, given by the next iteration, and to prove that such corrections are small in the high-frequency limit (Heifets and Kheifets, 1989). Recently, Gluckstern (1989a) has shown that Eq. (6.32) holds for a cylindrically symmetric cavity of a general shape.

D. The high-frequency impedance of an array of cavities

Consider now an array consisting of M identical cells. In this case the interference of waves generated in different cells must be taken into account. We describe the interaction of a particle with each cell in a manner similar to the previous treatment of a single cavity. Therefore, we consider Eq. (6.15) in the diagonal approximation for the lower indices, retaining only the terms $m=n=n_0$, but keeping the summation over the upper indices N'. This gives (Heifets and Kheifets, 1988, 1989):

$$B_n^N y(k)=\frac{iV_n^*}{ka^2}+\sum_{\substack{N'=0,\\ N'\neq N}}^{M-1}\Gamma_{nn}^{N-N'}B_n^{N'} , \tag{6.43}$$

where $N=0,1,\ldots,M-1$; $\Gamma_{nn}^{N-N'}$ is defined in Eq. (6.17); and $y(k)$ is defined by Eq. (6.37).

It should be noted that the system Eq. (6.43) is difficult to solve numerically for an interesting case, namely $M\sim ka\gg 1$. Indeed, the rank of the corresponding matrix is M. In addition, the coefficients in Eq. (6.43) oscillate rapidly with a typical period of $1/M$. Therefore, the computational time for the calculation of the averaged impedance increases with M as M^3.

To simplify Eq. (6.43), consider the behavior of its matrix elements given in Eq. (6.17). All the elements with $N<N'$ contain factors which oscillate with large sum frequencies $u_l+k\sim 2k$. After averaging over a frequency interval, their contribution is negligibly small. On the other hand, all the matrix elements with $N>N'$ contain factors which oscillate with small difference frequencies u_l-k. These terms describe the interaction of a particle with the waves traveling in the same direction. Therefore, we may assume that

$$\Gamma_{nn}^{N-N'}=0 \quad \text{for } N<N' \tag{6.44}$$

and rewrite Eq. (6.43) in the form

$$B_n^N y(k)=\frac{iV_n^*}{ka^2}+\sum_{N'=0}^{N-1}\Gamma_{nn}^{N-N'}B_n^{N'} . \tag{6.45}$$

By omitting the terms with $N'>N$ we neglect the interaction of a particle with the waves traveling in the opposite direction. In particular, we neglect the decay of the modes inside cavities into these waves. Since we do that in the nondiagonal terms, for consistency, the same should be done in the diagonal terms as well. In other words, ImΓ_{nn}^0 in the definition of $y(k)$, Eq. (6.37), should be divided by 2.

Equations (6.45) are the recurrence relations between coefficients B_n^N. Thus the coefficients can be found sequentially starting with the zeroth one:

$$B_n^0=\frac{iV_n^*}{ka^2y(k)} . \tag{6.46}$$

Notice that this expression gives the impedance of a single cavity.

It is also possible to solve the system of Eqs. (6.45) explicitly. To do that we notice that the Nth coefficient is expressed through coefficients with indices $N'<N$. Although we are interested in only the first M coefficients, the procedure can be formally extended to any N. Since the matrix $\Gamma_{nn}^{N-N'}$ depends only on the differences $N-N'$, Eq. (6.45) can be solved by applying the discrete Laplace transformation. The Laplace transforms of B_n^N and Γ_{nn}^N are defined for a complex argument s as follows:

$$B_n(s,k)=\sum_{N=0}^{\infty}e^{-Ns}B_n^N , \tag{6.47}$$

$$\Gamma_n(s,k)=\sum_{N=1}^{\infty}e^{-Ns}\Gamma_{nn}^N , \tag{6.48}$$

with $\sigma\equiv\text{Re}s>0$.

Then the Laplace transform of a solution of Eq. (6.45) is

$$B_n(s,k)=\frac{iV_n^*}{ka^2}\frac{1}{[y(k)-\Gamma_n(s,k)](1-e^{-s})} . \tag{6.49}$$

The inverse transformation now gives the solution of Eq. (6.45):

$$B_n^N=\int_{-i\pi+\sigma}^{i\pi+\sigma}\frac{ds}{2\pi i}e^{Ns}B_n(s,k), \quad \sigma>0 . \tag{6.50}$$

Hence, the impedance of an array with arbitrary number of cells M is given by the following expression [cf. Eq. (6.20)]:

$$Z(k)=-\frac{Z_0}{4\pi ka^2}\sum_{n=0}^{\infty}|V_n(k)|^2\int_{-i\pi+\sigma}^{i\pi+\sigma}ds\frac{e^{Ms}-1}{[y(k)-\Gamma_n(s,k)](\cosh s-1)}\ . \tag{6.51}$$

Here

$$\Gamma_n(s,k)=\sum_{l=0}^{\infty}\frac{2\pi i|V_n(u_l)|^2}{a^2u_l(e^{iL(k-u_l)+s}-1)} \tag{6.52}$$

and

$$u_l=\sqrt{k^2-(\nu_l/a)^2+2ki\varepsilon},\quad \nu_l\approx\pi l\ . \tag{6.53}$$

The integrand in Eq. (6.51) has the same value on two parallel lines, $s=-i\pi+\sigma$ and $s=+i\pi+\sigma$, $-\infty<\sigma<0$. Therefore, we can add and subtract integrals over these two lines, thereby extending the contour of integration in the complex plane s from $-\infty-i\pi$, then from $-i\pi+\sigma$ to $i\pi+\sigma$, and back to $-\infty+i\pi$. The integral is then equal to the sum of the residues at the roots of the respective equations $\cosh s=1$ and

$$y(k)=\Gamma_n(s,k)\ . \tag{6.54}$$

It is easy to see that all the roots of Eq. (6.54) are purely imaginary. Using that fact, we average the impedance over the interval $\Delta k=\pi/2g$; see Eq. (6.29), as in Sec. VI.C for a single cavity (Heifets and Kheifets, 1987). The result is

$$\left\langle\mathrm{Re}\left[\frac{Z}{M}\right]\right\rangle=\frac{2Z_0}{(ka)^{3/2}}\left[\frac{2L}{\pi a}\right]^2\left[\frac{\pi a}{g}\right]^{1/2}\Phi(k,M)\ , \tag{6.55}$$

where

$$\Phi(k,M)=k\pi g\left[\frac{a}{4L}\right]^2\int_{-\pi}^{\pi}dt\frac{F(t,M)}{2\pi}\Xi(\xi)\ , \tag{6.56}$$

$$F(t,M)=\frac{\sin^2(Mt/2)}{M\sin^2(t/2)}\ , \tag{6.57}$$

$$\Xi(\xi)=\frac{1}{\xi^2}\left[1-\frac{\arctan\xi}{\xi}\right], \tag{6.58}$$

$$\xi=\frac{a}{2L}\sqrt{k\pi g}\,\frac{J_1(p)}{pJ_0(p)}\ , \tag{6.59}$$

and

$$p=\left[-\frac{2ka^2}{L}t\right]^{1/2} \tag{6.60}$$

For an array with only a few cavities ($M\approx1$) the expansion of the expression Eq. (6.51) is obtained in the paper by Heifets and Kheifets (1989). Apart from small corrections, the impedance per cavity is the same as that for a single cavity; see Eq. (6.32).

To evaluate the average impedance for $M\gg1$ we notice that, for large M, function $F(t,M)$ has a very sharp peak at $t\sim0$. Hence, a good approximation for it is

$$F(t,M)\approx\begin{cases}M & \text{if } |t|<\pi/M\ ,\\ 0 & \text{if } |t|>\pi/M\ .\end{cases} \tag{6.61}$$

Then Eq. (6.56) can be simplified:

$$\Phi(k,M)=\frac{M}{8}\frac{g}{a}\left[\frac{a}{4L}\right][R_1(P)+R_2(P)]\ , \tag{6.62}$$

where

$$R_1(P)=\int_0^P p\,dp\,\Xi(\xi_1)\ , \tag{6.63}$$

$$R_2(P)=\int_0^P p\,dp\,\Xi(\xi_2)\ , \tag{6.64}$$

$$\xi_1=\frac{a}{2L}\sqrt{k\pi g}\,\frac{J_1(p)}{pJ_0(p)}\ , \tag{6.65}$$

$$\xi_2=\frac{a}{2L}\sqrt{k\pi g}\,\frac{I_1(p)}{pI_0(p)}\ , \tag{6.66}$$

and

$$P=(2\pi ka^2/LM)^{1/2}\ . \tag{6.67}$$

We shall evaluate integrals R_1 and R_2 in two regions of the parameter P.

(a) Suppose first that $P\ll1$ or

$$M\gg ka^2/L\ . \tag{6.68}$$

Since $P\ll1$, we can expand functions ξ_1 and ξ_2 in the vicinity of $p=0$: $\xi_1=\xi_2=(a/4L)\sqrt{\pi kg}$. Both values are large for large k everywhere inside the interval of the integration in Eqs. (6.63) and (6.64). Hence, function $\Xi\approx\xi^{-2}\approx(4L/a)^2(1/\pi kg)$. For the integrals R_1 and R_2 we get $R_1=R_2\approx16L/gM$ and $\Phi(k,M)\approx1$. Thus we obtain

$$\left\langle\mathrm{Re}\left[\frac{Z}{M}\right]\right\rangle=\frac{2Z_0}{(ka)^{3/2}}\left[\frac{2L}{\pi a}\right]^2\left[\frac{\pi a}{g}\right]^{1/2}\quad\text{for } M\gg ka^2/L\ . \tag{6.69}$$

In other words, the real part of the average impedance per cell decreases with frequency as $\omega^{-3/2}$.

(b) Suppose now that $P\gg1$ or

$$1\ll M\ll ka^2/L\ . \tag{6.70}$$

In this case, the main contribution to the integral R_1 comes from the vicinities of the roots of $J_1(p)$: $p_m=\nu_{1m}$, where $\xi_1\approx0$. Near the root p_m, the function Ξ can be approximated by

$$\Xi\approx\frac{1}{3+[\xi'\cdot(p-\nu_{1m})]^2}\ . \tag{6.71}$$

This expression has the correct behavior in the vicinity of the roots $p=\nu_{1m}$, and decreases as ξ^2 far from them. The estimate of the integral R_1 is then

$$R_1 \approx \frac{\pi k a^2}{M\sqrt{gML}} , \tag{6.72}$$

where we used the formula

$$\sum_{m=1}^{[P/\pi]} \nu_{m1}^2 \approx \frac{P^3}{3\pi}, \quad P \gg 1 .$$

Unlike the situation with R_1, the integrand of R_2 does not oscillate, and the relative contribution of R_2 to Eq. (6.62) is small [it is of order of $(gM/L)^{-1/2} \ll 1$ with respect to R_1]. The physical reason for such a difference is that the interaction of a particle with the diffracted waves is substantial only when both travel in the same direction. Therefore, in this case

$$\left\langle \mathrm{Re}\left[\frac{Z}{M}\right]\right\rangle = \frac{Z_0}{2\pi}\left[\frac{g}{\pi k a^2}\right]^{1/2}\left[\frac{\sqrt{2L}}{\sqrt{gM}}\right] ,$$

$$1 \ll M \ll k a^2/L . \tag{6.73}$$

In other words, the real part of the average impedance per cell decreases as $(kaM)^{-1/2}$. This result was first qualitatively obtained by Palmer (1987). A result similar to Eq. (6.73) was later obtained by Gluckstern (1989b, 1989c), albeit with a different coefficient.

An intermediate parameter region $M \sim ka^2/L$ is the transition area. The transition from one regime to another is illustrated in Fig. 28 (Heifets and Kheifets, 1989). The curves represent function Φ versus ka^2/ML for different values M, and were obtained by numerically integrating Eq. (6.56).

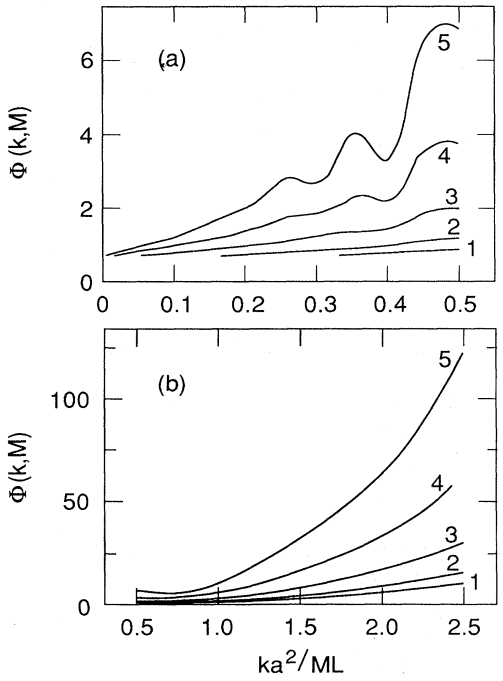

FIG. 28. The transition from a cavity regime to an array regime. The function Φ is plotted versus the parameter ka^2/ML for different values of the number M of cavities. (a) Blowup of the region of small values ka^2/ML of (b). Curves are labeled as follows: 1, $M=500$; 2, $M=1000$; 3, $M=3000$; 4, $M=10\,000$; 5, $M=30\,000$.

Let us summarize the results (Heifets and Kheifets, 1989). The real part of the impedance per cell for a small number of cavities decreases with frequency as $k^{-1/2}$. For a large number of cavities the asymptotic frequency region is divided into two parts. For an extremely high frequency, the real part of the impedance depends on frequency in a way similar to that for a single cavity, i.e., as $k^{-1/2}$, but falls off as $M^{-1/2}$, with the number of cells M due to the interference of the radiated waves emitted from different cavities. The interference also takes place for moderate (but still large) frequencies satisfying the criterion Eq. (6.70), resulting in a much faster decrease of the impedance $\sim k^{-3/2}$. There is a continuous transition from the regime where the parameter M satisfies Eq. (6.70) to another where M satisfies Eq. (6.68). This result agrees both with numerical calculations performed for a small number of cavities (Bane and Sands, 1990) and with the optical resonator model (Vainshtein, 1963; Keil, 1972; Sessler, 1972; Brandt and Zotter, 1982).

The rapid decrease of the real part of the impedance as $k^{-3/2}$ has a direct implication on the design of a short bunch accelerator. Indeed, had the asymptotic decrease of the longitudinal impedance followed the law $k^{-1/2}$, the main contribution to the total energy loss would be given by the high-frequency tail of the impedance and the total energy loss would depend on the longitudinal rms size of the bunch σ as $\sigma^{-1/2}$. The situation is quite different when the impedance falls off as $k^{-3/2}$. In this case, the total energy loss is defined by the low-frequency range of the impedance and, in general, is smaller than in the first case.

E. The high-frequency impedance of a collimator

The longitudinal impedance of a collimator in the high-frequency region (and in the relativistic case $\gamma \gg 1$) can be found analytically using formula (4.28). Since asymptotically $\tilde{\lambda}_b \approx \tilde{k}$, only the diffracted field, i.e., the field depending on coefficients z_n, contributes to the impedance. Physically that arises from the fact that only the diffracted field radiated forward can reach a relativistic particle. Hence,

$$Z_{\mathrm{col}}(k) = -2(Z_0/\pi)\tilde{k}\sum_n z_n J_0(\nu_n/p) , \tag{6.74}$$

where $p = b/a$, a is the pipe radius, and b is the collimator radius.

Coefficients z_n can be found from the matrix Eq. (4.23), with the matrix elements and the right-hand side taken from Table II:

$$z_l \tilde{k} J_1^2(\nu_l) = -J_0(\nu_l/p)/\nu_l^2 + 2p^{-2}\tilde{k}\sum_m (t_m - y_m E_-)\phi_{lm}(p^{-1}) , \tag{6.75}$$

where quantities $\phi_{lm}(p^{-1})$ are defined in Eq. (4.24) and E_- in Table II. Dividing Eq. (6.75) by $J_1^2(\nu_l)$, multiplying by $J_0(\nu_l/p)$, and summing over l, we obtain

$$\tilde{k}\sum_l z_l J_0(\nu_l/p)=-\sum_l J_0^2(\nu_l/p)/\nu_l^2 J_1^2(\nu_l) +2\tilde{k}\sum_l J_0^2(\nu_l/p)J_1^{-2}(\nu_l)\sum_m (t_m-y_m E_-)\nu_m J_1(\nu_m)(\nu_m^2 p^2-\nu_l^2)^{-1} . \tag{6.76}$$

Summation here can be performed explicitly using the following particular form of the Kneser-Sommerfeld formula (Watson, 1944; Erdelyi *et al.*, 1953)

$$\sum_l J_0^2(\nu_l/p)(\nu_l^2-x^2)^{-1}J_1^{-2}(\nu_l) =\pi J_0(x/p)[J_0(x/p)Y_0(x) -J_0(x)Y_0(x/p)]/4J_0(x) , \tag{6.77}$$

where Y_0 is a Bessel function of the second kind. From here it follows that the second term of the right-hand side of Eq. (6.76), containing coefficients t_m and y_m, vanishes, since the sum over l is zero. The first sum in Eq. (6.76) according to the same formula is

$$\sum_l J_0^2(\nu_l/p)/\nu_l^2 J_1^2(\nu_l) =(\pi/4)\lim[Y_0(x)-Y_0(x/p)]_{x\to 0}=(\ln p)/2 . \tag{6.78}$$

Hence, in the high-frequency region, the impedance of a collimator does not depend on frequency and is the following constant:

$$Z(\tilde{k})=(Z_0/\pi)\ln(a/b), \quad \text{for } \gamma>\tilde{k}\gg 1 . \tag{6.79}$$

The same expression holds for the high-frequency impedance of a pipe cross section step for the case of a bunch exiting the narrow pipe. In the opposite case, the impedance is zero; see Sec. IV.C.

Formula (6.79) is not valid for $\tilde{k}>\gamma$. In this range of frequencies the impedance decreases at least as k^{-2}.

It is interesting to estimate the total energy loss $\Delta\mathcal{E}$ of a charge passing through a collimator; cf. Eqs. (2.1) and (2.15). For a Gaussian bunch of rms length σ, the total energy loss is

$$\Delta\mathcal{E}=\frac{2q^2}{\sigma\sqrt{\pi}}\ln\frac{a}{b} . \tag{6.80}$$

This expression is valid for $\sigma>1/\gamma$, and agrees with the formula for the total energy loss of a charge passing through a sudden change in a pipe cross section obtained by Balakin and Novokhatski (1983) and by Kheifets (1987).

If one assumes that ReZ is constant for $\tilde{k}<\gamma$ and is zero for $\tilde{k}>\gamma$, as previously discussed, then the total energy loss of a *point* charge, $\sigma=0$, is proportional to γ. For a charge passing through a hole in a screen, this conclusion is in agreement with the estimate obtained by Lawson (1968), and with numerical calculations (Dnestrovskii and Kostomarov, 1959a, 1959b).

F. The impedance of a semi-infinite circular waveguide

In this subsection we describe the application of the Wiener-Hopf factorization method (Wiener and Hopf, 1931; Vainshtein, 1969), for calculating the impedance of a semi-infinite waveguide with a circular cross section of radius a (Kheifets *et al.*, 1985, 1987; Kheifets and Palumbo, 1987). A similar structure—a semi-infinite circular pipe inside an infinite circular pipe of a larger radius—is considered in the paper of Palumbo (1990). These structures have a unique feature: the Maxwell equations in these cases can be solved exactly. The same method was used by Levine and Schwinger (1948) to obtain an explicit solution to the problem of the radiation of sound from the end of a pipe.

As discussed in Sec. III.D, the impedance in this case depends on the direction of the charge motion. Consider for example, a charge entering a waveguide whose open end is placed at $z=0$. Due to the axial symmetry of the problem, the current density has only the z component, and can be expressed as the sum of the current densities of the source charge and the induced charge.

The starting point of the method is a set of integral equations for the longitudinal current density distribution induced in the wall of the pipe. The system can be obtained from Eq. (6.2). In the ultrarelativistic limit $\gamma\to\infty$, Eq. (6.2) can be rewritten in the following way:

$$E_{z\omega}(r,z)=-iQe^{ikz}K_0(\tau r) -\frac{q}{2cka}\int_{-\infty}^{\infty}dp\,F(p)\chi_p^2 J_0\left[\chi_p\frac{r}{a}\right] \times H_0^{(1)}(\chi_p)e^{ipz} , \tag{6.81}$$

where $k=\omega/c$, $\tau=k/\gamma$, $Q=qk/\pi c\gamma^2$, and $\chi_p=a\sqrt{k^2-p^2+2ki\varepsilon}$. In Eq. (6.81) the unknown function $A(p)$ was replaced by another function $F(p)$ according to the formula

$$A(p)=-\frac{\pi}{2ka}\chi_p^2 H_0^{(1)}(\chi_p)F(p) . \tag{6.82}$$

As shown by the paper by Kheifets *et al.* (1985), function $F(p)$ defined in this way can be interpreted as the Fourier component of the induced current density. In Eq. (6.81) we have also replaced $G_0(r,a)$ by $K_0(\tau r)$ to take into account the fact that the second term in Eq. (4.4) also comes from the induced current (see Sec. V.B), and thus is already included in the second term of Eq. (6.81).

Function $F(p)$ is defined by the boundary condition which here can be written as

$$E_{z\omega}(a,z)=0 \quad \text{for } z>0 . \tag{6.83}$$

We define

$$L(p)=\pi\chi_p^2 J_0(\chi_p)H_0^{(1)}(\chi_p)\ ; \tag{6.84}$$

then Eq. (6.83) gives

$$\int_{-\infty}^{\infty} dp\, F(p)L(p)\exp(ipz)=\hat{Q}\exp(ikz)\quad \text{for } z>0\ , \tag{6.85}$$

where $\hat{Q}=-2ik^2aK_0(\tau a)/\gamma^2$. Since there is no metallic surface for $z<0$, the induced current density for negative z is zero:

$$\int_{-\infty}^{\infty} dp\, F(p)\exp(ipz)=0\quad \text{for } z<0\ . \tag{6.86}$$

Equations (6.85) and (6.86) constitute a system of linear integral equations for function $F(p)$. Provided the function $F(p)$ is found, the longitudinal impedance can be found by integrating Eq. (6.81) according to formula (2.5).

The solution of the system (6.85), (6.86) can be obtained by factoring the kernel $L(p)$ in such a way as to satisfy the following requirements (Vainshtein, 1969):

(1) In the upper half-plane of the complex variable p, the product $F(p)L(p)$ has one pole at $p_0=k$. The value of the residue of this pole is $\hat{Q}/2i\pi$. In all other points of the upper half-plane this product is an analytic function. As $|p|\to\infty$ in the upper half-plane, $F(p)L(p)\to 0$.

(2) In the lower half-plane $F(p)$ is an analytic function and tends to zero as $|p|\to\infty$.

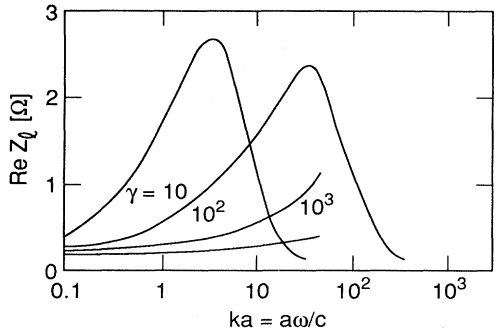

FIG. 29. The real part of the longitudinal impedance of a semi-infinite circular waveguide as a function of parameter $ka=a\omega/c$ for three different values of the Lorentz factor γ.

The analytic behavior of $F(p)$ and $F(p)L(p)$ listed in (1) and (2) causes $F(p)$ to be the solution of the system defined by Eqs. (6.85) and (6.86). The function $F(p)$ satisfying both the above requirements is (Vainshtein, 1969):

$$F(p)=\frac{i\hat{Q}}{2\pi\Gamma_+(ka)\sqrt{ka}}\frac{\Gamma_-(pa)}{(ka-pa)^{3/2}}\ , \tag{6.87}$$

where functions $\Gamma_\pm$ are

$$\Gamma_\pm(u)=[2\rho I_0(\rho)K_0(\rho)]^{\pm 1/2}\exp\left[-\frac{u}{i\pi}\int_0^{ka}dt\frac{\ln[\pi\sigma_1 J_0(\sigma_1)H_0(\sigma_1)]}{u^2-t^2}+\frac{u}{i\pi}PV\int_{ka}^{\infty}dt\frac{\ln[2\sigma_2 I_0(\sigma_2)K_0(\sigma_2)]}{t^2-u^2}\right]\ , \tag{6.88}$$

where $\rho=\sqrt{u^2-(ka)^2}$, $\sigma_1=\sqrt{(ka)^2-t^2}$, and $\sigma_2=\sqrt{t^2-(ka)^2}$. Note that at $u=ka$ there is no singularity.

In terms of these functions, the impedance produced by the radiation on the open end of the waveguide (Kheifets *et al.*, 1985) for $\beta\approx 1$ is

$$Z(k)=\frac{Z_0 kaK_0(\tau a)}{2\pi\gamma^2 I_0(\tau a)}\left[\frac{\gamma I_1(\tau a)}{I_0(\tau a)}-\frac{\Gamma_+'(ka)}{\Gamma_+(ka)}-\frac{1}{4ka}\right]\ . \tag{6.89}$$

Figure 29 presents the real part of the longitudinal impedance $\mathrm{Re}Z(k)$, Eq. (6.89), for several values of the Lorentz factor γ.

In the asymptotic region $ka\gg 1$, the contribution of the discontinuity to the longitudinal impedance is

$$Z(k)=\frac{Z_0}{2\pi}\ln\frac{2\gamma}{ka}\ . \tag{6.90}$$

This result is similar to that of a step with the infinitely large outer radius.

VII. CONCLUSIONS

Substantial progress has recently been achieved in understanding the physics of the bunch-environment interaction in modern accelerators and, correspondingly, in the development of analytical and numerical methods of estimation of the coupling impedances and the loss factors. In this paper, we have tried to describe the present level of understanding and the main theoretical results in the field. Clearly, the presented methods are limited to rather simple cylindrically symmetric geometries. Nevertheless, it is difficult to overestimate the importance of the comprehension and insight which they help to develop. Certainly much more work is needed for other geometries such as tapers, bellows, etc. This is especially true for cylindrically nonsymmetric structures.

ACKNOWLEDGMENTS

We are grateful to B. Zotter, R. Gluckstern, P. Wilson, M. Sands, and K. Bane for their valuable comments. This work was supported by the U. S. Department of Energy under contract DE-AC03-76SF00515.

REFERENCES

Balakin, V. E., A. V. Novokhatski, 1983, "VLEPP: Longitudinal Beam Dynamics," in *Proceedings of the 12th International Conference on High-Energy Accelerators,* edited by Francis T. Cole and Rene Donaldson (Fermilab, Batavia, IL, 1984), pp. 117 and 118.

Bane, K., 1980, "Constructing the Wake Potentials from the Empty Cavity Solutions of Maxwell's Equations," European Organization for Nuclear Research Report CERN/ISR-TH/80-47.

Bane, K. F. L., 1986, "Wakefield Effects in Linear Colliders," Stanford Linear Accelerator Center Report SLAC-PUB-4169.

Bane, K. F. L., and P. B. Wilson, 1980, "Longitudinal and Transverse Wake Potentials in SLAC," in *Proceedings of the 11th International Conference on High-Energy Accelerators, Geneva, Switzerland, 1980,* edited by W. S. Newman (Birkhäuser Verlag, Basel), pp. 592-596.

Bane, K. F. L., P. B. Wilson, and T. Weiland, 1984, "Wakefields and Wakefield Acceleration," Stanford Linear Accelerator Center Report SLAC-PUB-3528.

Bane, K. L., and M. Sands, 1987, "Wakefields of Very Short Bunches in an Accelerating Cavity," Stanford Linear Accelerator Center Report SLAC-PUB-4441.

Bane, K. L., and M. Sands, 1990, "Wakefields of Very Short Bunches in an Accelerating Cavity," Part. Accel. **25**, 73-96.

Bassetti, M., and D. Brandt, 1986, "Transverse Electro-Magnetic Force in Circular Trajectory," European Organization for Nuclear Research Report CERN/LEP-TH/86-04.

Bethe, H. A., 1944, "Theory of Diffraction by Small Holes," Phys. Rev. **66**, 163–182.

Bisognano, J. J., 1990a, "Comments on the High-Frequency Behavior of the Coupling of an Accelerator Beam to its Environment," Part. Accel. **25**, 253–262.

Bisognano, J. J., 1990b, "On the Independence of the Longitudinal Wakefield on Direction of Transit through a Cavity," Continuous Electron Beam Accelerator Facility Report CEBAF-TN-0109.

Bisognano, J. J., S. A. Heifets, and B. C. Yunn, 1988, "The Loss Parameters for Very Short Bunches," Continuous Electron Beam Accelerator Facility Report CEBAF-PR-88-005.

Bisognano, J. J., S. A. Heifets, and B. C. Yunn, 1988, "Loss Parameters for Very Short Bunches", in *Proceedings of EPAC European Particle Accelerator Conference,* Rome, Italy, 1988, Vol. 2, edited by S. Tazzari (World Scientific, Singapore), pp. 708-710.

Brandt, D., and B. Zotter, 1982, "Calculation of the Wakefield with the Optical Resonator Model," European Organization for Nuclear Research Report CERN-ISR/TH/82-13.

Chan, K. C. D., and R. Schweinfurth, 1987, "Beam Energy Spread Induced by Beampipe Steps," Los Alamos National Laboratory Report LANL-AT-6:ATN-87-24.

Channell, P. J., 1986, "Energy Independent Radial Space Charge Forces in Circular Machines," Los Alamos National Laboratory Accelerator Theory Note LANL-AT-6: ATN-86-15.

Chao, A., 1982, "Coherent Instabilities of a Relativistic Bunched Beam," Stanford Linear Accelerator Center Report SLAC-PUB-2946.

Chao, A., 1983, "Coherent Instabilities of a Relativistic Bunched Beam," in *Physics of High Energy Particle Accelerators,* Stanford Linear Accelerator Center Summer School 1982, AIP Conference Proceedings No. 105, edited by Melvin Month (AIP, New York), pp. 353–523.

Chatard-Moulin, M., and A. Papiernik, 1979, "Energy Losses of an Electron Bunch Moving along the Axis of a Circular Waveguide with Periodically Perturbed Wall," IEEE Trans Nucl. Sci. **NS-26**, 3523–3525.

Chin, Y. H., 1988, "ABCI (Azimuthal Beam Cavity Interaction) User's Guide," European Organization for Nuclear Report CERN/LEP-TH/88-3.

Collin, R. E., 1966, *Foundations for Microwave Engineering* (McGraw Hill, New York), p. 56.

Cooper, R. K., S. Krinsky, and P. L. Morton, 1982, "Transverse Wake Force in Periodically Varying Waveguide," Part. Accel. **12**, 1–12.

Coplen, B., L. Ludeking, J. MacDonald, G. Warren, and R. Worl, 1988, "MAGIC User's Manual," Mission Research Corp. Report MRC/WDC-R-184, Mission Research Corp., 8560 Cinderbed Road, Suite 700, Newwington, VA 22122.

DeFord, J. F., G. D. Craig, and R. McLeod, 1989, "The AMOS (Azimuthal Mode Simulation) Code," in *Proceedings of the 1989 IEEE Particle Accelerator Conference, Chicago,* Vol. 2, edited by Floyd Bennet and Joyce Kopta (IEEE, Piscataway, NJ, 1989), pp. 1181–1183.

Dolen, R., D. Horn, and C. Schmid, 1968, "Finite-energy sum rules and their application to πN charge exchange," Phys. Rev. **166**, 1768–1781.

Dôme, G. D., 1985, "Wake Potentials of a Relativistic Point Charge Crossing a Beam-Pipe Gap: An Analytic Approach," IEEE Trans. Nucl. Sci. **NS-32**, 2531–2534.

Dnestrovskii, Yu. N., and D. P. Kostomarov, 1959a, "Radiation of a Modulated Beam of Charged Particles in Passing through a Round Opening in a Flat Screen," Dokl. Akad. Nauk SSSR **124**, 792–795 [Sov. Phys. Dokl. 132–135 (1959)].

Dnestrovskii, Yu. N., and D. P. Kostomarov, 1959b "A Study of Ultrarelativistic Charges Passing through a Circular Aperture in a Screen," Dokl. Akad. Nauk SSSR **124**, 1026–1029 [Sov. Phys. Dokl. **4**, 158–160 (1959)].

Erdelyi, A., W. Magnus, F. Oberhettinger, F. G. Tricomi, D. Bertin, W. B. Fulks, A. R. Harvey, D. L. Thomsen, M. A. Weber, and F. L. Whitney, 1953, *Higher Transcendental Functions,* Vol. 2 (McGraw-Hill, New York) Sec. 7.15, p. 10.

Fornaca, S., H. Boehmer, J. A. Edighoffer, A. Maschke, G. R. Neil, J. L. Orthel, M. Rhodes, C. E. Hess, H. A. Schwettman, and T. I. Smith, 1987, "Experimental Investigation of Low Frequency Modes of a Single Cell RF Cavity," in *Proceedings of the 1987 Particle Accelerator Conference, Washington, D.C.,* Vol. 3, edited by Eric R. Lindstrom and Louise S. Taylor (IEEE, Piscataway, NJ, 1988), pp. 1818–1820.

Gluckstern, R., and B. Zotter, 1988, "The Coupling Impedance of Asymmetric Cavities," European Organization for Nuclear Research Report CERN/LEP Note 613.

Gluckstern, R. L., 1989a, "High-Frequency Behavior of the Longitudinal Impedance for a Cavity of General Shape," Phys. Rev. D **39**, 2773–2779.

Gluckstern, R. L., 1989b, "High-Frequency Dependence of the Coupling Impedance for a Large Number of Obstacles," in *Proceedings of the 1989 IEEE Particle Accelerator Conference, Chicago,* Vol. 2, edited by Floyd Bennet and Joyce Kopta (IEEE, Piscataway, NJ, 1989), pp. 1157–1159.

Gluckstern, R. L., 1989c, "Longitudinal Impedance of a Periodic Structure at High Frequency," Phys. Rev. D **39**, 2780–2783.

Gluckstern, R. L., and R. Li, 1990, "Analysis of Coaxial Wire Measurement of Longitudinal Coupling Impedance," Part. Accel. **29**, 159–165.

Gluckstern, R. L., and F. Neri, 1985, "Longitudinal Coupling Impedance for a Beam Pipe with a Cavity," IEEE Trans. Nucl.

Sci. **NS-32**, 2403–2404.
Gluckstern, R. L., and F. Neri, 1987a, "Characteristic of the Broad Resonance in the Longitudinal Coupling Impedance," in *Proceedings of the 1987 IEEE Particle Accelerator Conference, Washington, D.C.,* Vol. 2, edited by Eric R. Lindstrom and Louise S. Taylor (IEEE, Piscataway, NJ, 1988), pp. 1069–1071.
Gluckstern, R. L., and F. Neri, 1987b, "Computation of Coupling Impedance Using Cavity Codes," in *Proceedings of the 13th International Conference on High-Energy Accelerators, Novosibirsk, 1986,* Vol. 2, edited by A. N. Skrinskii (Nauka, Novosibirsk, 1987), pp. 170–173.
Gluckstern, R. L., and F. Neri, 1989, "Longitudinal Coupling Impedance of a Small Obstacle," in *Proceedings of the 1989 IEEE Particle Accelerator Conference, Chicago,* Vol. 2, edited by Floyd Bennet and Joyce Kopta (IEEE, Piscataway, NJ, 1989), pp. 1271–1273.
Gradshteyn, I. S., and I. M. Ryzhik, 1980, *Tables of Integrals, Series, and Products* (Academic, New York).
Gygi-Hanney, P. M., A. Hofmann, K. Hubner, and B. Zotter, 1983, "Program BBI: Bunched-Beam Instabilities in High-Energy Storage Rings," European Organization for Nuclear Research Report CERN/LEP-TH/83-2.
Halbach, K., and R. F. Holsinger, 1976, "SUPERFISH—A Computer Program for Evaluation of RF Cavities with Cylindrical Symmetry," Part. Accel. **7**, 213–222.
Heifets, S. A., 1988, "Analytic Study of the High-Frequency Impedance," presented at the Workshop on FEL's and Storage Rings, Dortmund, Germany, Continuous Electron Beam Accelerator Facility Report CEBAF-PR-89-014.
Heifets, S. A., 1989, "Diffraction Model of the High-Frequency Impedance," Phys. Rev. D **40**, 3097–3106.
Heifets, S. A., 1990a, "Determination of the High-Frequency Behavior of the Impedance from the Low-Frequency Data," Continuous Electron Beam Accelerator Facility Report CEBAF-TN/90/206.
Heifets, S. A., 1990b, "Impedance of a Taper," Continuous Electron Beam Accelerator Facility Report CEBAF-TN/90/202.
Heifets, S. A., 1990c, "On Directional Symmetry of the Impedance," Stanford Linear Accelerator Center Report SLAC-AP/79.
Heifets, S. A., 1990d, "Perturbation Method for Calculation of Narrow-Band Impedance and Trapped Modes," Part Accel. **25**, 217–228.
Heifets, S. A., and S. A. Kheifets, 1987, "High-Frequency Limit of the Longitudinal Impedance," Continuous Electron Beam Accelerator Facility Report CEBAF-PR-87-030.
Heifets, S. A., and S. A. Kheifets, 1988 "High-Frequency Limit of the Longitudinal Impedance of an Array of Cavities," Stanford Linear Accelerator Center Report SLAC-PUB-4625.
Heifets, S. A., and S. A. Kheifets, 1989, "High-Frequency Limit of the Longitudinal Impedance of an Array of Cavities," Phys. Rev. D **39**, 960–970.
Heifets, S. A., and S. A. Kheifets, 1990, "High-Frequency Limit of the Longitudinal Impedance," Part. Accel. **25**, 61–72.
Henke, H., 1985a, "Charge Passing Off Axis through a Cylindrical Resonator with Beam Pipes," IEEE Trans. Nucl. Sci. **NS-32**, 2335–2337.
Henke, H., 1985b, "Point Charge Passing a Resonator with Beam Tubes," European Organization for Nuclear Research Report CERN/LEP-RF/85-41.
Hereward, H. G., 1975, "Coupling Impedance of a Cross-Section Change for High Frequencies," European Organization for Nuclear Research Report CERN/ISR-D1/75-47.
Hofmann, A., 1976, "Single Beam Collective Phenomena—Longitudinal," in *Theoretical Aspects of the Behavior of Beams in Accelerators and Storage Rings,* Proceedings, First Course of International School of Particle Accelerators, Erice, Italy, edited by M. H. Blewett, A. Z. Zichichi, and K. Johnsen (CERN, Geneva, 1977) (European Organization for Nuclear Research Report CERN-77-13), p. 139.
Hofmann, A., and B. Zotter, 1989, "Analytic Models for the Broad Band Impedance," in *Proceedings of the 1989 Particle Accelerator Conference, Chicago,* Vol. 2, edited by Floyd Bennet and Joyce Kopta (IEEE, Piscataway, NJ, 1989), pp. 1041–1043; European Organization for Nuclear Research Report CERN/LEP-TH/89-16.
Jackson, J. D., 1975, *Classical Electrodynamics,* 2nd ed. (Wiley, New York).
Keil, E., 1972, "Diffraction Radiation of Charged Rings Moving in a Corrugated Cylindrical Pipe," Nucl. Instrum. Methods **100**, 419–427.
Keil, E., 1985, "Notes on the First Workshop on Radiation Impedance," European Organization for Nuclear Research Report CERN/LEP-TH/85-40.
Keil, E., and B. Zotter, 1972, "Longitudinal Stability of a Coasting Beam in a Corrugated Chamber," Part. Accel. **3**, 11–20.
Kheifets, S. A., 1981, "Electromagnetic Fields in an Axial Symmetric Waveguide with Variable Cross Section," IEEE Trans. Microwave Theory Technique **MTT-29**, 222–228.
Kheifets, S. A., 1986, "Longitudinal Impedance of Simple Cylindrically Symmetric Structures," Stanford Linear Accelerator Center Report SLAC-PUB-4133.
Kheifets, S. A., 1987, "Longitudinal Impedance of Simple Cylindrically Symmetric Structures," IEEE Trans. Microwave Theory Technique **MTT-35**, 753–760.
Kheifets, S. A., K. L. F. Bane, and H. Bizek, 1987a, "Transverse Impedances of Cavities and Collimators," in *Proceedings of the 1987 Particle Accelerator Conference, Washington, D.C.,* Vol. 3, edited by Eric R. Lindstrom and Louise S. Taylor (IEEE, Piscataway, NJ, 1988), pp. 1916–1918.
Kheifets, S. A., K. L. F. Bane, and H. Bizek, 1987b, "Transverse Impedances of Cavities and Collimators," Stanford Linear Accelerator Center Report SLAC-PUB-4097.
Kheifets, S. A., and P. M. Gygi, 1985, "IMPASS—A Computer Program for Calculations of Impedances of Periodic Axially Symmetric Smooth Structures (Bellows)," IEEE Trans. Nucl. Sci. **NS-32**, 2338–2340.
Kheifets, S. A., and S. A. Heifets, 1986a, "Radiation of a Charge in a Perfectly Conducting Cylindrical Pipe with a Jump in its Cross Section," in *Proceedings of the 1986 Linear Accelerator Conference* (Stanford Linear Accelerator Center Report SLAC-303), pp. 493–495.
Kheifets, S. A., and S. A. Heifets, 1986b, "Radiation of a Charge in a Perfectly Conducting Cylindrical Pipe with a Jump in its Cross Section," Stanford Linear Accelerator Center Report SLAC-PUB-3965.
Kheifets, S. A., and L. Palumbo, 1987, "Analytical Calculation of the Longitudinal Impedance of a Semi-Infinite Circular Waveguide," European Organization for Nuclear Research Report CERN/LEP Note 580.
Kheifets, S. A., L. Palumbo, and V. G. Vaccaro, 1985, "Longitudinal Impedance of a Semi-Infinite Circular Waveguide," European Organization for Nuclear Research Report CERN/LEP-TH/85-23.
Kheifets, S. A., L. Palumbo and V. G. Vaccaro, 1987, "Elec-

tromagnetic Fields Scattered by a Charge Moving on the Axis of an Infinite Circular Waveguide: Radiation Spectrum and Longitudinal Impedance," IEEE Trans. Nucl. Sci. **NS-34**, 1094–1100.

Kheifets, S. A., and B. Zotter, 1986, "Longitudinal and Transverse Impedances of Bellows in the Low-Frequency Range," Nucl. Instrum. Methods A **243**, 13–27.

Klatt, R., F. Krawczyk, W. R. Novender, C. Palm, B. Steffen, T. Weiland, T. Barts, M. J. Browman, R. Cooper, C. T. Mottershead, G. Rodenz, and S. G. Wipf, 1986, "MAFIA—A Three-Dimensional Electromagnetic CAD System for Magnets, RF Structures and Transient Wake-Field Calculations," in *Proceedings of the 1986 Linear Accelerator Conference* (Stanford Linear Accelerator Center Report SLAC-303), pp. 276–278.

Krinsky, S., 1980, "Resonant Impedance of Bellows above Cutoff," in *Proceedings of the 11th International Conference on High-Energy Accelerators, Geneva, Switzerland, 1980,* edited by W. S. Newman (Birkhäuser Verlag, Basel), pp. 576–580.

Krinsky, S., and R. Gluckstern, 1981, "Higher-Order Terms in a Perturbation Expansion for the Impedance of a Corrugated Wave Guide," IEEE Trans. Nucl. Sci. **NS-28**, 2621–2623.

Kurennoy, S. S., and S. V. Purtov, 1989, "Method for Calculation of Longitudinal and Transverse Coupling Impedances of Periodic Structures in Accelerators," U.S.S.R. Institute of Physics of High Energy Report IPHE 89-1.

Lambertson, G. R., 1989, "Electromagnetic Detectors," in *Frontiers of Particle Beams; Observation, Diagnosis, and Correction,* edited by M. Month and S. Turner, Lecture Notes in Physics Vol. 343 (Springer-Verlag, Berlin), pp. 380–402.

Landau, L. D., and E. M. Lifshitz, 1982, *Electrodynamics of Continuous Media* (Pergamon, New York), p. 292.

Laslett, L. J., 1963, "On Intensity Limitations Imposed by Transverse Space-Charge Effects in Circular Particle Accelerators," in *Proceedings of the Brookhaven Summer Study on Storage Rings, Accelerators and Experimentation at Super-High Energies,* edited by J. W. Bittner (BNL, Upton, NY) (Brookhaven National Laboratory Report BNL-7534), p. 324.

Lawson, J. D., 1968, "Radiation From a Ring Charge Passing Through a Resonator," Rutherford High Energy Laboratory Report M-144.

Lawson, J. D., 1990, "Radiation From a Ring Charge Passing Through a Resonator," Part. Accel. **25**, 107–112.

Lee, E. P., 1990, "Cancellation of the Centrifugal Space-Charge Force," Part. Accel. **25**, 241–252.

Levine, H., and J. Schwinger, 1948, "On the Radiation of Sound from an Unflanged Circular Pipe," Phys. Rev. **73**, 383–406.

Mankofsky, A., 1988, "Three-Dimensional Electromagnetic Particle Codes and Applications to Accelerators," in *Linear Accelerator and Beam Optics Codes,* AIP Conference Proceedings No. 177, edited by C. R. Eminhizer (AIP, New York).

Morton, P. L., V. K. Neil, and A. M. Sessler, 1966, "Wake Fields of a Pulse of Charge Moving in a Highly Conducting Pipe of Circular Cross Section," J. Appl. Phys. **37**, 3875–3883.

Ng, K.-Y., 1988, "Resonant Impedance in a Toroidal Beam Pipe," Superconducting Supercollider Laboratory and Fermi National Laboratory Report FERMILAB-FN-477-Rev.

Ng, K.-Y., 1990, "Resonant Impedance in a Toroidal Beam Pipe," Part. Accel. **25**, 153–182.

Ng, K.-Y., and Warnock, R. L., 1989, "Reactive Impedance of a Smooth Toroidal Chamber Below the Resonance Region," Stanford Linear Accelerator Center Report SLAC-PUB-4783, SSC-194, FN-500.

Novokhatski, A. V., 1988, "On the Estimation of the Wake Potential for an Ultrarelativistic Charge in an Accelerating Structure," Inst. Nucl. Phys. Preprint 88–39, Novosibirsk, U.S.S.R.

Palmer, R. B., 1986, "Wakefields for Short Bunches," Stanford Linear Accelerator Center Report SLAC-AAS-23.

Palmer, R. B., 1987 "A Qualitative Study of Wakefields for Very Short Bunches," Stanford Linear Accelerator Center Report SLAC-PUB-4433.

Palmer, R. B., 1989, "A Diffraction Analysis of Longitudinal Wakes of Short Bunches," Stanford Linear Accelerator Center Report SLAC-AAS-44.

Palmer, R. B., 1990, "A Qualitative Study of Wakefields for Very Short Bunches," Part. Accel. **25**, 97–106.

Palumbo, L., 1990, "Analytical Calculation of the Impedance of a Discontinuity," Part. Accel. **25**, 201–216.

Palumbo, L., and V. G. Vaccaro, 1989, "Wake Fields Measurements," in *Frontiers of Particle Beams; Observation, Diagnosis, and Correction,* Lecture Notes in Physics, Vol. 343 edited by M. Month and S. Turner (Springer-Verlag, Berlin), pp. 312–354.

Panofsky, W. K. H., and W. A. Wenzel, 1956, "Some Considerations Concerning the Transverse Deflection of Charged Particles in Radio-Frequency Fields," Rev. Sci. Instrum. **27**, 967.

Pellegrini, C., 1982, "Single Beam Coherent Instabilities in Circular Accelerators and Storage Rings," in *Physics of High Energy Particle Accelerators,* AIP Conference Proceedings No. 87, edited by R. A. Carrigan, F. R. Huson, and M. Month (AIP, New York), pp. 77–146.

Piwinski, A., 1985, "On the Transverse Forces Caused by the Curvature," European Organization for Nuclear Research Report CERN/LEP-TH/85-43.

Sands, M., and J. R. Rees, 1975, "A Bench Measurement of the Energy Loss of a Stored Beam to a Cavity," Stanford Linear Accelerator Center Report PEP-0095.

Sands, M., 1977, "Energy Loss from Small Holes in the Vacuum Chamber," Stanford Linear Accelerator Center Report PEP-253.

Sessler, A., unpublished monograph cited in E. Keil, 1972.

Slatter, J. C., 1950, *Microwave Electronics* (Van Nostrand, New York).

Stratton, J. A., 1941, *Electromagnetic Theory* (McGraw-Hill, New York).

Talman, R., 1986, "A novel relativistic effect important in accelerators," Phys. Rev. Lett. **56**, 1429–1432.

van Rienen, U., and T. Weiland, 1986, "Impedance of Cavities with Beam Ports above Cutoff," in *Proceedings of the 1986 Linear Accelerator Conference* (Stanford Linear Accelerator Center Report SLAC-303), pp. 289–291.

Vainshtein, L. A., 1963 Zh. Eksp. Teor. Fiz. **44**, 1415–1417 [Sov. Phys. JETP **17**, 709–719 (1963)].

Vainshtein, L. A., 1969, *The Theory of Diffraction and the Factorization Method* (Golden, Boulder, CO). Vainshtein solved the related problem of the diffraction of a wave (electromagnetic or acoustic) on an open end of a circular waveguide. His book contains the description of the Wiener-Hopf-Fock method, which he calls the factorization method.

von Meixner, J., 1949, "Die Kantenbedingungen in der Theory der Beugung von Electro-Magnetischer Wellen an Vollkommen Leitenden Ebenen Schirmen," Ann. Phys. (Leipzig) **6**, 2–9.

Vos, L., 1986, "Computer Calculation of the Longitudinal Impedance of Cylindrically Symmetric Structures and its Application to the SPS," European Organization for Nuclear

Research Report CERN/SPS/86-21(MS).

Vos, L., 1987, "Computer Calculation of the Longitudinal Impedance of Cylindrically Symmetric Structures and its Application to the SPS," in *Proceedings of the 1987 Particle Accelerator Conference, Washington, D.C.*, edited by Eric R. Lindstrom and Louise S. Taylor (IEEE, Piscataway, NJ, 1988), pp. 1237–1239.

Wang, T.-S. F., and B. Zotter, 1989, "An Expansion Method for Calculating Wake Potentials," European Organization for Nuclear Research Report CERN/LEP-TH/89-75.

Warnock, R. L., and G. R. Bart, 1984, "Longitudinal Stability of a Coasting Beam in a Resistive Vacuum Chamber with Cylindrical Resonant Cavity. Part II. Graphs and Formula for the Coupling Impedance," Part. Accel. **15**, 1–33.

Warnock, R. L., G. R. Bart, and S. Fenster, 1982, "Longitudinal Stability of a Coasting Beam in a Resistive Vacuum Chamber with Cylindrical Resonant Cavity. Part I. Self-Consistent Field Equations and a Method to Improve Convergence," Part. Accel. **12**, 179–203.

Warnock, R. L., and P. Morton, 1988, "Fields Excited by a Beam in a Smooth Toroidal Chamber," Stanford Linear Accelerator Center Report SLAC-PUB-4562.

Warnock, R. L., and P. Morton, 1990, "Field Excited by a Beam in Smooth Toroidal Chamber," Part. Accel. **25**, 113–151.

Watson, G. N., 1944, *A Treatise on the Theory of Bessel Functions* (Cambridge University Press, Cambridge, England), Section 15.42; note that the formula here contains several misprints.

Weiland, T., 1980, "On the computation of electromagnetic fields excited by relativistic bunches of charged particles in accelerator structures," European Organization for Nuclear Research Report CERN/ISR-TH/80-07.

Weiland, T., 1982, "Transverse Beam Cavity Interaction. Part I: Short Range Forces," Deutsches Electronen-Synchrotron Report DESY 82-015.

Weiland, T., 1983a, "Transverse Beam Cavity Interaction. Part I: Short Range Forces," Nucl. Instrum. Methods **212**, 13–21.

Weiland, T., 1983b, "Comment on Wakefield Computation in Time Domain," Nucl. Instrum. Methods **216**, 31–34.

Weiland, T., 1983c, "On the Computation of Resonant Modes in Cylindrically Symmetric Cavities," Nucl. Instrum. Methods **216**, 329–348.

Wiener, N., and E. Hopf, 1931, "Ueber eine Klasse Singulaerer Integralgleichungen", Sitzungsber. Dtsch. Akad. Wiss., Berlin, Kl. Math. Phys. Tech., pp. 696–706. Reproduced in N. Wiener, "Collected Works with Commentaries," Vol. 3, edited by P. Masani (MIT Press, Cambridge, MA), pp. 33-43. A short but sufficient description of the method can be found also in the book by P. M. Morse and H. Feshbach, 1953, *Methods of Theoretical Physics* (McGraw-Hill, New York), Vol. 1, Section 8.5.

Wilson, P. B., 1978, "Parasitic Mode Losses to Small Vacuum Chamber Gaps," European Organization for Nuclear Research Report CERN/LEP-70/62.

Wilson, P. B., 1982, "High Energy Electron Linacs; Application to Storage Ring RF Systems and Linear Colliders," in *Physics of High Energy Particle Accelerators,* AIP Conference Proceedings No. 87, edited by R. A. Carrigan, F. R. Huson, and M. Month (AIP, New York), pp. 450–558.

Yokoya, K., 1990, "Impedance of Slowly Tapered Structures," European Organization for Nuclear Research Report CERN SL/90-88 (AP).

Yunn, B., 1989, "A Note on Tapering a Step," Continuous Electron Beam Accelerator Facility Report CEBAF-TN-0134.

Zisman, M. S., S. Chattopadhyay, and J. Bisognano, 1986, "ZAP User's Manual," Lawrence Berkeley Laboratory Report LBL-21270.

Zotter, B., and K. Bane, 1979, "Transverse Resonances of Periodically Widened Cylindrical Tubes with Circular Cross section," Stanford Linear Accelerator Center Report PEP-308.